To the Graduate Council:

I am submitting herewith a dissertation written by Baldomero O. Westermann entitled "Optimal Speed of Response of a Roller Follower Cam Driven System." I have examined the final copy of this dissertation for form and content and recommend that it be accepted in partial fulfillment of the requirements for the degree of Doctor of Philosophy, with a major in Mechanical Engineering.

James A. Euler

James A. Euler, Major Professor

We have read this dissertation
and recommend its acceptance:

Edward G. Keshock

R. L. Maxwell

C. W. Lee

Accepted for the Council:

Vice Provost
and Dean of The Graduate School

OPTIMAL SPEED OF RESPONSE OF A ROLLER FOLLOWER CAM DRIVEN SYSTEM

A Dissertation

Presented for the

Doctor of Philosophy

Degree

The University of Tennessee, Knoxville

Baldomero O. Westermann

December 1987

To Mery, Wermer, Ingrid, and Isabel

ACKNOWLEDGMENTS

I would like to thank Dr. James A. Euler for his efforts and help as advisor and major professor. Thanks are also given to Professors F. H. Speckhart, R. L. Maxwell, C. W. Lee and E. G. Keshock for serving on my committee. Thanks to the department head Dr. Donald R. Pitts for his financial support in giving me a teaching assistantship. Thanks to the authorities of the Universidad de Santiago de Chile for their support and for giving me the opportunity to pursue this Doctor of Philosophy degree. I wish to thank Ms. Jennifer Brewster and Mrs. Beverly Owens for typing this manuscript.

ABSTRACT

This dissertation analyzes the problem of determination of the maximal speed of response of a roller follower plate cam driven system. The solution to the problem of the lift of a roller from lower to upper dwelling conditions under the dual constraints of (1) a maximal allowed stress, and (2) no undercutting of the cam, was obtained using the analogy of the "Bang Bang Problem"; this problem has a very simple analytical solution, but its implications can be very usefully applied to the problem of cam lift. After applying this analogy in the present study, a technique of nonlinear programming was used to deal with the process of minimizing the angle of rotation of the cam under the constraint of a maximum allowable stress.

Using the stress constraint at its limiting value (i.e., at the border of the domain) an initial value problem of a second order non-linear differential equation is defined, which can be solved numerically. The study of the singular solution of this problem and the study of this ODE in the phase plane provide important information about the existence of restrictions in the phase plane as well as its singular points. The maximum stress constraint is found to provide a maximum rate of deceleration for a low angular velocity problem. Also for low angular velocity it was necessary to add an additional constraint of a maximum acceleration rate, because the dual constraint did not bound the acceleration.

In the region of high angular velocity it was found that the maximal stress constraint provides a maximum acceleration rate but a maximum deceleration rate is obtained using a low stress.

The geometrical constraint of no undercutting determines the area of the phase plane for a feasible solution.

TABLE OF CONTENTS

LIST OF TABLES

LIST OF FIGURES

NOMENCLATURE

a: Arm distance of the rocker arm to the point of action of the push rod.

b: Arm distance of the rocker arm to the point of action of the valve.

c: Parameter for Hertz stress; also constant of integration.

d: diameter of the wire of the spring.

D: Working stroke.

D_e: Exterior diameter of the coil.

E: Elasticity moduli.

EXP: Exponential.

F: Function of μ.

F_n: Normal load.

g: Acceleration of gravity.

G: Shear modulus.

h: Total lift of the follower.

h*: Nondimensional h.

h_v: Total lift of the valve.

J: Polar moment of inertia of the rocker arm with respect to the axis of rotation.

k: Spring rate.

K_t: Curvature of the cutting tool used to manufacture the cam.

l: Length of the rocker arm; also free height of the spring valve.

l_n: Natural logarithm.

L: Displacement in the Bang-Bang problem.

m: Total mass of the follower.

m_A: Equivalent mass at point A.

m_r: Mass of the rocker arm.

m_s: Mass of the spring.

m_v: Mass of the valve plus spring retainer.

M: Bound positive value of the control value.

n: Number of turns of the coil.

p: Independent variable in the linear O.D.E.

P: Force between cam and follower; also numerator of a fraction.

P_o: Spring force at $y = 0$.

P_f: Spring force at $R = 0$.

q: Parameter function of α.

Q: Denominator of a fraction.

r: Nondimensional radius to pitch curve.

r_m: Mean radius of the coil.

R: Radius to pitch curve.

R_f: Radius of the roller follower.

s: Upper limit of the nondimensional stress.

S: Square of the maximum permissible contact stress.

t: Time; also independent variable in the modified Able equation.

u: Displacement shifted to a center; also change of variable in the quadrature of the linear equation.

U: Control variable.

v: Nondimensional velocity.

w: Width of the roller follower.

X: State variable in the Bang-Bang problem.

y: Lift of the follower.

y^*: Nondimensional y.

z: Dependent variable.

Z: Trinomial on z.

Greek Symbols

α: Nondimensional stress.

β: Nondimensional prestress.

γ: Angular velocity ratio.

δ: Diameter of circle of singularity.

Δ: Discriminant of second order algebraic equation; also maximum deflection of the spring valve.

μ: Poisson's ratio.

ω: Angular velocity of the cam.

ϕ: Lower limit of the control variable; also integrating factor.

ψ: Angle of pressure; also upper limit of the control variable.

ρ: Radius of curvature of the pitch curve.

ρ^*: Nondimensional ρ.

ρ_c: Radius of curvature of the cam.

σ: Contact stress.

Θ: Angle of rotation of the cam.

Subscripts

0: Initial.

n: Natural number for polynomial coefficient; also for roots of algebraic equation.

min: Minimum.

max: Maximum.

f: Final.

Superscripts

$*$: Nondimensional.

a: Transition point.

CHAPTER 1

INTRODUCTION

This dissertation is a continuation of the "Fast Movement of a Roller Follower Plate Cam Driven System" [38]. The central idea is the study of the speed of response of a cam lift problem to find optimal results by minimizing the angle of rotation for a given lift (see Fig. 1.1). This type of problem appears in the valve timing of big size internal combustion engines used in electrical power generation or for powering ships where units as high as 40,000 HP have been built. Also the roller follower is used in piston aircraft engine, where a long period of operation between overhauls is required.

The development of the cam lifter mechanism was considered in the beginning from a kinematics point of view (see Figs. 1.2 and 1.3). The displacement, velocity and acceleration of the follower were studied. It has been recognized that the continuity of the velocity versus rotation of the cam is a must, otherwise an infinite discontinuity in the acceleration at the acceleration diagram will occur. Because of that the linear displacement was modified in the beginning and final part of the movement using arcs of circles or parabolas.

For a given lift and permissible angle of rotation of the cam, the acceleration was intended to be a minimum value. Thus the parabolic displacement diagram was used, which has a constant acceleration during half of the rise stroke and a negative acceleration of the same

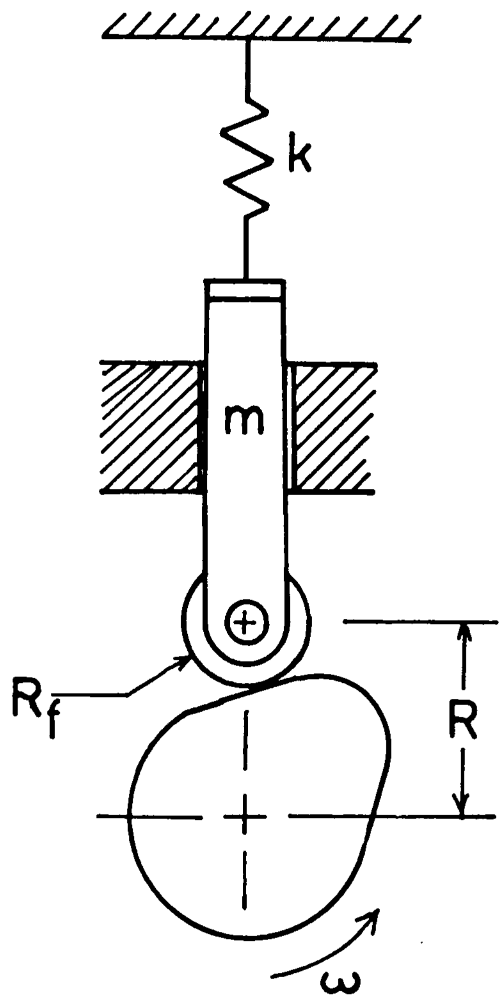

Figure 1.1. Cam driven mechanism.

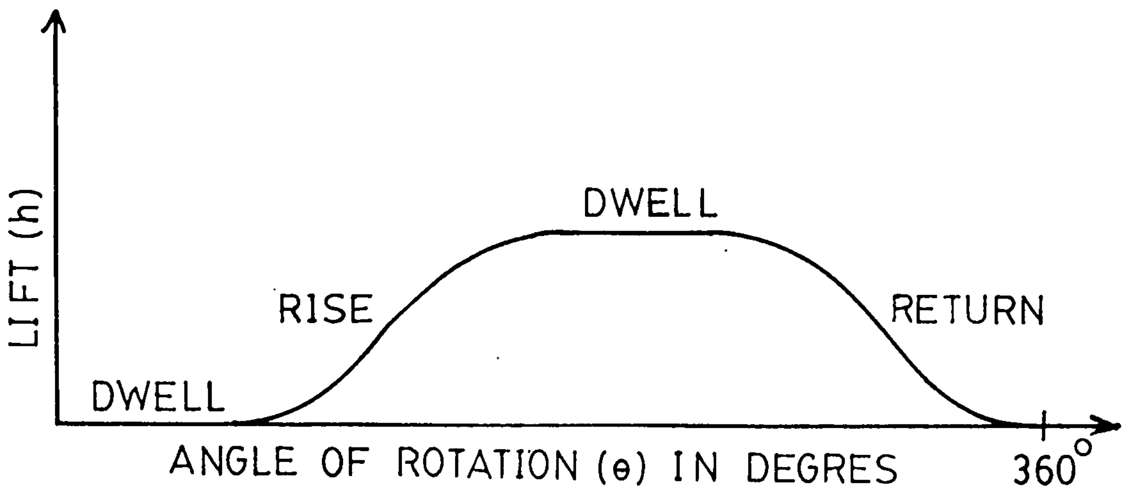

Figure 1.2. Cam displacement diagram: dwell-rise-dwell-return.

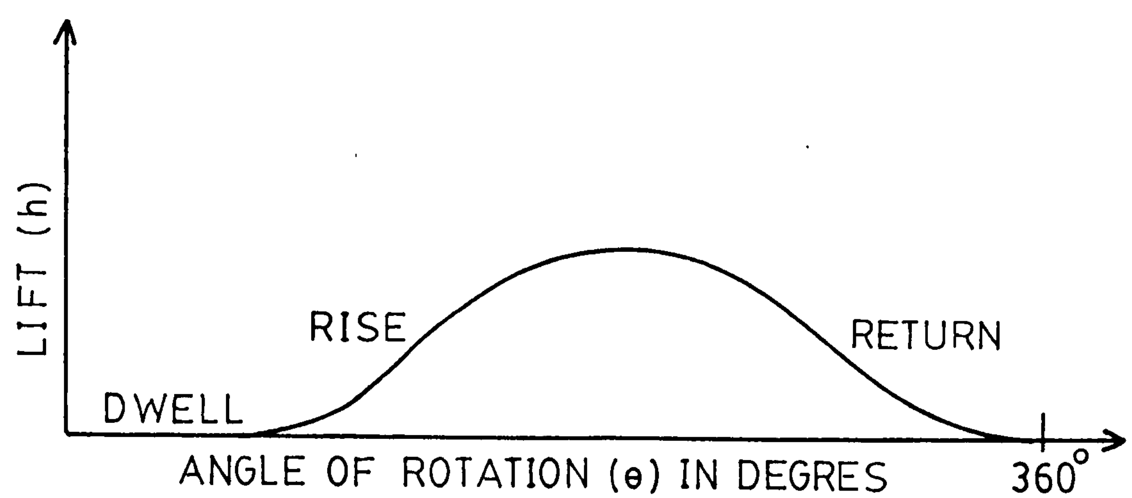

Figure 1.3. Cam displacement diagram: dwell-rise-return.

numerical value in the second half of it, and therefore, the maximum absolute value of the acceleration is kept at a minimum.

This interest in the acceleration diagrams existed because the acceleration is related to the inertial forces between the cam and follower and was important to keep the forces at a minimum. Later another problem arose in cam systems. The cam applications increased in angular velocity. Then designers focused their interest on the third derivative of the displacement, which is called the jerk and causes vibration due to the elasticity of the components of the cam lifter mechanism. Then designers tried avoiding discontinuity in the acceleration which is infinite jerk. Cycloidal shapes in the displacement curve were used since they have the quality that the acceleration curve is smooth and no discontinuity is encountered. But a disadvantage was coming. The maximum of the absolute value of the acceleration was bigger than it was for the parabolic shape. A further increase in the angular velocity of the mechanism was forcing, in part, a return to the parabolic motion, which has a shape of two rectangles for positive and negative acceleration respectively. The so called trapezoidal acceleration curve was the response for keeping the jerk low and not having too high an acceleration. Also the stress between the cam and roller now played an important role, otherwise the wear of the cam reduced the life of the cam system.

With all this development only one method of solution was used by designers, they defined the displacement versus cam rotation diagram, the base and prime circles were selected empirically, then the pitch curve and cam profile was determined. If no undercutting appeared in the negative acceleration part of the lift, the selection of the displacement curve was acceptable. Meanwhile the maximum angle of pressure was checked and 30° was considered an upper limit. In some cases, because of space restrictions, 45° was accepted. After that the spring was designed to be able to provide the required negative acceleration. The last step was to check the contact stress between the cam and the roller follower. The whole design process consisted of many steps with high empirical input, much necessary experience, and many trail and error loops.

During this time, some theoretical understanding was reached. For example, the integral of the acceleration curve has to be zero in going from lower to upper dwelling position and vice versa. Also the second order differential equation of the curvature of the pitch curve in polar coordinates allowed a proof that no finite positive acceleration will undercut the cam. But in the negative acceleration phase undercutting occurred if the selected empirical values were improper. However, there was no clear understanding of the relation between acceleration and contact stresses. That was expected because of the high nonlinearity displayed by the curvature equation of the pitch curve.

With the introduction of computer facilities more research was conducted but the methods were the same. Researchers were using the acceleration curve as a control variable and the bidimensional state space (i.e., velocity and displacement) was not understood. The geometrical constraint and stress constraint were introduced after the empirical design.

The designer began approaching good results only after much empirical work. The computer data by itself did not help in understanding the limitations of the design.

In this dissertation the author approaches the problem of minimizing the angle of rotation of a cam for a given lift under two differential inequality constraints. They are the stress constraint given by the materials used in the system and the geometrical constraint of no undercutting.

The method used for optimization under the inequality constraint is very general. First, one tries to optimize with no constraint and determines if there exists a limit where the solution approaches an optimum. If an optimum exists the inequality is checked to see if it holds. If it does then the problem is already solved.

Second, if the preceding method does not work then the inequalities are introduced one by one and one tries to find an optimal in the border of the inequality. If there exists an optimal then it is checked to see if the other inequality holds, if it does then the problem is solved.

In the problem of this dissertation the first method does not work because if no constraints are put on the stress then the answer is to apply infinite positive acceleration for half of the displacement, and then to switch to infinite deceleration in the second half of the displacement. The optimal rotation equals zero, but in checking both inequalities, it is found that they do not hold.

The second method works and is presented in this dissertation. Furthermore, the author studied the types of solutions and determined under what conditions they appear. This is a typical study of nonlinear mechanics where not only the parameters influence the solution but also the initial conditions play an important role.

CHAPTER 2

MODEL FOR OPTIMAL SPEED OF RESPONSE

The problem of the optimal speed of response in lifting a follower from a lower to an upper position beginning and ending at rest is related to the simple Bang-Bang [11] problem in which the actual extreme control function U(t) is piecewise continuous and is required to satisfy a pointwise inequality constraint of the form,

$$\phi(t) \leqq U(t) \leqq \psi(t) \qquad \text{for } t_0 \leqq t \leqq t_2 \tag{2.1}$$

where $\phi(t)$ and $\psi(t)$ are given known piecewise continuous functions for $t_0 \leqq t \leqq t_2$.

Let us now consider a particle moving in free space with the second order equation

$$\ddot{X}(t) = U(t) \tag{2.2}$$

where x is the position in a one dimensional trajectory, U(t) is the acceleration provided by a thrust system, which is the control function. Let us limit the control variable by:

$$-M \leqq U(t) \leqq M \qquad \text{for } t_0 \leqq t \leqq t_2 \tag{2.3}$$

It is known that an optimal time in the change of position of a particle is obtained by accelerating at a maximum rate and then switching in the middle of the trajectory to a maximum decelerating rate. Let us integrate the equation of the trajectory which is discontinuous at the switch point.

Recall from Eq. (1.2) that

$$\ddot{X} = U(t), \qquad U(t) = \begin{cases} M \text{ if } 0 < t < t_1 \\ -M \text{ if } t_1 < t < t_2 \end{cases} .$$

The initial conditions are the following

$$t = 0,\ \dot{X}(0) = X(0) = 0 \ ,$$

and the final conditions:

$$t = t_2,\ \dot{X}(t_2) = 0 \text{ and } X(t_2) = L \ .$$

This lead to the following results

$$\dot{X} = Mt \text{ and } X = \tfrac{1}{2}Mt^2, \text{ for } 0 \leq t \leq t_1. \tag{2.4}$$

and

$$\dot{X}(t) = -Mt + 2Mt_1$$

$$X(t) = \tfrac{1}{2}Mt^2 + 2Mt_1t - Mt_1^{\,2}, \text{ for } t_1 \leq t \leq t_2. \tag{2.5}$$

Imposing the final conditions at the end of the interval i.e.m $t = t_2$ yields the set of two algebraic equations,

$$-Mt_2 + 2Mt_1 = 0 \tag{2.6}$$

$$-\tfrac{1}{2}Mt_2^{\ 2} + 2Mt_1t_2 - Mt_1^{\ 2} + L. \tag{2.7}$$

Solving the system for t_2 and t_1, one obtains

$$t_2 = 2t_1,$$

and

$$t_1 = \sqrt{\frac{L}{M}} \ . \tag{2.8}$$

Now let us define

$$T \equiv t_2,$$

which is the minimum time for change from state $X(0) = 0$, $\dot{X}(0)$ to state $X(T) = L$, $\dot{X}(T) = 0$.

Then the state at the midpoint can be rewritten as follows

$$t_1 = \frac{T}{2} \ .$$

Thus,

$$\dot{X}(\tfrac{T}{2}) = \tfrac{1}{2}MT, \tag{2.9}$$

and

$$X(\tfrac{T}{2}) = \frac{L}{2} \ . \tag{2.10}$$

The relations $\ddot{X}(t)$, $\dot{X}(t)$ and $X(t)$ can be seen in Fig. 2.1.

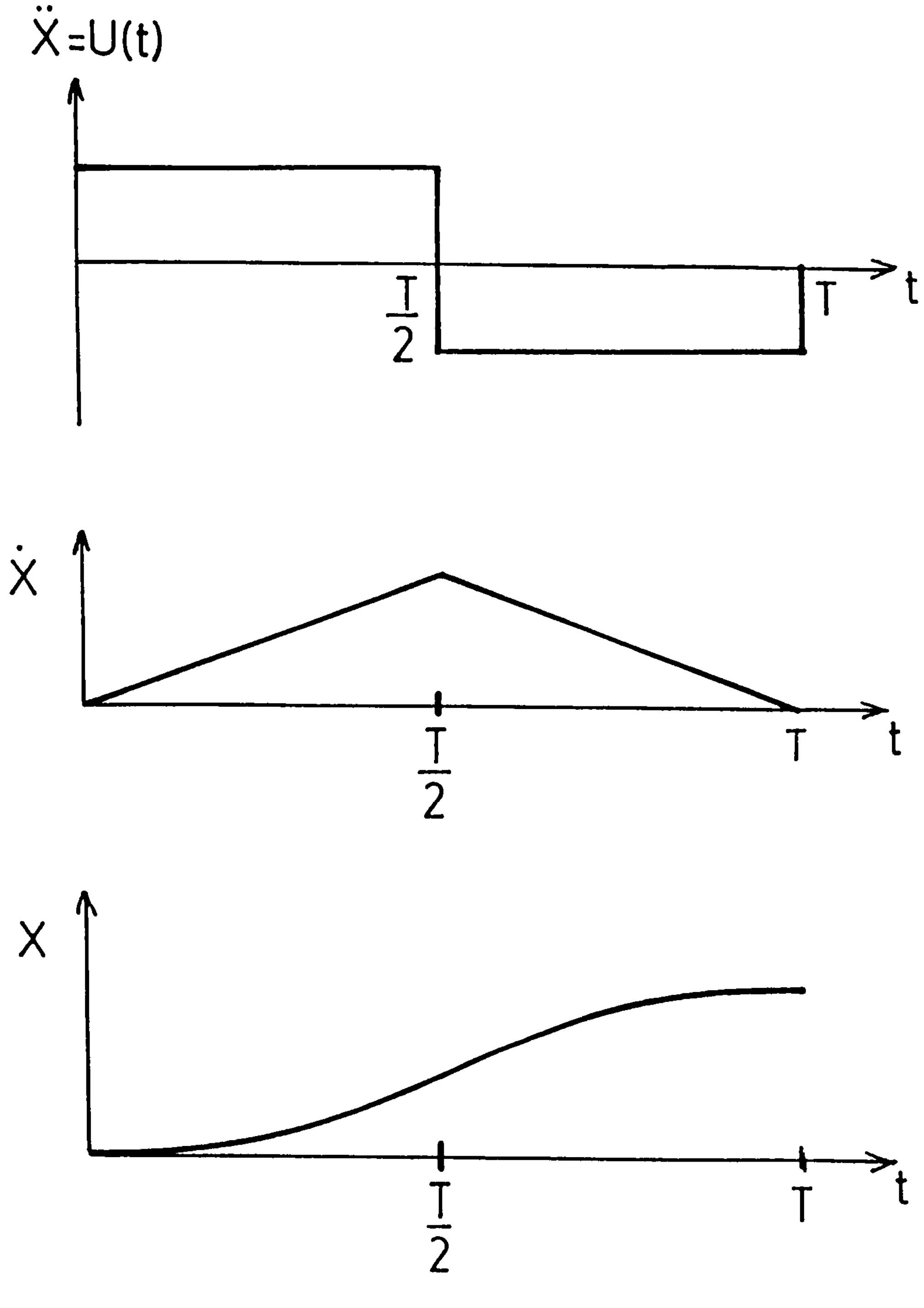

Figure 2.1. Kinematics of the bang-bang problem.

Trajectories in the Phase Plane of the Bang-Bang Problem

The phase plane is a graph in which is plotted the velocity as a function of the displacement and the variable time does not appear.

Recall Eq. (2.4) and its derivative

$$X(t) = \tfrac{1}{2}Mt^2$$

$$\dot{X}(t) = Mt$$

solving for t in the second equation and substituting in the first equation, one obtains

$$X = \frac{(\dot{X})^2}{2M}\,, \tag{2.11}$$

which is a parabola.

Recall Eq. (2.5) and its derivative

$$\dot{X}(t) = -Mt + 2Mt_1$$

$$X(t) = -\tfrac{1}{2}Mt^2 + 2Mt_1t - Mt_1{}^2\,,$$

solving for t in the first equation, using Eq. (2.8) and substituting in the second equation yields

$$X = L - \frac{(\dot{X})^2}{2M} \tag{2.12}$$

which is the second parabola for the decelerating process. The complete trajectory in the phase plane can be seen in Fig. 2.2.

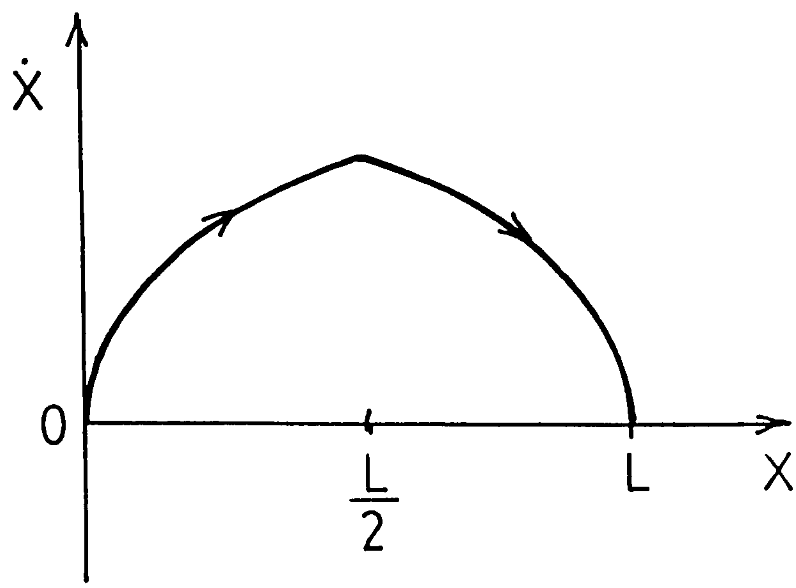

Figure 2.2. Trajectory in the phase plane of the bang-bang problem.

The conclusion of the simple Bang-Bang problem is that it is necessary that only one discontinuity occur in the piecewise continuous control. This is where you switch from maximal acceleration to maximal deceleration.

The next analysis will have a different governing equation and different constraints but the general point of view is the same.

Model for the Optimal Cam's Profile

First it is important to establish a general approach for the solution of an optimal cam profile in a roller follower cam drive system. It is already known that a quick response is obtained by a positive acceleration in the first stage, followed by a shift to deceleration in the second stage. In general the actual methods try to avoid a discontinuity in the acceleration, but in this work it will be allowed, specifically in the beginning position, the transition point (where the acceleration shifts sign), and the final position of the follower.

Description of the Model of a Roller Follower Cam Driven System

Let us present quickly the ideas, definition of parameters and restrictions already described in reference [38], "Fast Movement of a Roller Follower Plate Cam Driven System."

First the problem was described in terms of the independent variable θ, which is the angle of rotation, and the dependent variable R, which is the radial distance from the center of the cam to the pitch curve. Later on the variable R was nondimesionalized to r. Now in brief the problem can be stated as follows:

It is required to minimize θ_f

where θ_f, the total angle of rotation for a given lift, is subject to (1) restrictions in the contact stress between roller and follower, and (2) to the geometrical constraint of no undercutting.

At this moment one can identify r and r' as state variables. Later it will be possible to identify the control variables which will be related to the two constraints already mentioned.

The constraints can be written as in [38]

$$0 < \sigma^2 = CP\left(\frac{1}{R_f} + \frac{1}{\rho_c}\right) \leq S$$

and

$$\frac{1}{\rho_c} > \max\left(-K_t, -\frac{1}{R_f}\right) \qquad (2.14)$$

where S = upperbound of the square of the contact stress,

P = force between cam and follower,

$$\frac{1}{C} = \pi w\left(\frac{1 - \mu_1^2}{E_1} + \frac{1 - \mu_2^2}{E_2}\right),$$

μ_1 and μ_2 = Poissons ratio for cam and follower respectively,

E_1 and E_2 = moduli of elasticity for cam and follower, respectively,

w = width of cam and follower,

R_f = radius of the roller follower,

ρ_c = radius of curvature of cam at the point of contact, and

K_t = curvature of the cutting tool used to manufacture the cam, always positive.

The radius of curvature of the pitch curve in polar coordinates is given by,

$$\rho = \frac{[R^2 + (R')^2]^{3/2}}{R^2 + 2(R')^2 - RR''} , \tag{2.15}$$

$$R = R_0 + y , \tag{2.16}$$

$$\rho_c = \rho - R_f , \tag{2.17}$$

where ρ = radius of curvature of the pitch curve and is positive for a convex radius,

y = cam lift,

R_0 = prime circle radius, and

R' and R'' = first and second derivatives of R with respect to the cam rotation, respectively.

By using Newton's second law and summing forces on the follower in the direction of positive lift, the following expression for the force between the cam and the follower is obtained, as in [38] (see Fig. 2.3).

$$P = [P_0 + ky + m\omega^2 y''] \, [1 + (\frac{y'}{R})^2]^{1/2} , \tag{2.18}$$

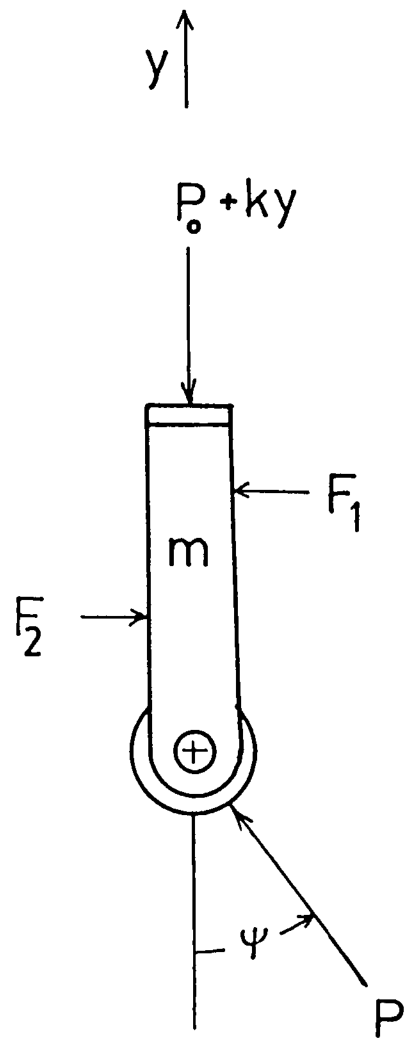

Figure 2.3. Free body diagram of the follower.

where P_0 = spring force at $y = 0$,

k = spring rate,

m = total mass of the follower, and

ω = angular velocity of cam.

In expression (2.18) y can be written in terms of R. Let us define a new parameter (see Fig. 2.4)

$$P_f = P_0 - kR_0 \ . \tag{2.19}$$

Equation (2.18) now yields

$$P = [P_f + kR + m\omega^2 R''] \ [1 + (\frac{R'}{R})^2]^{1/2} \quad , \tag{2.20}$$

which is plotted in Fig. 2.4. On substituting Eq. (2.20) into (2.14) it follows that

$$\sigma^2 = C[P_f + kR + m\omega^2 R''] \ [1 + (\frac{R'}{R})^2]^{1/2} \ (\frac{1}{R_f} + \frac{1}{\rho_c}) \tag{2.21}$$

Notice that the right most factor on the right hand side of Eq. (2.21) must satisfy the relation

$$\frac{1}{R_f} + \frac{1}{\rho_c} > 0 \quad . \tag{2.22}$$

Otherwise an undercutting condition will occur. Also notice that the first factor must satisfy the relation

$$P_f + kR + m\omega^2 R'' > 0 \quad . \tag{2.23}$$

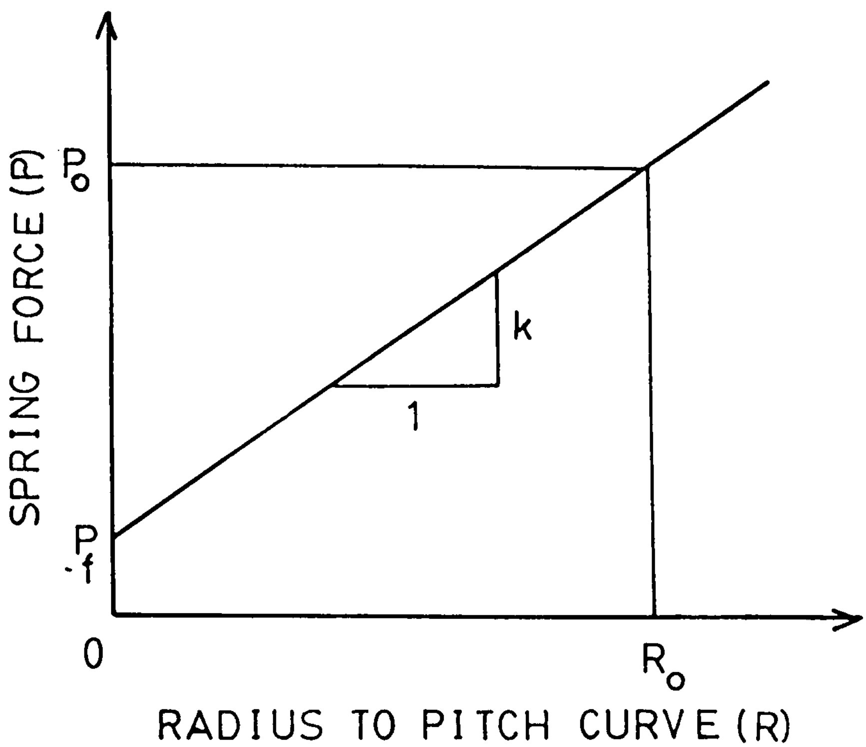

Figure 2.4. Prestress diagram.

In other words the cam pushes the roller follower and never pulls it.

It is important to realize that negative values of Eqs. (2.22) and (2.23) at the same time represent only a mathematical solution without physical meaning for our cam configuration.

Equation (2.22) can be written in terms of ρ and R_f only as follows.

$$\frac{1}{R_f} + \frac{1}{\rho_c} = \frac{1}{R_f} + \frac{1}{\rho - R_f} = \frac{\rho}{R_f(\rho - R_f)} \; .$$

Now, replace ρ using Eq. (2.15). Thus,

$$\frac{1}{R_f} + \frac{1}{\rho_c} = \frac{1}{R_f} \; \frac{[R^2 + (R')^2]^{3/2}}{[R^2 + (R')^2]^{3/2} - R_f[R^2 + 2(R')^2 - RR'']} \; . \tag{2.24}$$

The numerator of Eq. (2.24) is always positive which means that inequality (2.22) holds only if the denominator of the right-hand side of Eq. (2.24) is positive. In the limit when the denominator approaches +0, a second order differential equation is defined, which is very useful for avoiding undercutting.

Let us now substitute Eq. (2.24) into Eq. (2.21) to obtain the following expression.

$$\sigma = \frac{C}{R_f} \, \frac{1}{R} \, \frac{[P_f + kR + m\omega^2 R''] \; [R^2 + (R')^2]^2}{\{[R^2 + (R')^2]^{3/2} - R_f[R^2 + 2(R')^2 - RR'']\}} \; . \tag{2.25}$$

Now define nondimensional parameters as follows,

$$\alpha \equiv \frac{\sigma^2}{Ck}$$

$$s \equiv \frac{S}{Ck}$$

$$\beta \equiv \frac{P_f}{kR_f}$$

$$\gamma \equiv \frac{m\omega^2}{k} \equiv \frac{\omega^2}{k/m}$$

$$r \equiv \frac{R}{R_f} \tag{2.26}$$

where α = nondimensional stress (involves a proportionality to the square of the allowable stress and to the inverse of the spring rate; also C represents the effect of w, E, and μ,

s = upper limit of the nondimensional stress,

β = nondimensional prestress,

γ = angular velocity ratio (this is the ratio between angular velocity of the cam and the angular frequency of the spring mass system),

r = nondimensional radial coordinate to the pitch curve,

r' and r'' = first and second derivatives of r with respect to the cam rotation, respectively, and

θ = angle of rotation of the cam in radius.

Eq. (2.25) can be put into the following nondimensional form.

$$\alpha = \frac{1}{r} \frac{(\beta + r + \gamma r'')\,[r^2 + (r')^2]^2}{[r^2 + (r')^2]^{3/2} - r^2 - 2(r')^2 + rr''} \quad . \tag{2.27}$$

From Eq. (2.27) the following inequality can be generated:

$$\frac{1}{r}\,\frac{(\beta + r + \gamma r'')\,[r^2 + (r')^2]^2}{[r^2 + (r')^2]^{3/2} - r^2 - 2(r')^2 + rr''} \leq s\ . \qquad (2.28)$$

This is the basic nondimensional inequality constraint for stress, with s being the maximal permissible nondimensional stress.

The geometrical constraint can also be written in nondimensional form as follows.

$$[r^2 + (r')^2]^{3/2} - r^2 - 2(r')^2 + rr'' > 0 \qquad (2.29)$$

There is a discontinuity in Eq. (2.27) if

$$r'' = \frac{r^2 + 2(r')^2 - [r^2 + (r')^2]^{3/2}}{r}\ ,$$

since α becomes unbounded. Also, it is found that when r" approaches infinity, as α, given by Eq. (2.27) approaches the following asymptote:

$$\lim_{r'' \to \infty} \alpha = \frac{\gamma\,[r^2 + (r')^2]^2}{r^2}\ .$$

Now the optimum control problem can be visualized as minimizing θ, using r" as a control variable, subject to the inequality constraints (2.28) and (2.29). The state variables are r and r' define the phase plane.

Let us notice that the left-hand side of the inequality (2.28) can be a decreasing, constant or increasing function of r" depending on the parameters β and γ and the state variables r and r'. Let us take the derivative of the right-hand side of inequality (2.28) with respect to r".

$$\frac{\partial\alpha}{\partial r''} = \frac{[r^2 + (r')^2]^2}{r} \, \frac{\{[r^2 + (r')^2]^{3/2} - r^2 - 2(r')^2\}\,\gamma - r(\beta + r)}{\{[r^2 + (r')^2]^{3/2} - r^2 - 2(r')^2 + rr''\}^2} \tag{2.30}$$

The sign of the $\partial\alpha/\partial r''$ is only dependent on a factor in the numerator of the right-hand side of Eq. (2.40) which is as follows:

$$\{[r^2 + (r')^2]^{3/2} - r^2 - 2(r')^2\} \;\; \gamma - r(\beta + r) \; . \tag{2.31}$$

Notice that for small values of γ the stress is a decreasing function with respect to the acceleration, while for large values of γ the stress is an increasing function with respect to the acceleration. For intermediate values of γ the nondimensional stress, α, is affected by both of the state variables r and r', which makes the response of the system more complicated. It should be noted that the geometrical inequality (2.29) depends only on the state variables r and r' and the acceleration as a control variable but not on β and γ. The behavior mentioned in this paragraph is typical for a nonlinear system.

<u>Solution of the Model for Maximum Stress Constraint</u>

Recall the statement of the problem for maximal speed of response, i.e.,

$$\text{Minimize } \theta_f$$

subject to the dual constraints (2.28) and (2.29)

$$\frac{1}{r}\,\frac{(\beta + r + \gamma r'')\,[r^2 + (r')^2]^2}{[r^2 + (r')^2]^{3/2} - r^2 - 2(r')^2 + rr''} \leq s$$

$$[r^2 + (r')^2]^{3/2} - r^2 - 2(r')^2 + rr'' > 0 \; .$$

In the study of reference [38] it was found that (2.28), considered as an equality, provides a solution which, for low angular velocity, minimizes the angle of rotation in the negative acceleration stage of the follower (i.e., low value of γ) and minimizes the angle of rotation in the positive acceleration stage of the follower (i.e., high value of γ).

This can be explained in the following way. For low values of γ, the inequality (2.28) has a decreasing relation with respect to the acceleration. Therefore, a low value of γ results in requiring a negative acceleration to achieve the maximal stress. For this to happen, the profile of the cam has to be convex, which guarantees that the inequality (2.29) will hold. On the other hand for high values of γ the inertial forces are important and the left-hand side of the inequality (2.28) increases with respect to the acceleration and the maximal stress is achieved with a positive acceleration of the follower. Now the profile cam results in a concave or a convex profile depending on the value of γ, but undercutting will never occur, which guarantees again that inequality (2.29) will hold.

The equation for maximal stress constraint was solved by reference [38] but the study of the type of singular solution made therein was with a simplified model. On the present study the singularities are analyized directly from the exact equation (2.28).

Singular Solution for Constant Stress Constraint

The singular solution for the constant stress constraint is obtained by using the equality portion of inequality (2.28) and by setting r' and r" equal to zero (i.e., the equilibrium solution). This yields

$$\alpha = \frac{(\beta + r)\, r}{r - 1} = s \ . \tag{2.32}$$

Now on checking the geometrical constraint given by inequality (2.29), one obtains

$$r^2(r - 1) > 0 \tag{2.33}$$

which indicates that for a singular solution $r > 1$.

On solving for r in Eq. (2.32) it follows that,

$$r_{1,2} = \frac{(\alpha - \beta) \pm\sqrt{\Delta}}{2} \ , \tag{2.34}$$

where $\Delta = (\alpha - \beta)^2 - 4\alpha$, and $r_1 \geq r_2$.

The characteristic of Eq. (2.34) is such that for $\beta > -1$ one obtains two roots greater than unity, with a convex curve existing in the graph of Eq. (2.32) wherein α is plotted as a function of r as shown by Fig. 2.5. For $\beta < -1$ one obtains only one root greater than unity;

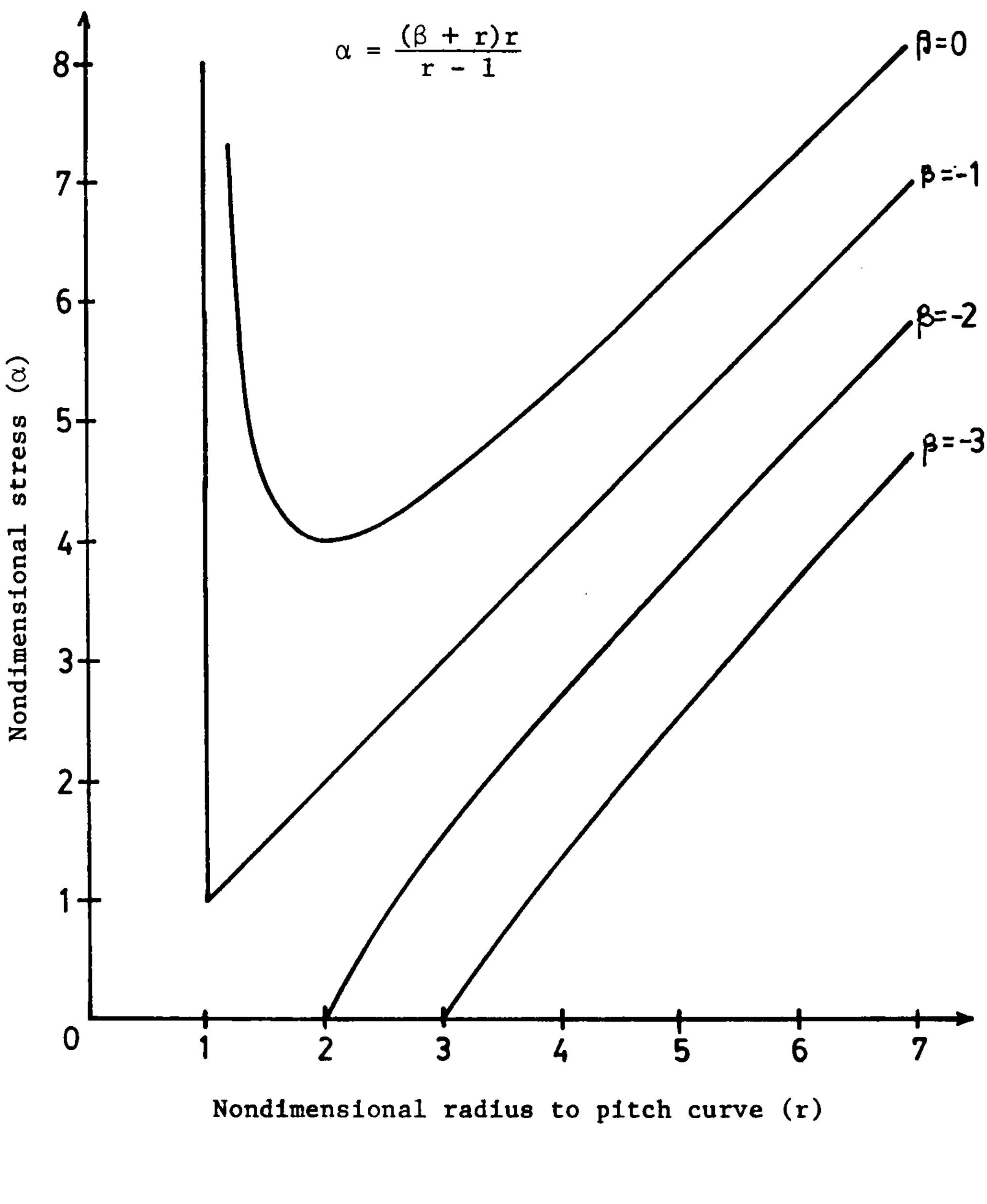

Figure 2.5. Contact stress for a cam in dwelling conditions. Velocity and acceleration of the follower are equal to zero.

The other root, being less than one, is discarded as a singular solution since $r \geqq 1$.

For $\Delta < 0$ the mathematical solution yields two complex conjugate roots, which indicates that no singular solution exists, that is no dwelling condition is possible. Now, the dwelling condition is a must for most of the applications in cam design.

Equation (2.27) can be written in the standard form of a nonlinear second order equation as follows:

$$r'' + \frac{\alpha r\{[r^2 + (r')^2]^{3/2} - r^2 - 2(r')^2\} - (\beta + r)[r^2 + (r')^2]^2}{\alpha r^2 - \gamma[r^2 + (r')^2]^2} = 0 \tag{2.35}$$

Equation (2.35) can be replaced by a system of two first order nonlinear differential equations, which yields

$$r' = v,$$

so that,

$$v' = \frac{(\beta + r)[r^2 + v^2]^2 - \alpha r\{[r^2 + v^2]^{3/2} - r^2 - 2v^2\}}{\alpha r^2 - \gamma\ (r^2 + v^2)^2} .$$

On dividing the second equation by the first, it follows that

$$\frac{dv}{dr} = \frac{(\beta + r)[r^2 + v^2]^2 - \alpha r\{[r^2 + v^2]^{3/2} - r^2 - 2v^2\}}{v[\alpha r^2 - \gamma(r^2 + v^2)^2]} . \tag{2.36}$$

Let us study the singularities of Eq. (2.36), which can be written in a general form as follows:

$$\frac{dv}{dr} = \frac{P(r,v)}{Q(r,v)} \tag{2.37}$$

where at the singularity,

$$P(r,v)\Big|_{\substack{r = r_0 \\ v = 0}} \equiv Q(r,v)\Big|_{\substack{r = r_0 \\ v = 0}} \equiv 0 \ . \tag{2.38}$$

In the present case,

$$P(r,v) = \frac{(\beta + r)[r^2 + v^2]^2 - \alpha r\{[r^2 + v^2]^{3/2} - r^2 - 2v^2\}}{\alpha r^2 - \gamma(r^2 + v^2)^2} \ , \tag{2.39}$$

and

$$Q(r,v) = v \ . \tag{2.40}$$

Let us make a linear expansion around the singular point $r = r_0$, $v = 0$ of $P(r,v)$. One obtains

$$P(r,v) = P(r_0,v_0) + \frac{\partial P(r,v)}{\partial r}\Big|_{\substack{r = r_0 \\ v = 0}}(r - r_0) + \frac{\partial P(r,v)}{\partial v}\Big|_{\substack{r = r_0 \\ v = 0}} v \tag{2.41}$$

From identity (2.38) it follows that

$$P(r_0,v_0) = 0 \ .$$

$P(r,v)$ can be written as a fraction

$$P(r,v) = \frac{A(r,v)}{B(r,v)} \quad ,$$

where:

$$A(r,v) = (\beta + r)[r^2 + v^2]^2 - \alpha r\{[r^2 + v^2]^{3/2} - r^2 - 2v^2\} \tag{2.42}$$

$$B(r,v) = \alpha r^2 - \gamma(r^2 + v^2) \quad , \tag{2.43}$$

provided that $B(r_0, v_0) \neq 0$.

$$P(r_0,v_0) = 0 \text{ , implies } A(r_0,v_0) = 0 \tag{2.44}$$

Let us now evaluate the partial derivatives of $P(r,v)$. One obtains,

$$\left.\frac{\partial P}{\partial r}\right|_{\substack{r = r_0 \\ v = 0}} = \left.\frac{B\frac{\partial A}{\partial r} - A\frac{\partial B}{\partial r}}{B^2}\right|_{\substack{r = r_0 \\ v = 0}} \quad .$$

Using the identity (2.44), this expression simplifies to

$$\left.\frac{\partial P}{\partial r}\right|_{\substack{r = r_0 \\ v = 0}} = \left.\frac{\frac{\partial A}{\partial r}}{B}\right|_{\substack{r = r_0 \\ v = 0}} \quad . \tag{2.45}$$

Let us evaluate $\partial A/\partial r$ which is needed in Eq. (2.45). Thus,

$$\frac{\partial A}{\partial r} = (r^2 + v^2)^2 + 4r(\beta + r)(r^2 + v^2)$$

$$- \alpha[(r^2 + v^2)^{3/2} + 3r^2(r^2 + v^2)^{1/2} - 3r^2 - 2v^2] \quad .$$

On evaluating at the singularity,

$$\left.\frac{\partial A}{\partial r}\right|_{\substack{r = r_0 \\ v = 0}} = r_0^{\,2}[r_0^{\,2} + 4r_0(\beta + r_0) - \alpha(4r_0 - 3)] \ .$$

After algebraic rearrangement, one obtains

$$\left.\frac{\partial A}{\partial r}\right|_{\substack{r = r_0 \\ v = 0}} = r_0^{\,2}[5r_0^{\,2} - 4(\alpha - \beta)r_0 + 3\alpha] \ . \tag{2.46}$$

In order to simplify Eq. (2.46), let us recall Eq. (2.32)

$$\alpha = \frac{(\beta + r)r}{r - 1} \quad ,$$

which can be written as a second degree identity at the singularity (i.e., dwelling condition) as follows:

$$r_0^{\,2} - (\alpha - \beta)r_0 + \alpha = 0 \ . \tag{2.47}$$

Using identity (2.47) in Eq. (2.46), simplifies to:

$$\left.\frac{\partial A}{\partial r}\right|_{\substack{r = r_0 \\ v = 0}} = r_0^{\,3}[2r_0 - (\alpha - \beta)] \ . \tag{2.48}$$

Now the singular points are functions of α and β, to show that let us recall Eq. (2.34)

$$r_{1,2} = \frac{(\alpha - \beta) \pm\sqrt{\Delta}}{2} \quad ,$$

from Eq. (2.34) follows that

$$2r_0 = (\alpha - \beta) \pm\sqrt{\Delta} \quad .$$

On substituting $2r_0$ into Eq. (2.48) yields

$$\left.\frac{\partial A}{\partial r}\right|_{\substack{r = r_0 \\ v = 0}} = \pm r_0^3 \sqrt{\Delta} \quad . \tag{2.49}$$

Let us evaluate B at the singularity, which is needed in Eq. (2.45). On doing this,

$$B\bigg|_{\substack{r = r_0 \\ v = 0}} = r_0{}^2(\alpha - \gamma r_0{}^2) \quad . \tag{2.50}$$

On substituting expressions (2.49) and (2.50) into Eq. (2.45) it follows that

$$\left.\frac{\partial P}{\partial r}\right|_{\substack{r = r_0 \\ v = 0}} = \pm\frac{r_0\sqrt{\Delta}}{\alpha - \gamma r_0{}^2} \quad . \tag{2.51}$$

Similarly,

$$\left.\frac{\partial P}{\partial v}\right|_{\substack{r = r_0 \\ v = 0}} ,$$

has to be evaluated. After some algebraic manipulation it leads to the result,

$$\left.\frac{\partial P}{\partial v}\right|_{\substack{r = r_0 \\ v = 0}} = 0 \ . \tag{2.52}$$

Finally on substituting Eq. (2.38), (2.51) and (2.52) into Eq. (2.41), one obtains

$$P(r,v) = \pm\frac{r_0\sqrt{\Delta}}{\alpha - \gamma r_0^{\,2}}\,(r - r_0) \quad . \tag{2.53}$$

On substituting Eqs. (2.40) and (2.53) into Eq. (2.37), one finds that

$$\frac{dv}{dr} = \pm\mu^2\,\frac{r - r_0}{v} \quad , \tag{2.54}$$

where

$$\mu = \left[\frac{r_0\sqrt{\Delta}}{\alpha - \gamma r_0^{\,2}}\right]^{\frac{1}{2}} ,$$

$$\Delta = (\alpha - \beta)^2 - 4\alpha \ ,$$

and

$$\alpha - \gamma r_0^{\,2} \neq 0 \ .$$

The positive sign denotes the upper root of Eq. (2.34) and the negative sign the lower root.

Integrating Eq. (2.54) leads to

$$v^2 \pm \mu^2 (r_0 - r)^2 = C \qquad (2.55)$$

where C is a constant of integration depending on the initial conditions.

It is seen that for the positive sign

$$v^2 + \mu^2 (r_0 - r)^2 = C_1$$

which is an ellipse and represents an oscillatory movement of frequency $\omega_0 = \mu$, while for the negative sign

$$v^2 - \mu^2 (r - r_0)^2 = C_2$$

which is a hyperbola and yields to nonoscillatory motion.

In the nonlinear analysis of differential equations [34] the elliptic trajectories are recognized as centers which leads to stability in the phase plane, and the hyperbolic trajectories are defined as saddles or unstable singular points (see Fig. 2.6).

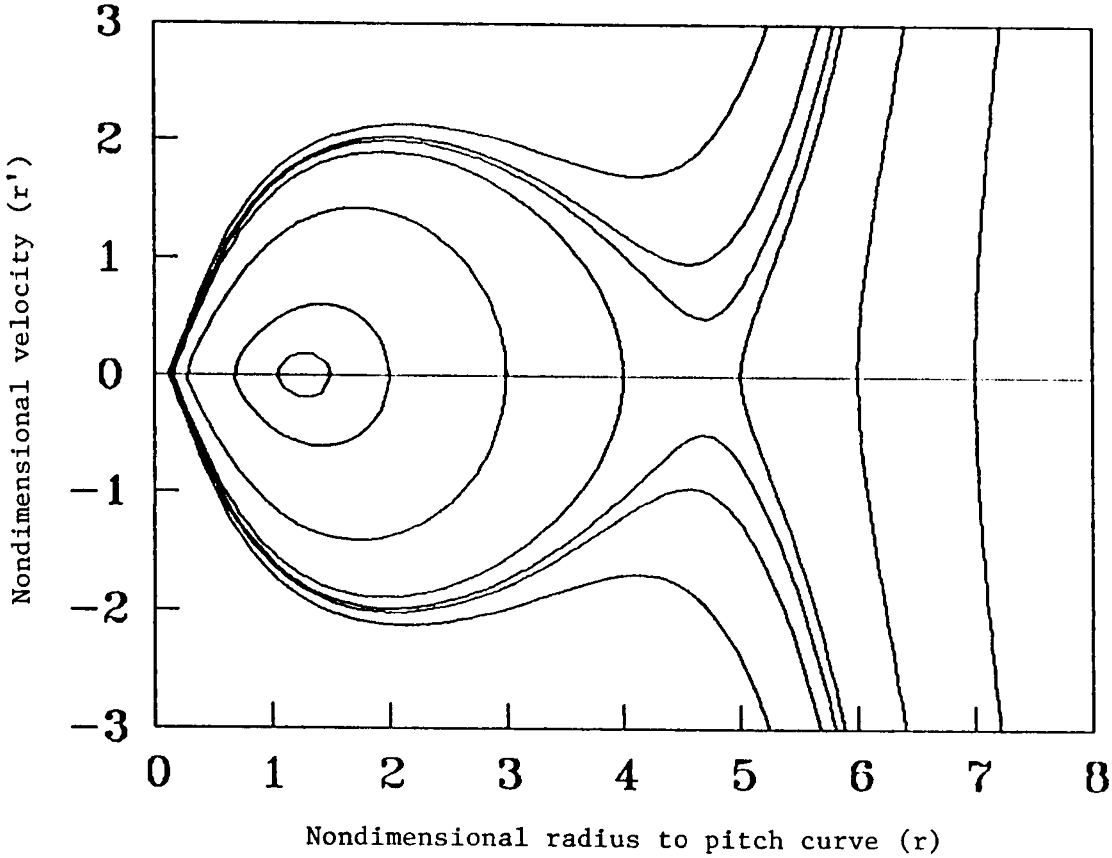

Figure 2.6. Phase plane shows singular points. $\alpha = 6$, $\beta = 0$, $\gamma = 0$; (1.27, 0) a center point, (4.73, 0) a saddle point.

On continuing with the analysis it is seen, therefore, that the stability of the singular point depends on the sign of $\pm\sqrt{\Delta}$ and the value of $\alpha - \gamma r_0^2$, for $r_0 > 1$. If both signs are equal, there is stability, and if the signs are different then there is instability. Figure 2.7 shows the case for $\alpha - \gamma r_1^2 < 0$. A complete list of possibilities is shown in Table 2.1.

It is interesting to notice that the study of the simplified model yielded the same conclusion, but the check using the exact equation is important since some simplifications can lead to erroneous conclusions.

Let us now summarize the results of this analysis. A model was defined for maximum stress constraint and was put into nondimensional form. This yielded a nonlinear differential equation for which the singular solutions were found (i.e., the equilibrium conditions or cam dwelling). In addition, the type of singular point was studied to define the stability of the system. A graph (Fig. 2.5, p. 26) was presented which gives the relation between nondimensional stress α, nondimensional prestress β and the nondimensional r (radius to the pitch curve in dwelling condition). Also, the cam in its extreme dwelling positions can be seen in Fig. 2.8.

Ordinary Solution of the O.D.E. for Stress Constraint

Having analyzed the singular solutions, the next logical step is to try to find ordinary solutions for the complete family of trajectories in the phase plane. These trajectories are unique and must agree with

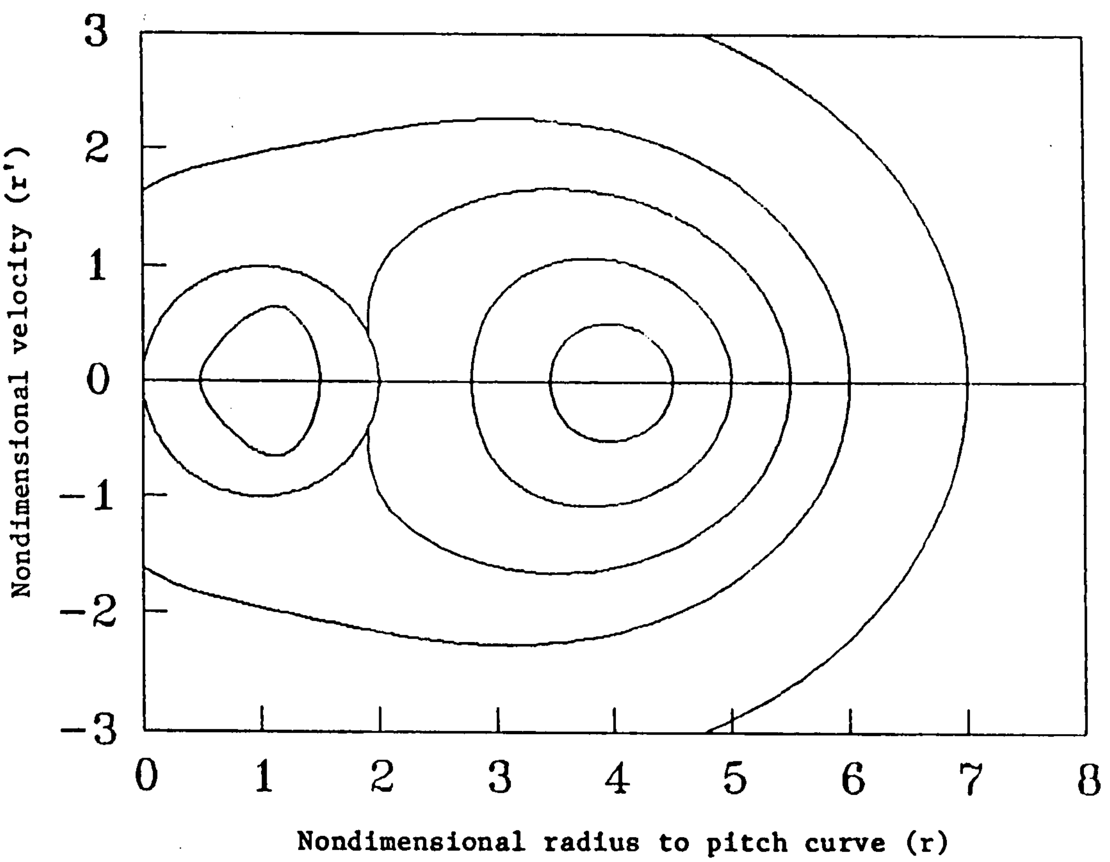

Figure 2.7. Phase plane shows two centers. $\alpha = 4$, $\beta = -1$, $\gamma = 1$; (1,0) and (4,0) centers.

Table 2.1. Types of Singular Points.

	r_2	r_1
$\alpha - \gamma r_1^{\;2} > 0$	center	saddle
$\alpha - \gamma R_2^{\;2} > 0 > \alpha - \gamma r_1^{\;2}$	center	center
$\alpha - \gamma r_2^{\;2} < 0$	saddle	center

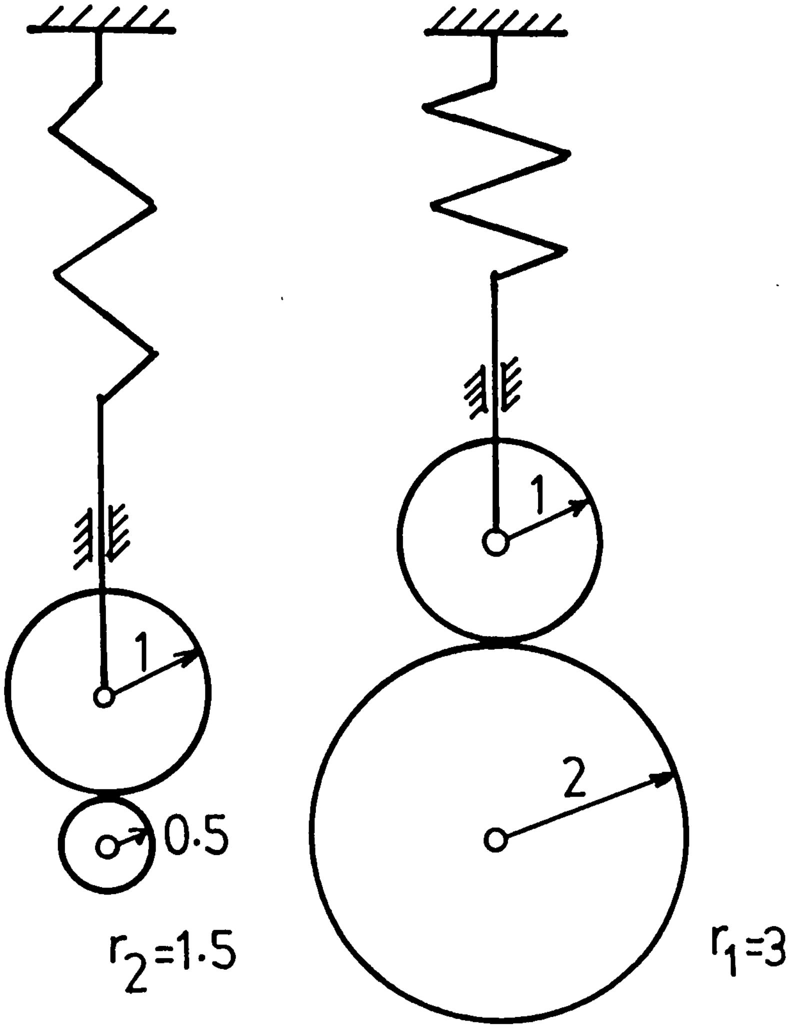

Figure 2.8. Cam dwelling in its extreme positions. $\beta = 0$, $s = \alpha_{max} = 4.5$.

the stress constraint and they must be checked to see that the geometric differential inequality is satisfied to avoid undercutting.

Recall Eq. (2.36)

$$\frac{dv}{dr} = \frac{(\beta + r)[r^2 + v^2]^2 - \alpha r\{[r^2 + v^2]^{3/2} - r^2 - 2v^2\}}{v[\alpha r^2 - \gamma(r^2 + v^2)^2]} .$$

On making the change of variable

$$z^2 = r^2 + v^2 ,$$

Equation (2.36) transforms as follows:

$$\frac{dz}{dr} = \frac{z[(1 - \gamma)rz^2 + \beta z^2 - \alpha r(z - 2)]}{\alpha r^2 - \gamma z^4} . \tag{2.56}$$

Equation (2.56) has a singularity when the denominator of the right-hand side is zero, this leads to a circle in the phase plane (r,v)

$$z^2 = \frac{\alpha}{\gamma} r$$

or

$$r^2 + v^2 = \delta r , \tag{2.57}$$

where

$$\delta = \sqrt{\frac{\alpha}{\gamma}} .$$

Equation (2.57) is a circle of radius $a = \delta/2$, with center at $(r,v) = (\delta/2,\ 0)$ (see Fig. 2.9). Equation (2.56) is a first order nonlinear differential equation.

Special Solution for Low Angular Velocity

On assigning the value zero to the parameter γ which is the limit case of low angular velocity Eq. (2.56) becomes the Abel equation reference [21]

$$\frac{dz}{dr} = \left(\frac{r + \beta}{\alpha r^2}\right) z^3 - \frac{1}{r} z^2 + \frac{2}{r} z \ . \tag{2.57}$$

Equation (2.57) has two parameters α and β but on making a change of variable it can be reduced to one parameter. Let us define a new independent variable

$$t = \frac{\beta}{\alpha r} \ , \quad \beta \neq 0 \ . \tag{2.58}$$

On substituting the new variable, one obtains

$$\frac{dz}{dt} = -\frac{1}{t}\left(\frac{1}{\alpha} + t\right) z^3 + \frac{1}{t} z^2 - \frac{2}{t} z \ . \tag{2.59}$$

Equation (2.59) can be solved numerically using the Runge-Kutta fourth order algorithm. A closed form solution appears too difficult to be found. Having found the family of solutions in t,z as $t = t(z)$, then r can be generated as a function of β and t. Solving for r from Eq. (2.58), yields

$$r = \frac{\beta}{\alpha t} \tag{2.60}$$

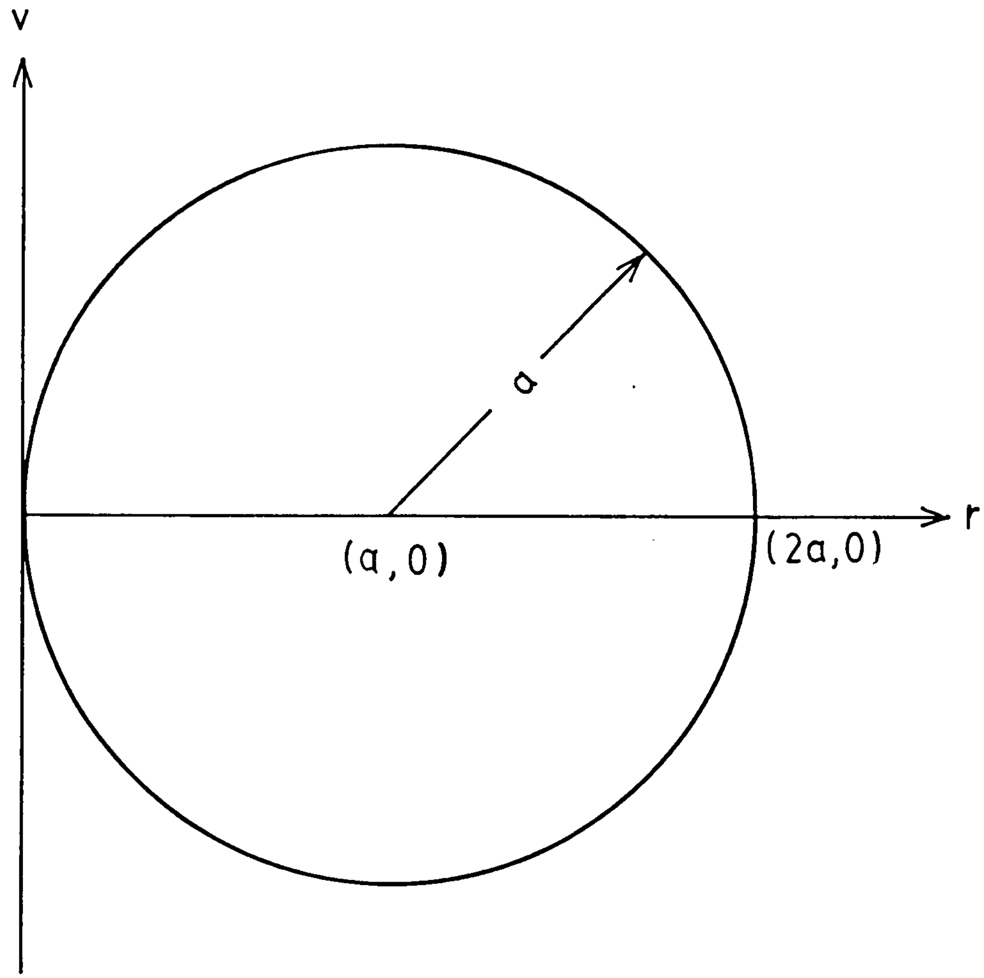

Figure 2.9. Circle of singularity in the phase plane. a = $\delta/2$.

or

$$r = r\ (\beta, z).$$

For the case $\beta = 0$, Eq. (2.57) directly reduces to the form,

$$\frac{dz}{dr} = \frac{1}{\alpha r} z \quad - \frac{1}{r} z^2 + \frac{2}{r} z \ . \tag{2.61}$$

Equation (2.61) may be solved by the method of separation of variables as in [38]. This family of solutions for $\gamma = 0$ has no interference with the circle of singularity since this circle has an infinite diameter and therefore, the solution may fill the phase plane r,v.

Equation (2.61) has a singular solution when the second degree polynominal in z has real roots. One can see this when Eq. (2.61) is written as follows:

$$\frac{dz}{dr} = \frac{z}{\alpha r} (z^2 - \alpha z + 2\alpha) \ .$$

The roots of the second degree polynominal are

$$z_{1,2} = \frac{\alpha \pm \sqrt{\alpha^2 - 8\alpha}}{2} \ ,$$

from which it is seen that real roots exist only for $\alpha \geq 8$ (see Fig. 2.10).

It follows for this case that

$$\frac{dz}{dr} = 0 \ .$$

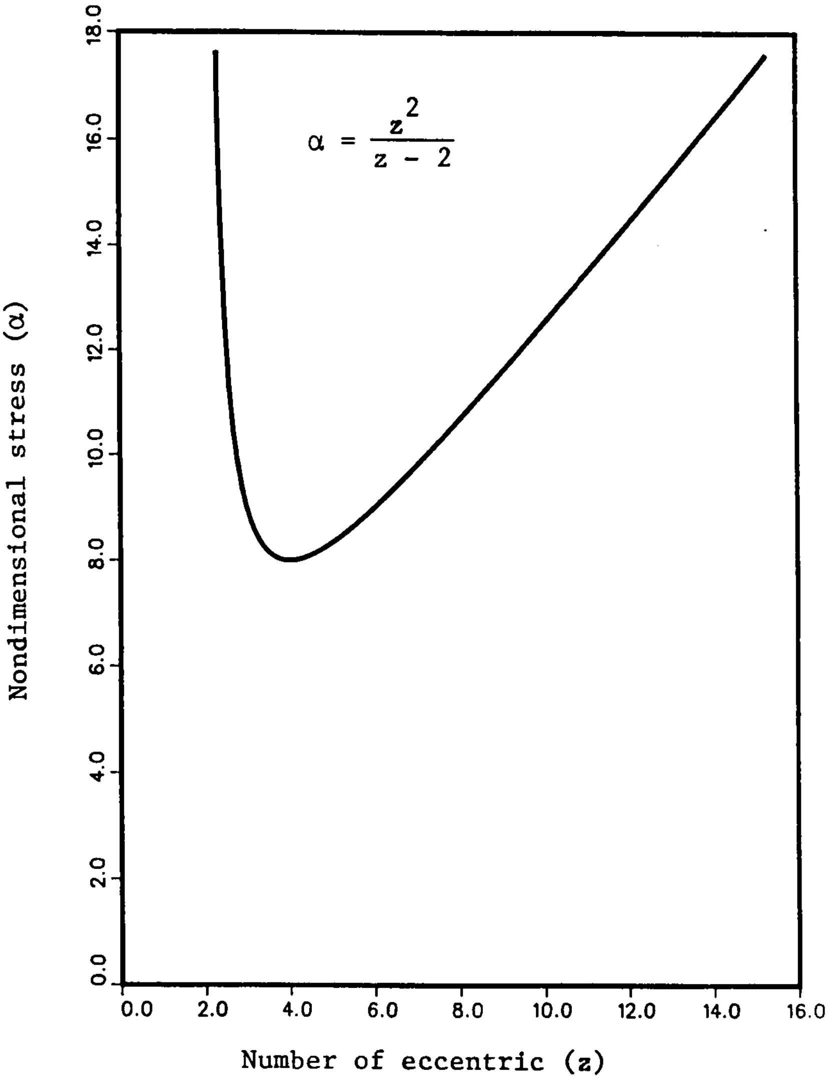

Figure 2.10. Family of eccentrics. $\beta = 0$, $\gamma = 0$.

Then z is a constant. This generates circles in the plane r,v with center at $(0,0)$ and radiis of z_1 and z_2, which are the roots of the second order polynomial. When solving for the cam profile it is found to be an eccentric (see Fig. 2.11).

The eccentric cam satisfy naturally the geometric constraint of no undercutting, because it is a convex profile. There is only one point of conflict. After 90° of rotation the pressure angle reaches 90°, which is not allowed. But in a solution, the eccentric cam profile is used only for generating a negative acceleration in the second part of the rising stroke. The first part of the rising stroke which generates positive acceleration, will be achieved by controlling the acceleration.

Range of the Upper and Lower Dwelling Condition

One must realize that all the trajectories of the ordinary solutions of O.D.E. in the phase plane obtained for the case $\gamma = 0$, $\alpha > 0$, and $\beta \neq 0$ will be not used. First it must be mentioned that the upper dwelling condition is not used at the value of the upper root for the dwelling condition, because this singular point is reached by the separatrices, and this involves an infinite amount of rotation to reach or leave the singular point. Therefore $r_{max} < r_1$.

The low dwelling position can reach the lower root for the case $\beta > -1$ where separation does not occur. But for $\beta \leq -1$, then $r_{min} > -\beta$, which will guarantee contact between cam and roller follower.

From the previous analysis it follows that only part of the ordinary solution is useful and even for those curves one has to check the geometric inequality constraint (2.29) to avoid undercutting.

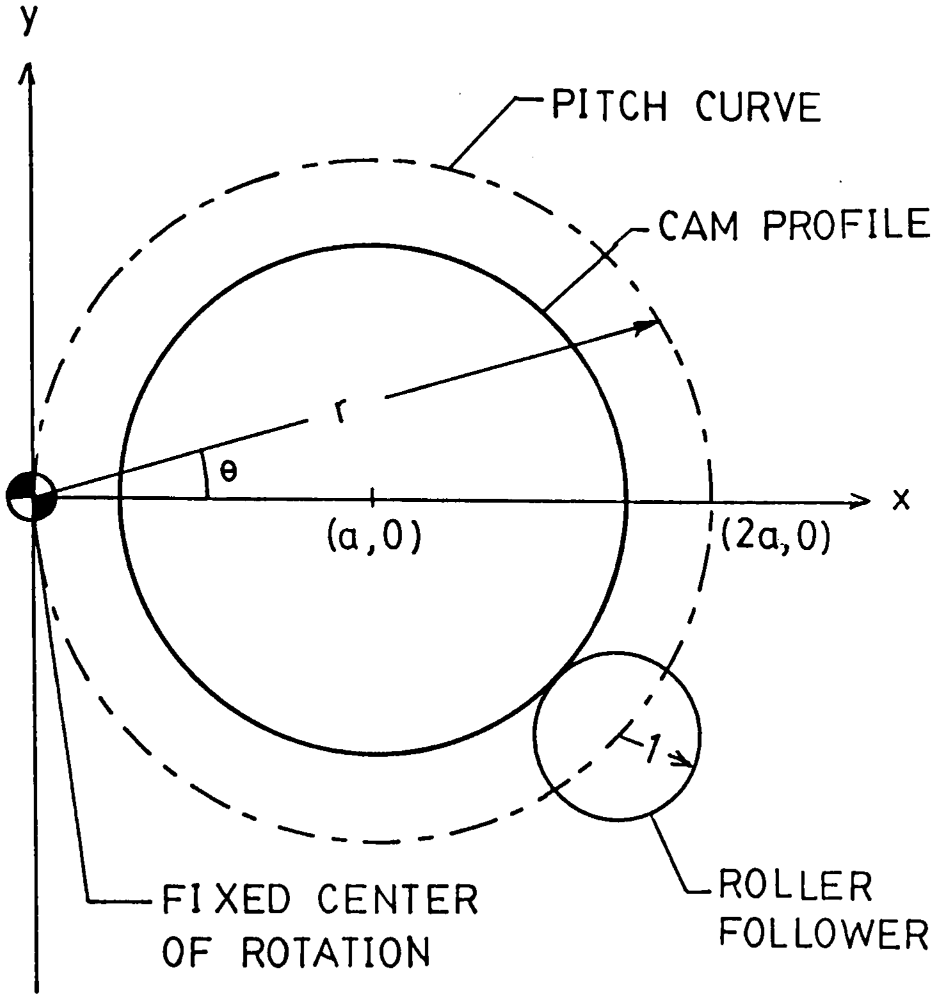

Figure 2.11. An eccentric.

A close form solution may be obtained for the case of the nondimensional parameters $\beta = 0$, $\gamma = 0$, that is the integration of the first order differntial equation (2.61) in the phase plane, which may be solved by the method of separation of variables.

<u>Special Solution for $\beta = \gamma = 0$</u>

The solutions for $\beta = \gamma = 0$, $\alpha > 0$, which were obtained in [38] and will be presented later, will also be checked by the geometrical constraint inequality (2.29). Let us recall Eq. 2.61

$$\frac{dz}{dr} = \frac{1}{\alpha r} z^3 - \frac{1}{r} z^2 + \frac{2}{r} z .$$

On separating variables of Eq. (2.61), we obtain the integral representation

$$\frac{1}{\alpha} \int \frac{dr}{r} = \int \frac{dz}{z(z^2 - \alpha z + 2\alpha)}$$

For the integration, we define

$$Z \equiv z^2 - \alpha z + 2\alpha$$

$$q \equiv \alpha(8 - \alpha)$$

The integration leads to three different solutions. From the reference [38] we show the general solution.

Initial condition: $r = r_0$, $z = r_0$.

<u>Case 1</u>. $q = 0$, (i.e., $\alpha = 8$)

$$r = \sqrt{\frac{(4 - r_0)r_0 z}{4 - z}} \; \exp \frac{2(z - r_0)}{(4 - z)(4 - r_0)} \tag{2.62}$$

Case 2. $q = \alpha(8 - \alpha) > 0$, (i.e., $\alpha < 8$)

$$r = \sqrt{r_0 z} \sqrt[4]{\frac{Z_0}{Z}} \; \frac{\mathrm{EXP}\left(\frac{\alpha}{2\sqrt{q}} \arctan \frac{2z - \alpha}{\sqrt{q}}\right)}{\mathrm{EXP}\left(\frac{\alpha}{2\sqrt{q}} \arctan \frac{2r_0 - \alpha}{\sqrt{q}}\right)} \tag{2.63}$$

Case 3: $q = \alpha(8 - \alpha) < 0$, (i.e., $\alpha > 0$

$$r = \sqrt{r_0 z} \sqrt[4]{\frac{Z_0}{Z}} \left[\frac{(2z - \alpha - \sqrt{-q})(2r_0 - \alpha + \sqrt{-q})}{(2z - \alpha + \sqrt{-q})(2r_0 - \alpha - \sqrt{-q})}\right]^{\frac{\alpha}{4\sqrt{-q}}} \tag{2.64}$$

The solutions for three different values of the nondimensional stress $\alpha = 6$, $\alpha = 8$, and $\alpha = 9$ are presented in Figs. 2.12, 2.13, 2.14. In the case of $\alpha = 6$ there is no eccentric, while for $\alpha = 8$ there is one eccentric at $z = 4$, and for $\alpha = 9$ there are two eccentrics for $z = 3$ and $z = 6$, respectively. These eccentrics satisfy naturally the geometric constraint because they result in convex cam profiles.

Now we will check the geometrical constraint given by the inequality (2.29) against the solutions mentioned by Eqs. (2.62) through (2.64).

Recall Eq. (2.35)

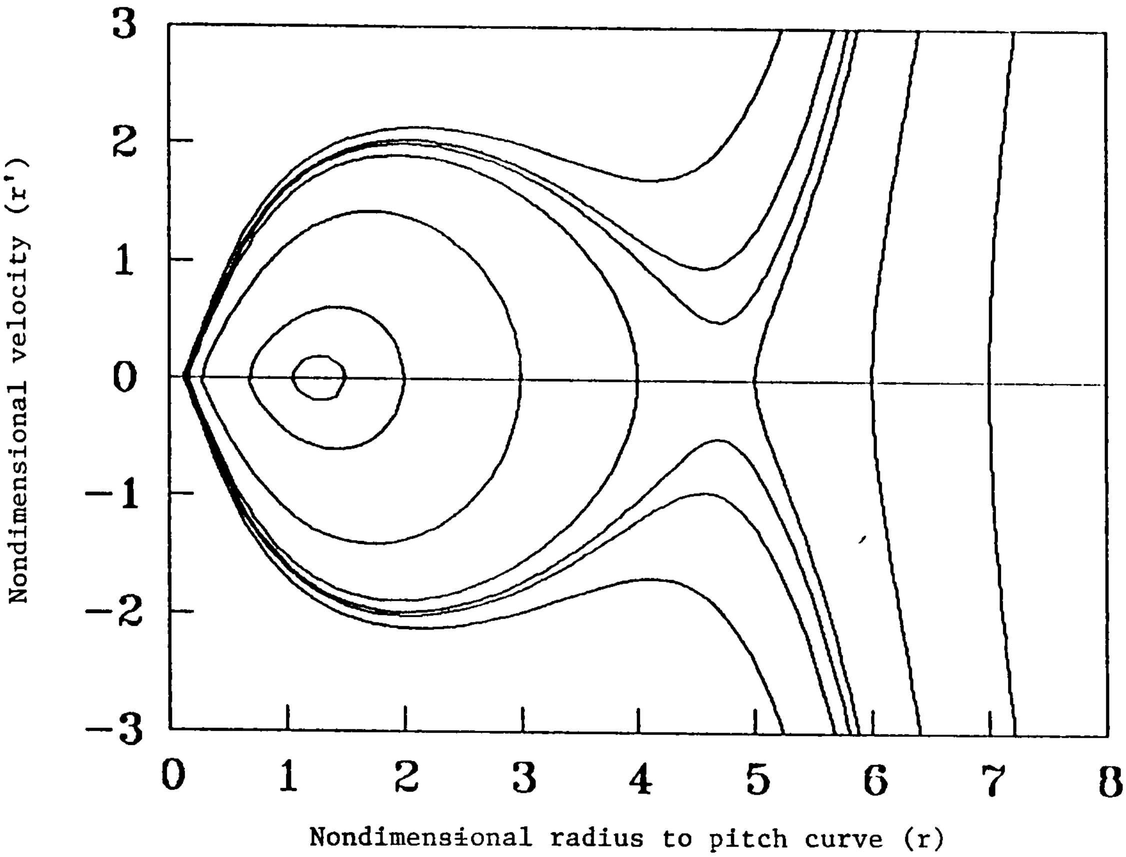

Figure 2.12. No eccentric in the phase plane. $\alpha = 6$, $\beta = 0$, $\gamma = 0$; $r_1 = 4.73$, $r_2 = 1.27$.

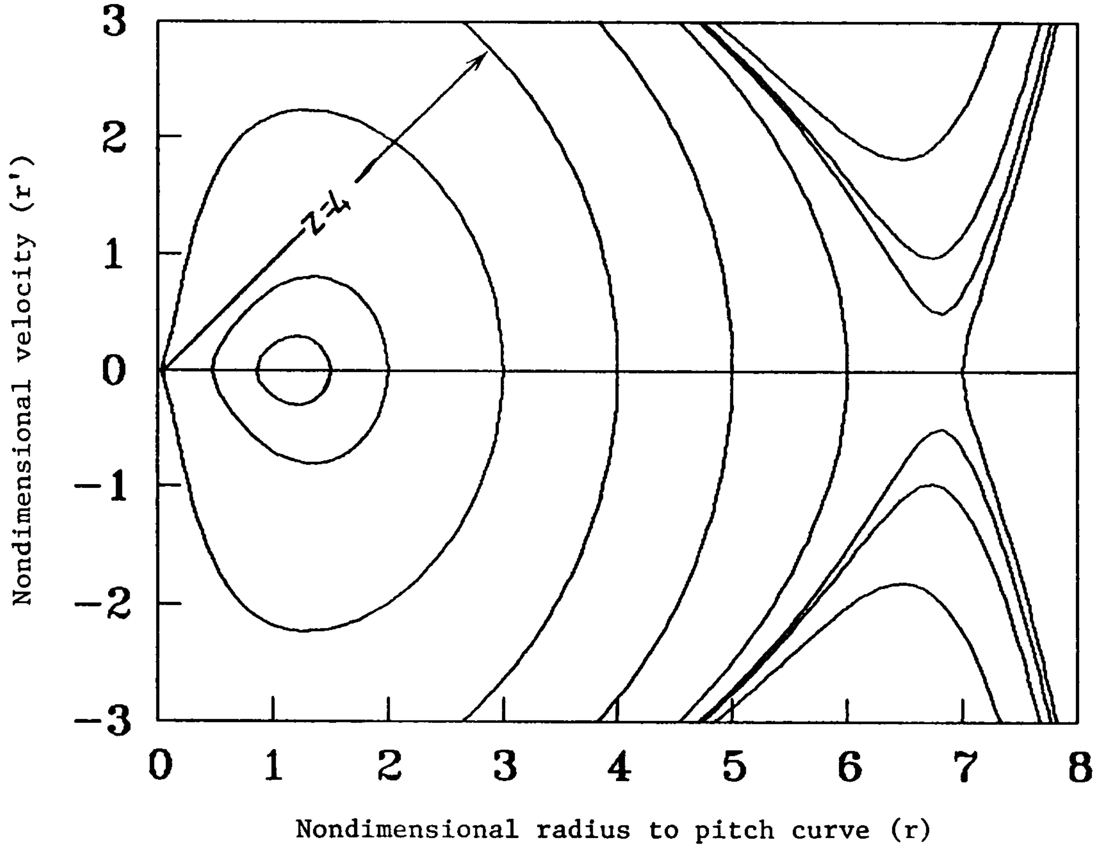

Figure 2.13. One eccentric in the phase plane. $z_1 = z_2 = 4$; $\alpha = 8$, $\beta = 0$, $\gamma = 0$; $r_1 = 6.83$, $r_2 = 1.17$.

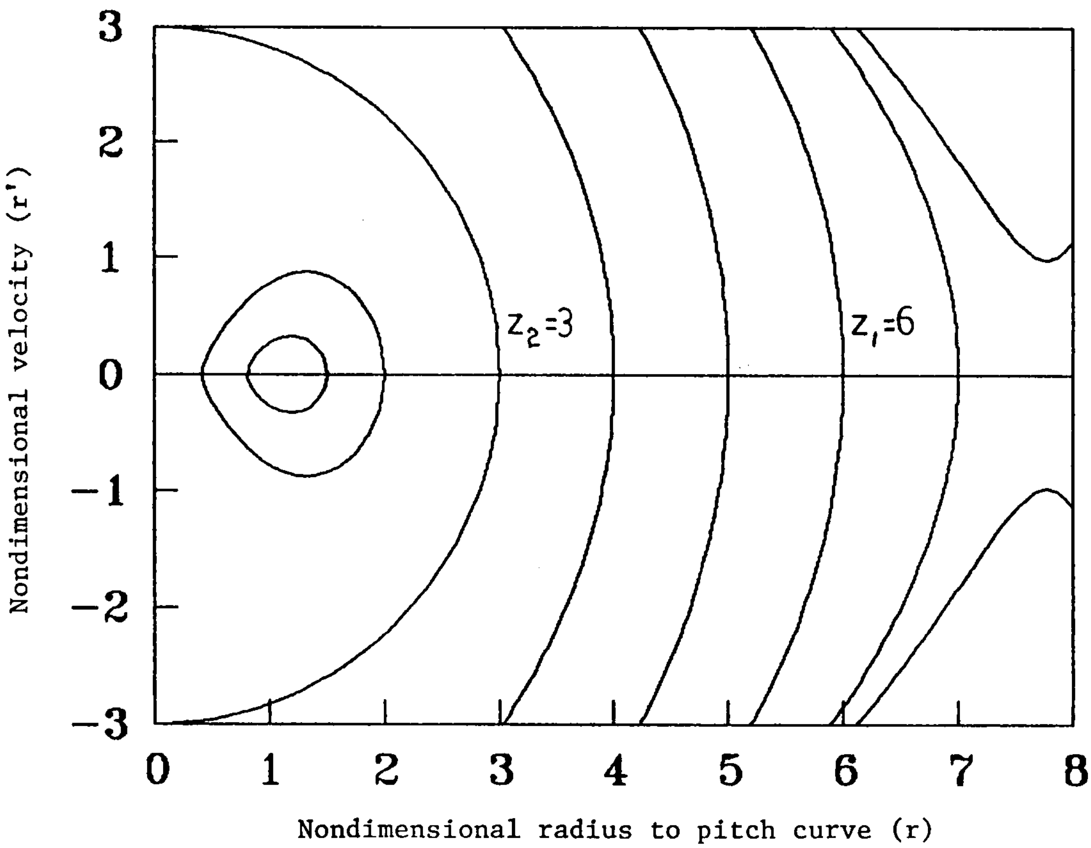

Figure 2.14. Two eccentrics in the phase plane. $z_1 = 6$, $z_2 = 3$; $\alpha = 9$, $\beta = 0$, $\gamma = 0$; $r_1 = 6.83$, $r_2 = 1.17$.

$$r'' + \frac{\alpha r\{[r^2 + (r')^2]^{3/2} - r^2 - 2(r')^2\} - (\beta + r)[r^2 + (r')^2]^2}{\alpha r^2 - \gamma[r^2 + (r')^2]^2} = 0 \ .$$

Solving for r'' for $\alpha > 0$, $\beta = \gamma = 0$, one obtains

$$r'' = \frac{[r^2 + (r')^2]^2 - \alpha\{[r^2 + (r')^2]^{3/2} - r^2 - 2(r')^2\}}{\alpha r} \ . \quad (2.65)$$

Recall inequality (2.29)

$$[r^2 + (r')^2]^{3/2} - r^2 - 2(r')^2 + rr'' > 0 \ .$$

Equation 2.65 comes from the maximal stress constraint. If we substitute the acceleration given by Eq. (2.65) into Eq. (2.29) we will find the region of the phase plane for which the solution holds. On making the substitution, it follows that

$$\frac{1}{\alpha}[r^2 + (r')^2]^2 > 0 \quad (2.66)$$

Equation 2.66 shows that the solutions obtained in the closed form solution by integrating the equation of maximal stress constraint for $\beta = \gamma = 0$ holds for the entire half phase plane (i.e., $r \geq 0$) with the exception of the origin $r = r' = 0$.

If the initial condition is given outside the envelope of the separatrices, the trajectory on the phase plane will yield an unstable trajectory. That is, the velocity will decrease, but will not reach zero. Instead it will reach a minimum positive value from which it will begin to increase. The lift will pass the maximal dwelling position and the cam will soon lock (see Figs. 2.15, 2.16).

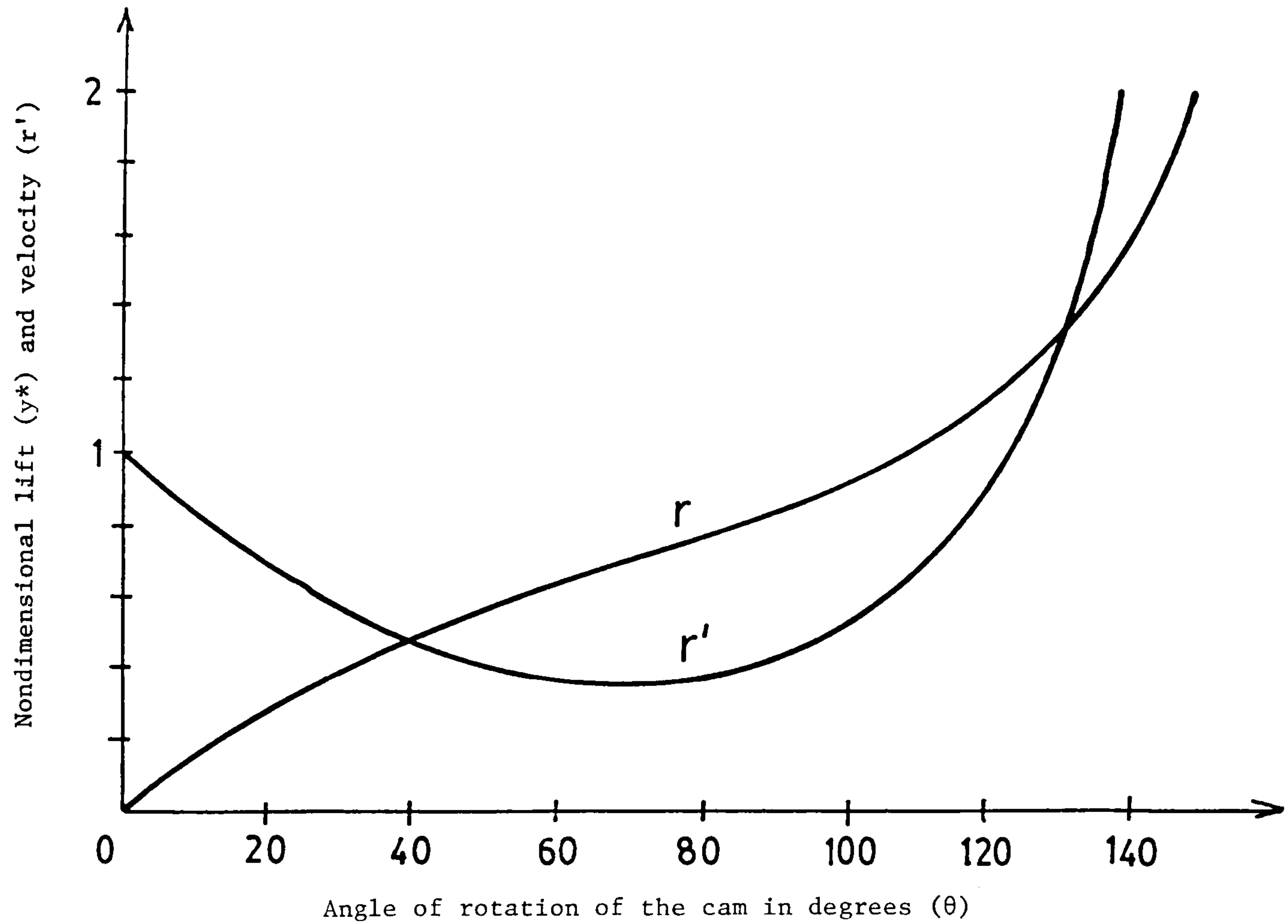

Figure 2.15. Cam working in unstable region.

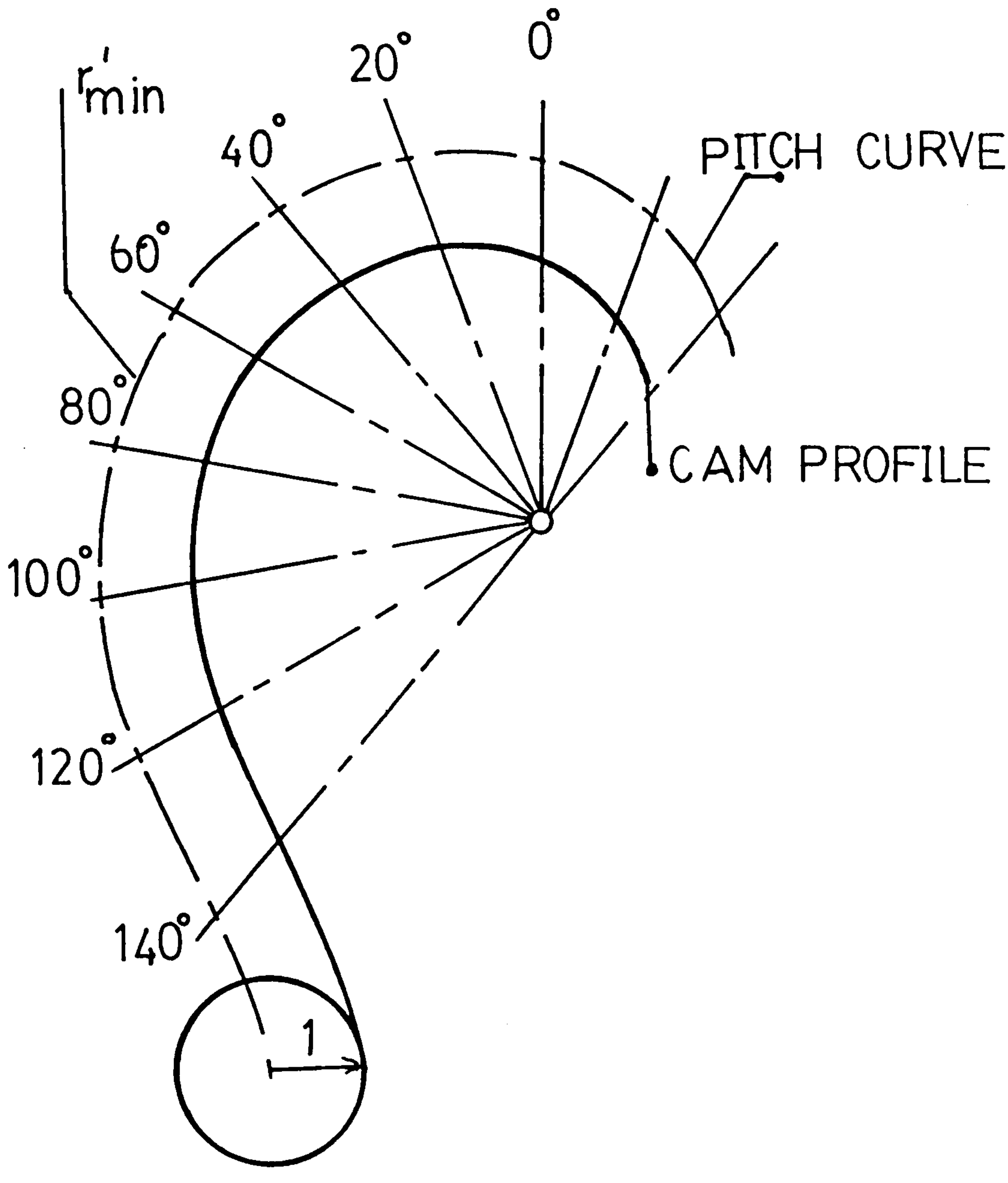

Figure 2.16. Profile of the cam working in the unstable region.

Special Solution for Prestress $\beta = 0$

The ordinary solution for $\beta = 0$, $\alpha > 0$ and $\gamma > 0$ can be studied in closed form because the differential equation can be reduced to a linear one.

Let us recall Eq. (2.56)

$$\frac{dz}{dr} = \frac{z[(1 - \gamma)rz^2 + \beta z^2 - \alpha r(z - 2)]}{\alpha r^2 - \gamma z^4} .$$

For the case under study in which β is equal to zero Eq. (2.56) reduces further to the form

$$\frac{dz}{dr} = \frac{rz[(1 - \gamma)z^2 - \alpha(z - 2)]}{\alpha r^2 - \gamma z^4} . \qquad (2.67)$$

Now, let us introduce the change of the independent variable

$$p \equiv r^2 , \qquad (2.68)$$

so that

$$dp \equiv 2rdr .$$

On substituting the change of variable from Eq. (2.68) into Eq. (2.67), it follws that,

$$\frac{dz}{dp} = \frac{z}{2} \frac{[(1 - \gamma)z^2 - \alpha(z - 2)]}{\alpha p - \gamma z^4} . \qquad (2.69)$$

On interchanging the roles of the dependent and independent variables, one obtains

$$\frac{dp}{dz} = \frac{2}{z} \frac{\alpha p - \gamma z^4}{[(1 - \gamma)z^2 - \alpha(z - 2)]} , \qquad (2.70)$$

which is a linear equation in p. This equation can always be solved by the method of quadratures.

Now we study the solution of the linear equation (2.70) for differents values of the parameters α (nondimensional stress) and γ (angular velocity ratio).

<u>Case 1</u>. $\gamma = 1$.

Equation (2.70) simplifies further to the following form

$$\frac{dp}{dz} = -\frac{2}{z} \frac{\alpha p - z^4}{\alpha(z - 2)} .$$

In standard form, this becomes

$$\frac{dp}{dz} + \frac{2p}{z(z - 2)} = \frac{2z^3}{\alpha(z - 2)} . \qquad (2.71)$$

The integrating factor $\phi(z)$ of Eq. (2.71) is:

$$\phi(z) = \mathrm{EXP}\left(\int \frac{2dz}{z(z - 2)}\right) ,$$

on integrating, one obtains

$$\phi(z) = \frac{z - 2}{z} .$$

On multiplying Eq. (2.71) by the integrating factor $\phi(z)$, it follows that,

$$\frac{(z - 2)}{z} \frac{dp}{dz} + \frac{2p}{z^2} = \frac{2z^2}{\alpha}$$

or

$$\frac{d}{dz} \left[\frac{(z - 2)p}{z}\right] = \frac{2z^2}{\alpha} \quad . \tag{2.72}$$

On integrating Eq. (2.72), one obtains

$$\frac{(z - 2)p}{z} = \frac{2z^3}{3\alpha} + C, \quad C = \text{constant},$$

or solving for p yields

$$p = \frac{z}{z - 2} \left(\frac{2z^3}{3\alpha} + C\right) \quad , \quad z \neq 2 \quad , \tag{2.73}$$

$$\text{and } \gamma = 1 \ .$$

The case z = 2 can be studied separately by substituting $\gamma = 1$ and z = 2 in Eq. (2.67) which yields,

$$\frac{dz}{dr} = 0 \quad ,$$

therefore,

$$z = C \quad , \quad C = \text{constant}$$

that is

$$z = 2 \quad . \tag{2.74}$$

Equation (2.74) represents a circle of radius equal to two with center in the origin of the phase plane.

Equation (2.73) for the initial condition $\theta = 0$, $z = r_0$, $p = r_0^2$ can be expressed in the following form

$$p = \frac{z}{z - 2}\left[\frac{2}{3\alpha}(z^3 - r_0^3) + r_0(r_0 - 2)\right]$$

or

$$r = \left\{\frac{z}{z - 2}\left[\frac{2}{3\alpha}(z^3 - r_0^3) + r_0(r_0 - 2)\right]\right\}^{1/2}, \qquad (2.75)$$

where $\gamma = 1$ and $z \neq 2$ (see Fig. 2.17).

Before continuing with the study of this case we have to check the geometrical inequality constraint (2.29) which represents the possibility of generating a true cam surface without undercutting.

The solution given by Eq. (2.74) $z = 2$ represents an eccentric, but in solving for the cam's profile one obtains a cam which corresponds to a limiting case. The eccentricity of the cam is seen to be equal to unity and the radius of the eccentric cam profile is equal to zero. Therefore this case is not physically realizable. Therefore the solution given by Eq. (2.74) must be discarded (see Fig. 2.18). The same result can be found by using inequality (2.29).

Recall inequality (2.29)

$$[r^2 + (r')^2]^{3/2} - r^2 - 2(r')^2 + rr'' > 0$$

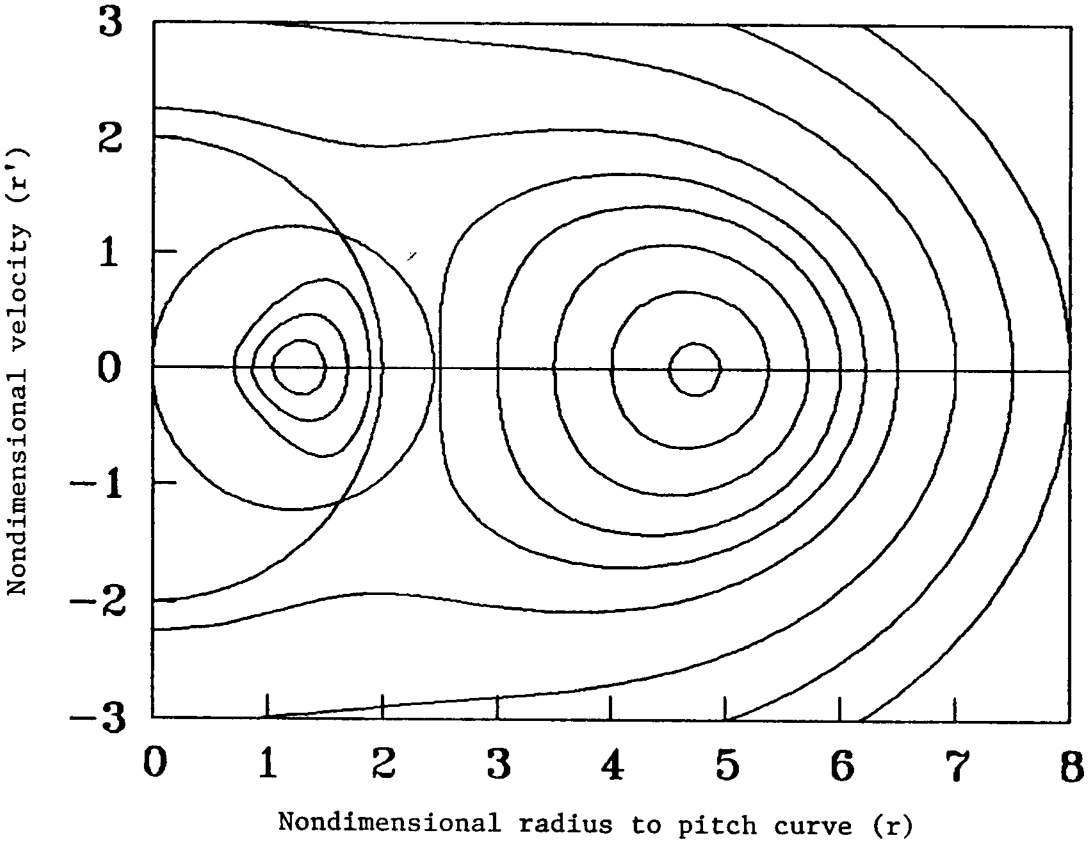

Figure 2.17. Phase plane of a cam working at γ = 1.

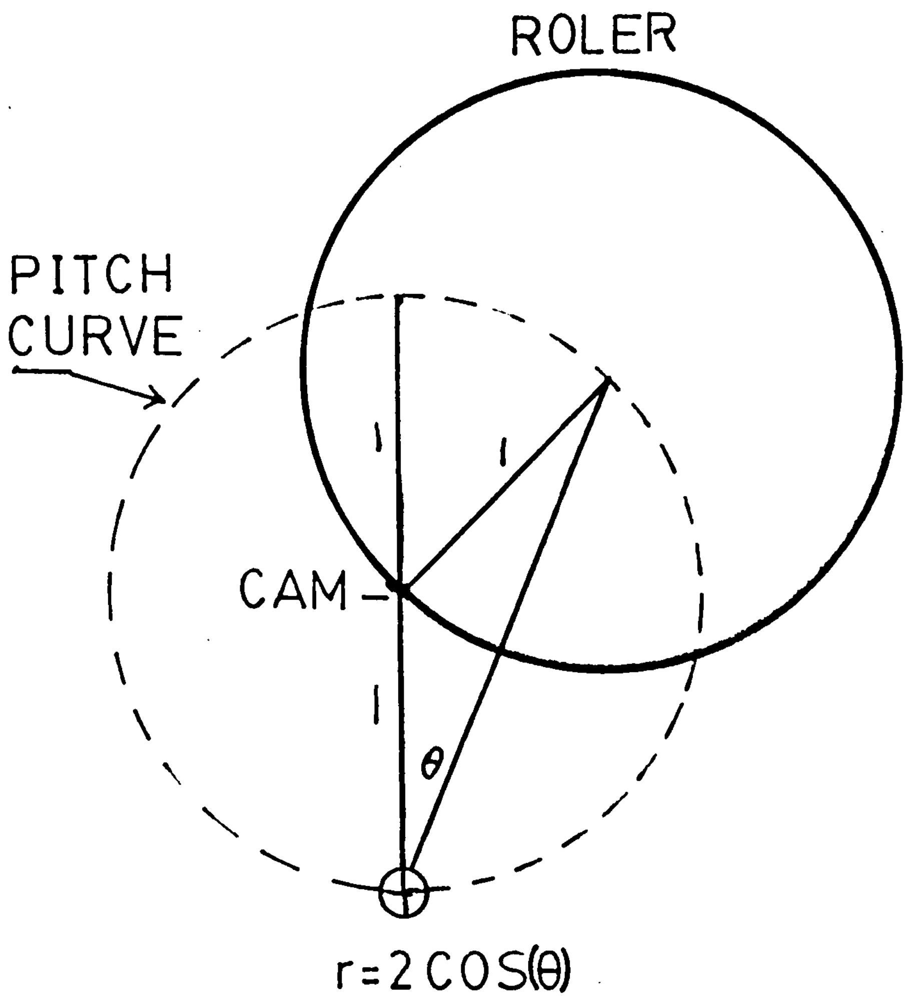

Figure 2.18. Eccentric for z = 2.

or

$$z^2(z - 2) + r^2 + rr'' > 0 \ . \tag{2.76}$$

For the case $z = 2$ the solution for r is as follows

$$r = 2\cos\theta \quad ,$$

where $\gamma = 1$, and $z = 2$, from which

$$r'' = - 2\cos\theta \quad .$$

Substituting these expressions into the inequality (2.76) leads to

$$z^2(z - 2) = 0 \quad , \quad \text{for } z = 2 \quad .$$

Thus, it is seen that the inequality (2.76) which is another form of inequality (2.29), does not hold, and therefore the cam is not physically realizable. This is the same conclusion reached by solving for the eccentric $z = 2$.

Another important conclusion is that $z = 2$ is the solution of the second order differential equation obtained when inequality (2.20) is set to a limit case, that is

$$[r^2 + (r')^2]^{3/2} - r^2 - 2(r')^2 + rr'' = 0 \quad . \tag{2.77}$$

Equation (2.77) has the solution given by

$$r = 2\cos\theta \quad .$$

The next step is to validate the solution given by Eq. (2.75). We proceed similarly as the case $\beta = 0$, $\gamma = 0$. Let us recall Eq. (2.35)

$$r'' + \frac{\alpha r\{[r^2 + (r')^2]^{3/2} - r^2 - 2(r')^2\} - (\beta + r)[r^2 + (r')^2]^2}{\alpha r^2 - \gamma[r^2 + (r')^2]^2} = 0 \ ,$$

On solving for r'' and substituting $\beta = 0$, $\gamma = 1$ one obtains

$$r'' = r \, \frac{[r^2 + (r')^2]^2 - \alpha\{[r^2 + (r')^2]^{3/2} - r^2 - 2(r')^2\}}{\alpha r^2 - [r^2 + (r')^2]^2}$$

or

$$r'' = r \, \frac{z^4 - \alpha[z^2(z - 2) + r^2]}{\alpha r^2 - z^4} \qquad (2.78)$$

Now recall Eq. (2.76), which is another form of Eq. (2.29)

$$z^2(z - 2) + r^2 + r'' > 0 \ .$$

Now on substituting Eq. (2.78), which is the O.D.E. for maximal stress constraint, into inequality (2.76), one obtains

$$z^2(z - 2) + r^2 + r^2 \, \frac{z^4 - \alpha[z^2(z - 2) + r^2]}{\alpha r^2 - z^4} > 0$$

After algebraic rearranging, one finds

$$\frac{z^6(2 - z)}{\alpha r^2 - z^4} > 0 \qquad (2.79)$$

Inequality (2.79) gives the region of the phase plane (r,v) which results in a physically meaningful solution.

The denominator of inequality (2.79) defines the circle of singularity with diameter δ given by

$$\delta = \sqrt{\frac{a}{\gamma}}$$

where, $\delta = \sqrt{\alpha}$ since $\gamma = 1$.

If the point of the phase plane is inside of that circle then

$$\alpha r^2 - z^4 > 0 \quad ,$$

and on being outside the circle, it yields

$$\alpha r^2 - z^4 < 0 \quad .$$

It is possible to find areas of solution that will satisfy the inequality constraint (2.79) for that happens the signs of numerator an denominator of the left hand side of inequality (2.79) have to be equal. That occurs outside the circle of singularity and outside the eccentric given by $z = 2$, on a second possibility occurs in the intersection between the circle of singularity and the circle generated by the eccentric $z = 2$ (see Fig. 2.19).

Case 2 $\gamma \neq 1$.

Before solving Eq. (2.71) we wish to determine the region in the phase plane (r,v) for which a physical solution exists.

Recall the inequality (2.76)

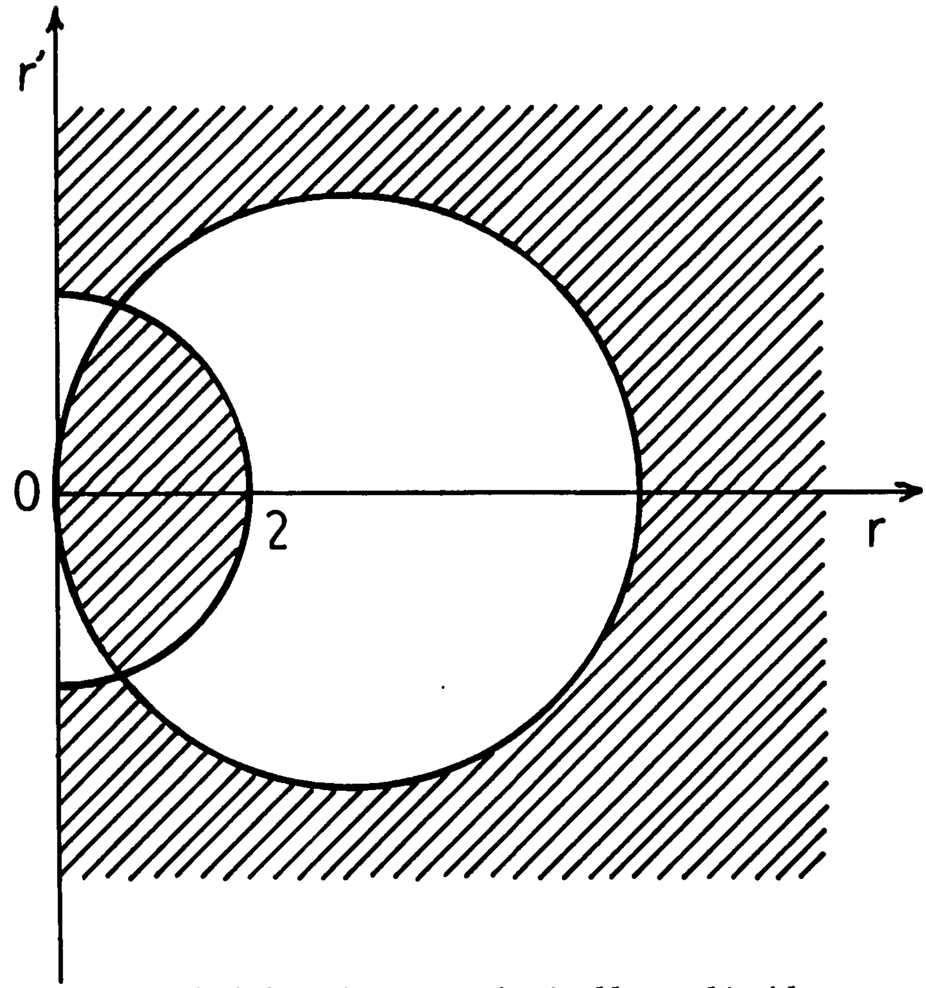

Shaded regions are physically realizable.

Figure 2.19. Regions of solutions in the phase plane for cams working at $\gamma = 1$. $\beta = 0$.

$$z^2(z - 2) + r^2 + rr'' > 0,$$

Recall Eq. (2.35) using the value $\beta = 0$

$$r'' = r\{\frac{z^4 - \alpha[z^2(z - 2) + r^2]}{\alpha r^2 - \gamma z^4}\} . \tag{2.80}$$

On substituting Eq. (2.80) into Eq. (2.76), it leads to

$$z^2(z - 2) + r^2 + r^2 \frac{z^4 - \alpha[z^2(z - 2) + r^2]}{\alpha r^2 - \gamma z^4} > 0 .$$

After algebraic simplification, one finds that

$$z^4 \frac{\gamma z^2(2 - z) + (1 - \gamma)r^2}{\alpha r^2 - \gamma z^4} > 0 . \tag{2.81}$$

In inequality (2.81) z^4 is greater than zero, which implies that the numerator and denominator of the fraction on the left hand side must have equal signs to agree with the geometrical constraints of no under-cutting. Again the denominator represents a circle with center at ($\delta/2$, 0) and radius $\delta/2$ drawn in the phase plane and inside the circle the function $\alpha r^2 - \gamma z^4$ is positive and outside the circle it is negative.

Now let us analyze the numerator

$$\gamma z^2(2 - z) + (1 - \gamma)r^2 .$$

We can obtain the limiting curve by setting the expression equal to zero. On doing so

$$\gamma z^2(2 - z) + (1 - \gamma)r^2 = 0 \ . \tag{2.82}$$

Transforming Eq. (2.82) into polar coordinates under the substitution r = zcosψ, we obtain

$$\gamma z^2(2 - z) + (1 - \gamma)z^2\cos^2\psi = 0 \ ,$$

or

$$z^2[\gamma(2 - z) + (1 - \gamma)\cos^2\psi] = 0 \ .$$

Being $z^2 > 0$, then follows that

$$\gamma(2 - z) + (1 - \gamma)\cos^2\psi = 0 \ .$$

On solving for z, we obtain

$$z = 2 + \frac{1 - \gamma}{2\gamma} + \frac{1 - \gamma}{2\gamma}\cos2\psi \ . \tag{2.83}$$

Because the domain of ψ which is the pressure angle is $\psi \in (-\pi/2, \pi/2)$ the third term correspond to two leaves of a four-leaved rose, being the first two terms a circle.

The intersection of the curve given by Eq. (2.38) and the ordinate of the phase plane can be determined as follows,

$$v = z \sin\psi \ .$$

Thus,

$$v = (2 + \frac{1 - \gamma}{2\gamma}) \sin\psi + \frac{1 - \gamma}{2\gamma}\cos2\psi \sin\psi \ .$$

Evaluating the first two derivatives with respect to ψ at $\psi = 90°$, one obtains,

$$\frac{dv}{d\psi} = (2 + \frac{1 - \gamma}{2\gamma}) \cos\psi + \frac{1 - \gamma}{2\gamma}[\cos 2\psi \cos\psi - 2\sin 2\psi \sin\psi]$$

with

$$\left.\frac{dv}{d\psi}\right|_{\psi = 90°} = 0, \text{ extremal point}$$

and,

$$\frac{d\ v}{d\psi^2} = -(2 + \frac{1 - \gamma}{2\gamma})\sin\psi - \frac{1 - \gamma}{2\gamma}[4 \sin 2\psi \cos\psi + 5 \cos 2\psi \sin\psi]$$

with

$$\left.\frac{d^2v}{d\psi^2}\right|_{\psi = 90°} = \frac{2(1 - 2\gamma)}{\gamma} . \tag{2.84}$$

From 2.84 may be predicted that the point (0,2) is a maximum or a minimum depending on γ.

$\gamma < 0.5$ $(r,v) = (0,2)$ is a local minimum.

$\gamma = 0.5$ $(r,v) = (0,2)$ is a point of inflexion.

$\gamma > 0.5$ $(r,v) = (0,2)$ is maximum.

See Fig. 2.20.

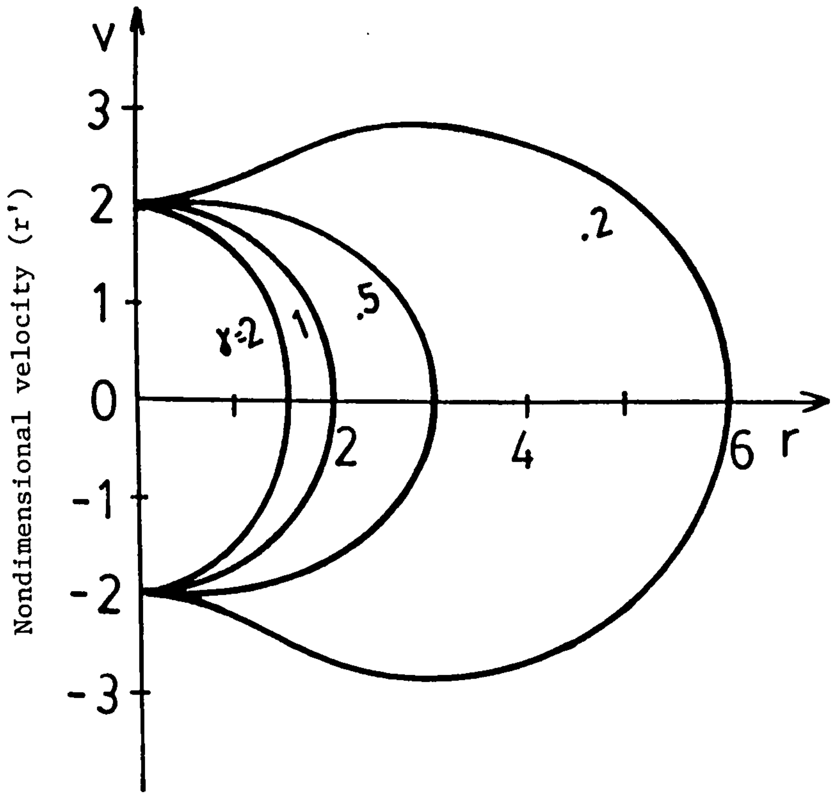

Nondimensional radius to pitch curve

Figure 2.20. Family of geometric constraint curves. β = 0.

The figure in the phase plane given by Eq. (2.83) is symmetric with respect to the abscissa. The intersection between the interior region of the curve of Eq. (2.83) and the interior region of the circle of singularity (radius $\delta/2$ and center at $(\delta/2, 0)$) is a feasible solution. Also the complement of the union of both surfaces defined above is a feasible solution. (See Fig. 2.21.)

Singular Solutions for $\beta = 0$

Equation (2.68) has singular solutions which are found by setting the second degree polynominal to zero. Then two root are found. If the roots are real then the singular solution are eccentrics, but if the roots are complex conjugate then the singular solutions are not physical solutions.

Let us recall Eq. (2.68).

$$\frac{dz}{dr} = \frac{rz[(1 - \gamma)z^2 - \alpha(z - 2)]}{\alpha r^2 - \gamma z^4} ,$$

from which is isolated the second degree polynominal

$$(1 - \gamma)z^2 - \alpha(z - 2) = 0 . \qquad (2.85)$$

It can be put into the form,

$$\frac{\alpha}{1 - \gamma} = \frac{z^2}{z - 2} , \qquad (2.86)$$

where $z > 2$, $\beta = 0$.

(See Fig. 2.22) z from Eq. (2.85) can be solved to yield,

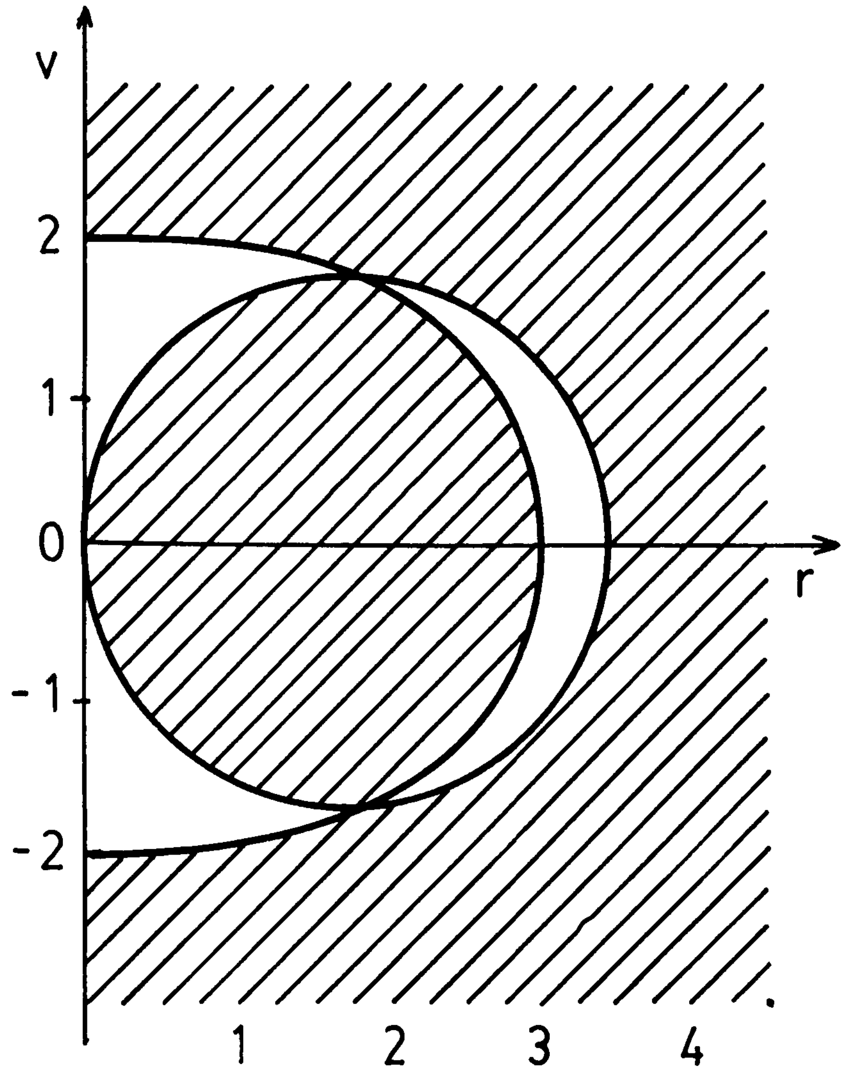

Shaded regions are physically realizable.

Figure 2.21. Regions of feasible solutions in the phase plane for cams working at $\gamma \neq 1$. $\beta = 0$, and $\gamma = 0.5$.

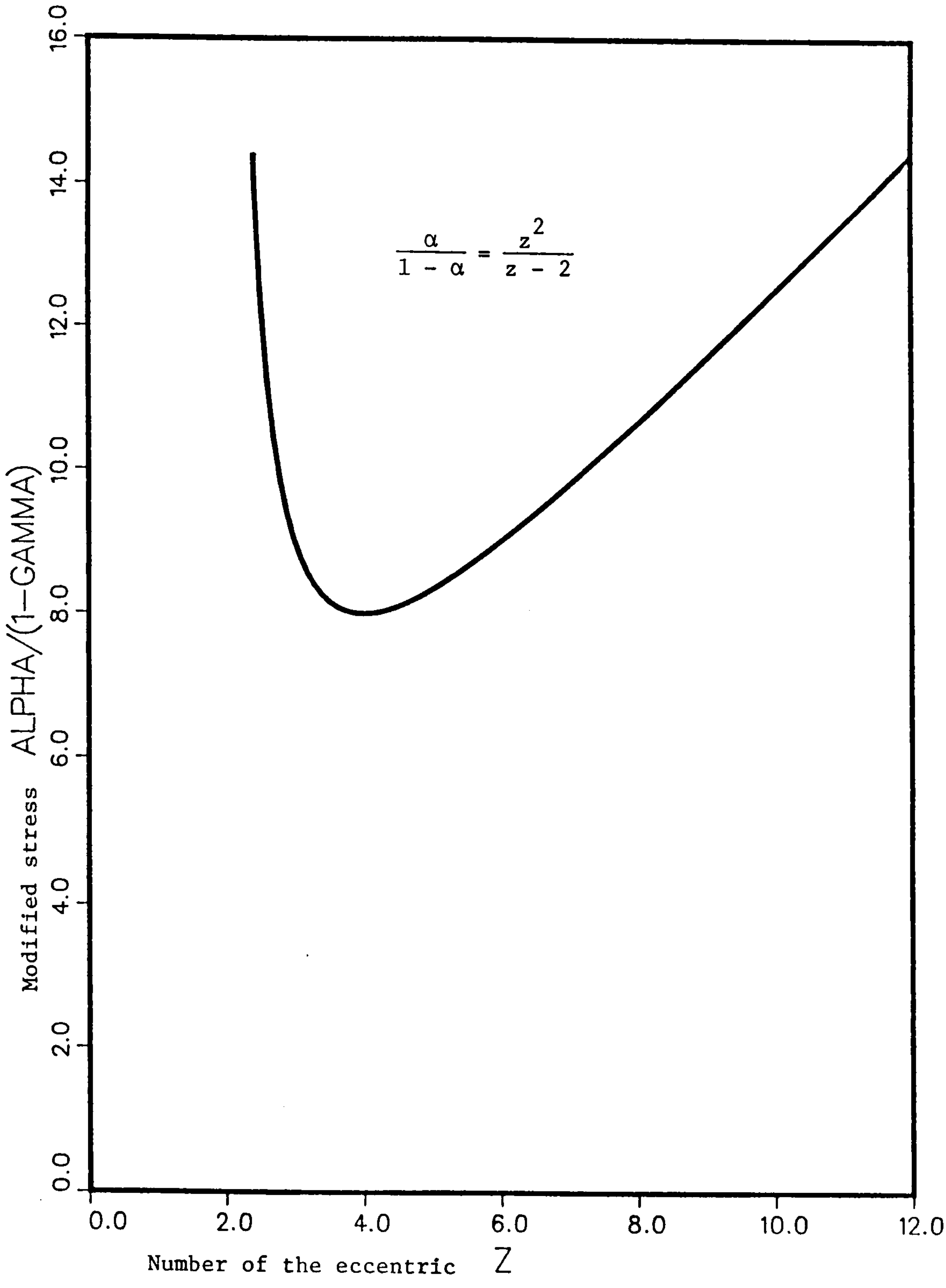

Figure 2.22. Family of eccentrics at $\gamma = 0$. $\beta = 0$.

$$z_{1,2} = \frac{\alpha \pm\sqrt{\alpha - 8(1 - \gamma)\alpha}}{2(1 - \gamma)} \ . \tag{2.87}$$

Equations (2.86) and (2.87) represent the same information and the singular solutions if they are real will be represented by z_1 and z_2 constants, which are eccentrics.

The solution for the pitch curve is represented by

$$r_i = z_i \cos\theta \ . \tag{2.88}$$

Equation (2.88) has to satisfy the inequality constrain (2.76),

$$z^2(z - 2) + r^2 + rr'' > 0 \ .$$

Substituting Eq. (2.88) into the left-hand side of Ineq. (2.76), we find

$$z_i^2(z_i - 2) > 0; \text{ for } i = 1, 2$$

from which

$$z_i - 2 > 0 \ . \tag{2.89}$$

No physical eccentric can exist with z_i less than or equal to two. From Eq. (2.86) it is seen that this forces the angular velocity ratio γ, to be less than one for the singular solutions.

Ordinary Solution for $\beta = 0$

The next step is to find the ordinary solutions of Eq. (2.71) for the general case $\gamma \neq 1$. Let us recall Eq. (2.71), and put it into the standard form of a linear O.D.E. It follows that,

$$\frac{dp}{dz} - \frac{2\alpha p}{z[(1-\gamma)z^2 - \alpha z + 2\alpha]} = -\frac{2\gamma z^3}{(1-\gamma)z^2 - \alpha z + 2\alpha} .$$

Let us define,

$$Z \equiv (1-\gamma)z^2 - \alpha z + 2\alpha$$

$$q \equiv \alpha[8(1-\gamma) - \alpha] .$$

Case 2. $q = 0$, this implies

$$\alpha = 8(1-\gamma) \tag{2.88}$$

and

$$Z = (1-\gamma)(z-4)^2 , \tag{2.89}$$

equation (2.88) also implies that $\gamma < 1$ because $\alpha > 0$.

Substituting Eqs. (2.88) and (2.89) into the linear equation (2.71) and simplifying leads to the following equation.

$$\frac{dz}{dp} - \frac{16p}{z(z-4)^2} = -\frac{2\gamma z^3}{(1-\gamma)(z-4)^2} . \tag{2.90}$$

The integrating factor for this equation is

$$\phi(z) = \exp \int -\frac{16\, dz}{z(z-4)^2}$$

$$= \exp\left(\frac{4}{z - 4} + \mathrm{Log}\ \frac{z - 4}{z}\right)$$

$$= \frac{z - 4}{z} \exp\left(\frac{4}{z - 4}\right) .$$

On multiplying Eq. (2.90) by the integrating factor, one gets

$$\frac{d}{dz}\left[\frac{p(z - 4)}{z} \exp\left(\frac{4}{z - 4}\right)\right] = - \left(\frac{2\gamma}{1 - \gamma}\right)\left(\frac{z^2}{4 - z}\right) \exp\left(\frac{4}{z - 4}\right) . \qquad (2.91)$$

Integrating Eq. (2.91) yields

$$\frac{p(z - 4)}{z} \exp\left(\frac{4}{z - 4}\right) = - \frac{2\gamma}{1 - \gamma} \int \frac{z^2}{(z - 4)} \exp\left(\frac{4}{z - 4}\right) dz .$$

On making the following change of variable

$$t = \frac{4}{z - 4} \qquad (2.92)$$

the expression can be reduced to

$$\frac{p \exp(t)}{t + 1} = \frac{8\gamma}{1 - \gamma} \int \frac{(1 + t)^2}{t^3} \exp(t)\ dt .$$

On solving the definite integral on the right-hand side, one obtains

$$\left.\frac{p \exp(t)}{t + 1}\right|_{t_0,\ p_0}^{t,\ p} = \left.\frac{4\gamma}{1 - \gamma} \left[7E_i(t) - \frac{(5t + 1) \exp(t)}{t^2}\right]\right|_{t_0}^{t} , \qquad (2.93)$$

where

$$E_i(t) = \int_{-\infty}^{t} \frac{\exp(u)}{u}\, du ,$$

which is the exponential integral function, and is tabulated in most mathematical tables. Finally, the explicit expression of the solution can be written as follows,

$$p = (t + 1) \left\{ \frac{p_0 \exp(t_0 - t)}{(t_0 + 1)} + \frac{4\gamma}{1 - \gamma} \left[\frac{7(E_i(t) - E_i(t_0))}{\exp(t)} + \frac{(5t_0 + 1) \exp(t_0 - t)}{t_0^2} - \frac{5t + 1}{t^2} \right] \right\} . \quad (2.94)$$

Case 3. $q > 0$ there is no eccentric, $q = 8\,\alpha\,(1 - \gamma) - \alpha^2 > 0$ implies $\gamma < 1 - \alpha/8$. Recall the linear equation for p given by Eq. (2.70), on putting in standard form,

$$\frac{dp}{dz} - \frac{2\alpha p}{z[(1 - \gamma)z^2 - \alpha z + 2\alpha]} = \frac{-2\gamma z^3}{(1 - \gamma)z^2 - \alpha z + 2\alpha}$$

this equation can be written more compact using

$$Z = (1 - \gamma)z^2 - \alpha z + 2\alpha .$$

With this substitution

$$\frac{dp}{dz} - \frac{2\alpha p}{zZ} = - \frac{2\gamma z^3}{Z} . \quad (2.95)$$

The integrating factor for this equation is given by,

$$\phi(z) = \exp\ (-2\alpha \int \frac{dz}{zZ}) \ .$$

On evaluating the integral it is found that,

$$\int \frac{dz}{zZ} = \frac{1}{4\alpha} \text{ Log } \frac{z^2}{Z} + \frac{1}{4} \int \frac{dz}{Z} \tag{2.96}$$

$$= \frac{1}{4\alpha} \text{ Log } \frac{z^2}{Z} + \frac{1}{2\sqrt{q}} \tan^{-1} \frac{2(1 - \gamma)z - \alpha}{\sqrt{q}} \ .$$

Thus, the integrating factor, becomes

$$\phi(z) = \exp \left[-\frac{1}{2} \text{ Log} \frac{z^2}{Z} - \frac{\alpha}{\sqrt{q}} \tan^{-1} \frac{2(1 - \gamma)z - \alpha}{\sqrt{q}} \right]$$

or

$$\phi(z) = \frac{Z^{\frac{1}{2}}}{z} \exp \left[- \frac{\alpha}{\sqrt{q}} \tan^{-1} \frac{2(1 - \gamma)z - \alpha}{\sqrt{q}} \right] .$$

Multiplying the linear O.D.E. Eq. (2.95) by the integrating factor $\emptyset(z)$ and we obtain the exact equation as follows,

$$\frac{d}{dz}[p\phi(z)] = -2\gamma \frac{z^2}{Z^{\frac{1}{2}}} \exp \left[-\frac{\alpha}{\sqrt{q}} \tan^{-1} \frac{2(1 - \gamma)z - \alpha}{\sqrt{q}} \right] \ .$$

On integrating, one obtains,

$$p\phi(z) = -2\gamma \int \frac{z^2}{Z^{\frac{1}{2}}} \exp\left[-\frac{\alpha}{\sqrt{q}} \tan^{-1} \frac{2(1-\gamma)z - \alpha}{\sqrt{q}}\right] dz \ . \qquad (2.97)$$

The integral on the right-hand side of Eq. (2.97) can be simplified under the change of variable.

$$u = \tan^{-1} \frac{2(1-\gamma)z - \alpha}{\sqrt{q}}$$

making this substitution, one finds

$$\int \frac{z^2}{Z^{\frac{1}{2}}} \exp\left[-\frac{\alpha}{\sqrt{q}} \tan^{-1} \frac{2(1-\gamma)z - \alpha}{\sqrt{q}}\right] dz$$

$$= \frac{1}{4(1-\gamma)^{5/2}} \int (\alpha^2 + 2\alpha\sqrt{q}\tan u + q \tan^2 u)(\sec u) \exp(-\frac{\alpha}{\sqrt{q}} u)\ du \ ,$$

this integral can be reduced to the form

$$\int (\sec u) \exp(-\frac{\alpha}{\sqrt{q}} u)\ du + F(u)$$

but even so the integral does not have an expression in terms of elementary functions and it has to be evaluated using numerical integration. At this point we stop the effort because we already have on hand a numerical solution of the differential equation for the general case.

Case 4. $q < 0$ there are two eccentrics, $q = 8\ \alpha(1-\gamma) - \alpha^2 < 0$, and $\gamma \neq 1$.

Following a procedure similar to Case 3 it is possible to calculate the integrating factor of the linear O.D.E., but the second quadrature can not be performed in terms of elementary functions. The integral has the form

$$\int \frac{z^2}{Z^{\frac{1}{2}}} \exp \frac{\alpha}{\sqrt{-q}} \tanh^{-1} \frac{2(1-\gamma)z-\alpha}{\sqrt{-q}} \; dz \; .$$

Using the transformation

$$u = \tanh^{-1} \frac{2(1-\gamma)z-\alpha}{\sqrt{-q}}$$

we obtain the integral

$$\int (\operatorname{sech} u) \exp \left(\frac{\alpha}{\sqrt{-q}} u\right) du \; ,$$

This integral also has no elementary solution. Therefore we stop here the effoort in trying to find close form solutions, and we will use the numerical solution to solve this type of problem.

Space of Solution for the General Case

For the general case for maximal stress constraint the nonlinear first degree differential equation in the phase plane namely Eq. (2.56) does not have a closed form solution.

However, we may obtain a numerical solution using the Runge Kutta method which is very accurate. We are interested in determining the part of the phase plane for which there are physical solutions. To accomplish this we recall the second order differential equation (2.35) that applies to maximal stress constraint, and is given by

$$r'' + \frac{\alpha r\{[r^2 + (r')^2]^{3/2} - r^2 - 2(r')^2\} - (\beta + r)[r^2 + (r')^2]^2}{\alpha r^2 - \gamma[r^2 + (r')^2]^2} = 0$$

and the geometrical inequality (2.29), which is given by

$$[r^2 + (r')^2]^{3/2} - r^2 - 2(r')^2 + rr'' > 0 ,$$

or the alternative form given by Inequality (2.76)

$$z(z - 2) + r^2 + rr'' > 0.$$

We introduce into Eq. (2.35) the following change of variable

$$z^2 = r^2 + (r')^2 ,$$

obtaining

$$r'' + \frac{\alpha r[z(z^2 - 2) + r^2] - (\beta + r)z^4}{\alpha r^2 - \gamma z^4} = 0 \quad . \qquad (2.98)$$

On solving for r" in Eq. (2.98), one obtains

$$r'' = \frac{(\beta + r)z^4 - \alpha r[z(z^2 - 2) + r^2]}{\alpha r^2 - \gamma z^4} \quad . \qquad (2.99)$$

Substituting r" from Eq. (2.99) into the geometrical inequality constraint (2.76), it follows that

$$z^2(z - 2) + r^2 + r\frac{(\beta + r)z^4 - \alpha r[z^2(z - 2) + r^2]}{\alpha r^2 - \gamma z^4} > 0 .$$

After algebraic simplication we obtain

$$\frac{z^4[(\beta + r)r - \gamma r^2 - \gamma z^2(z - 2)]}{\alpha r^2 - \gamma z^4} > 0 .$$

In this case $z^4 > 0$. Then the inequality reduces to

$$\frac{(\beta + r)r - \gamma r^2 - \gamma z^2(z - 2)}{\alpha r^2 - \gamma z^4} > 0 .$$

For the special case of $\gamma = 0$ inequality (2.100) reduces to

$$\frac{\beta + r}{\alpha r} > 0 .$$

Since α and r are both positive we obtain

$$r > -\beta \tag{2.101}$$

as a solution space.

Continuing with the analysis of inequality (2.100), we find that it holds if its numerator and denominator have equal signs.

Setting the numerator equal to zero we may find the limit curve in the phase plane where it change sign. Thus,

$$(\beta + r)r - \gamma r^2 - \gamma z^2(z - 2) = 0 . \tag{2.102}$$

With the change of variable $r = z \cos\psi$, Eq. (2.102) changes to polar form, with z being the distance from the origin to a point in the phase plane and ψ the polar angle which is the physically pressure angle. Thus,

$$z[(\beta + z\cos\psi)\cos\psi - \gamma z\cos^2\psi - \gamma z(z - 2)] = 0 .$$

Since $z > 0$, then

$$(\beta + z\cos\psi)\cos\psi - \gamma z\cos^2\psi - \gamma z(z - 2) = 0 .$$

On putting this expression in the form of a second degree polynominal in z, we get

$$-\gamma z^2 + [(1 - \gamma)\cos^2\psi + 2\gamma]z + \beta\cos\psi = 0 . \qquad (2.103)$$

On solving for z we obtain

$$z = \frac{2\gamma + (1 - \gamma)\cos^2\psi \pm\sqrt{[2\gamma + (1 - \gamma)\cos^2\psi]^2 + 4\beta\gamma\cos\psi}}{2\gamma} . \qquad (2.104)$$

For the special case of $\psi = 0$, then $z = r$ and the solution intercepts the abscissa at

$$r = \frac{1 + \gamma \pm\sqrt{(1 + \gamma)^2 + 4\beta\gamma}}{2\gamma} . \qquad (2.105)$$

For $\beta = -1$ there is a further reduction of the expression. Namely,

$$r = \frac{1 + \gamma \pm(1 - \gamma)}{2\gamma} \qquad (2.106)$$

which leads to the values

$$r = \frac{1}{\gamma} , \text{ and } r = 1 .$$

We can now study the solution in more depth for the case $\beta = -1$ and $\gamma = 0.5$, Eq. (2.104) becomes

$$z = \frac{2 + \cos^2\psi \pm\sqrt{(2 + \cos^2\psi)^2 - 8\cos\psi}}{2} ,$$

which yields real values of z in the domain

$$\psi \in [-\frac{\pi}{2}, \frac{\pi}{2}] .$$

Making a table of z as a function of ψ in the interval $[0, \pi/2]$ we obtain a curve in the phase plane (Fig. 2.23).

For the case under study ($\beta = -1$, $\gamma = 0.5$), a given polar angle ψ yields two real roots of the quadratic equation in z Eq. (2.103) which has a negative coefficient on the second order term in z (i.e., $-\gamma z^2$). This means the parabola has its vertex above the abscissa and the quadratic expression on z is positive between the roots given by Eq. (2.104) (see Fig. 2.24). If the roots of this second degree algebraic equation are complex conjugates, that means that the parabola of z versus ψ does not intercept the abscissa and all the values of the quadratic expression on z are negative.

Having found the areas of the phase plane where the numerator is positive and negative then we combine the solution with the sign of the denominator given by the circle of singularity which has center at $(\delta/2, 0)$ and radius $\delta/2$. The solution is physically feasible if the signs of numerator and denominator are alike.

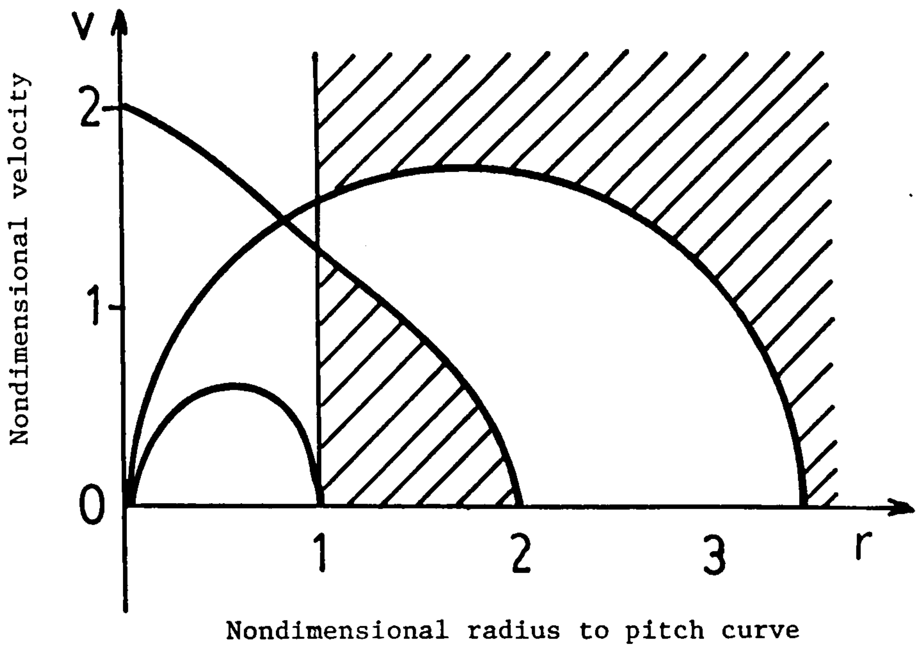

Figure 2.23. Feasible region in the phase plane for the general case. $\beta = -1$, $\gamma = 0.5$.

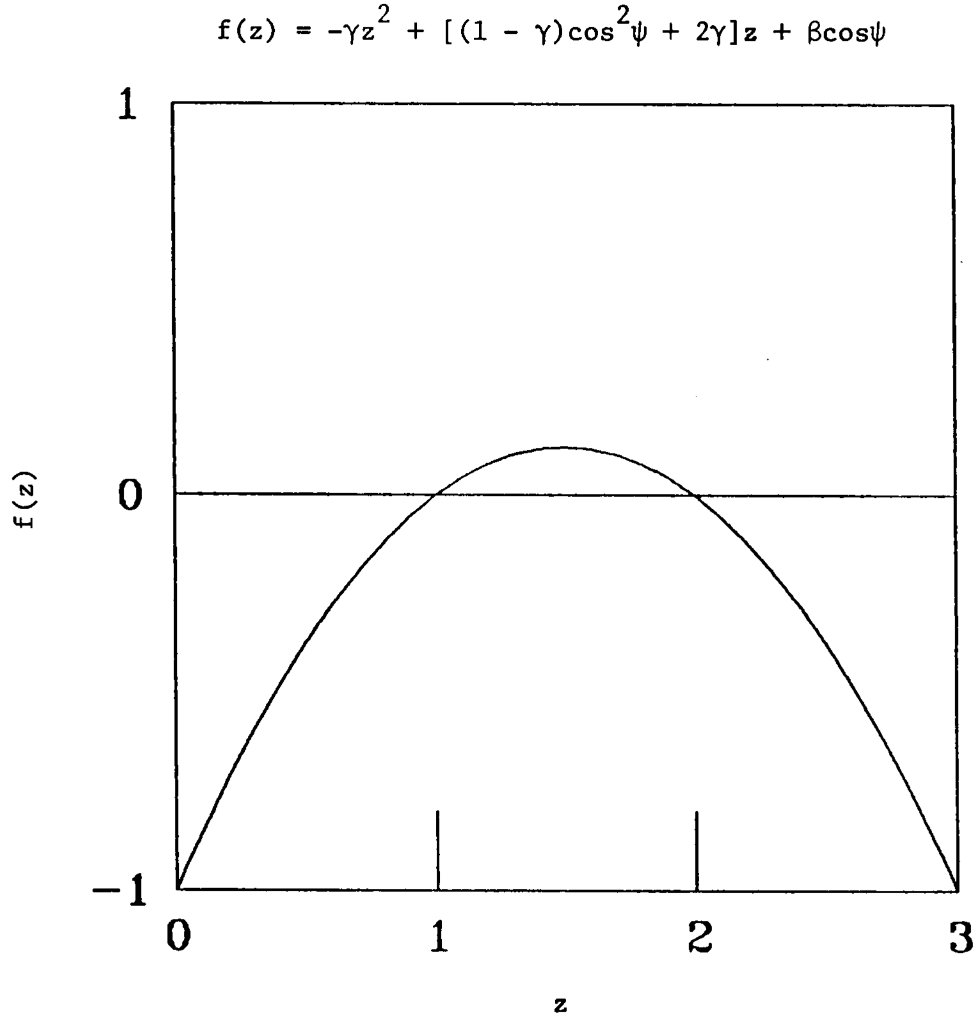

Figure 2.24. Second degree polynomial on z.

For the case of $\beta < -1$ we know that there the physical solution is for $r > -\beta$. That means that also the area in the phase plane between the lines $r = 0$ and $r = -\beta$ has to be discarded as a physical solution.

Solution for Low Stress at High Angular Velocity

This solution is interesting for negative acceleration on the roller follower but it is necessary to run the cam driven system at high angular velocity. In this case we set the nondimensional stress equal to zero and look for the space of feasible solution in the phase plane.

The case of low stress has the same solution as the general case for the values $\alpha > 0$, $\beta \neq 0$, $\gamma > 0$, that was studied where inequality (2.100) was the function that controlled the space of physical solutions. Let us recall inequality (2.100).

$$\frac{(\beta + r)r - \gamma r^2 - \gamma z^2(z - 2)}{\alpha r^2 - \gamma z^4} > 0 \ .$$

In the case for low stress we take the limit case when α goes to zero and find that the diameter of the circle of singularity goes to zero. That is, the circle is at the origin of the phase plane. For the rest of the space of the phase plane the denominator is negative. The numerator does not depend on α. Therefore, the sign of it is controlled by the second order polynominal on z Eq. (2.103). The roots where the polynominal shifts sign are given by Eq. (2.104).

Let us recall Eq. (2.104)

$$z = \frac{2\gamma + (1-\gamma)\cos^2\psi \pm\sqrt{[2\gamma + (1-\gamma)\cos^2\psi]^2 + 4\beta\gamma\cos\psi}}{2\gamma} .$$

The region between the roots given by Eq. (2.104) is forbidden, because the numerator is positive. Outside that region the sign of the numerator is negative and the solution becomes feasible.

The solution for low stress was studied in reference [38] and it was found that it corresponds to harmonic motion. This came from setting α equal to zero in Eq. (2.35).

Let us recall Eq. (2.35)

$$r'' + \frac{\alpha r\{[r^2 + (r')^2]^{3/2} - r^2 - 2(r')^2\} - (\beta + r)[r^2 + (r')^2]^2}{\alpha r^2 - \gamma[r^2 + (r')^2]^2} .$$

On setting $\alpha = 0$, and simplifying the fraction, Eq. (2.35) reduces to a linear second order equation as follows

$$r'' + \frac{\beta + r}{\gamma} = 0 ,$$

or

$$r'' + \frac{1}{\gamma} r = -\frac{\beta}{\gamma} . \qquad (2.107)$$

Its solution for the initial condition $\theta = 0$, $r = r_0$, and $r' = 0$ is:

$$r = (r_0 + \beta) \cos(\omega_0\theta) - \beta , \qquad (2.108)$$

where

$$\omega_0 = \sqrt{\frac{1}{\gamma}} .$$

The trajectory in the phase plane is an ellipse with the following equation

$$\frac{(r + \beta)^2}{(r_0 + \beta)^2} + \frac{(r')^2}{[\omega_0(r_0 + \beta)]^2} = 1 , \qquad (2.109)$$

(see Fig. 2.25).

Only the negative part of the acceleration is used, because in the positive part separation between the roller follower and cam would occur. However in a practical application it may be preferred to use a low positive value of the nondimensional stress α to avoid separation. For example using the value of α equal to the unity may be a good choice. In that case the movement will be governed by the general numerical solution but the shape will be similar to harmonic motion as defined by Eq. (2.108).

Model for Controlled Curvature

Controlled curvature is a second form of defining the movement of the roller follower. In this case we define directly the radius to the pitch curve $r = r(\theta)$ as a function of the angle of rotation. This definition has to agree with the geometric constraint. In this case it is rather simple to agree because any convex, straight line, or concave profile with nondimensional curvature greater than

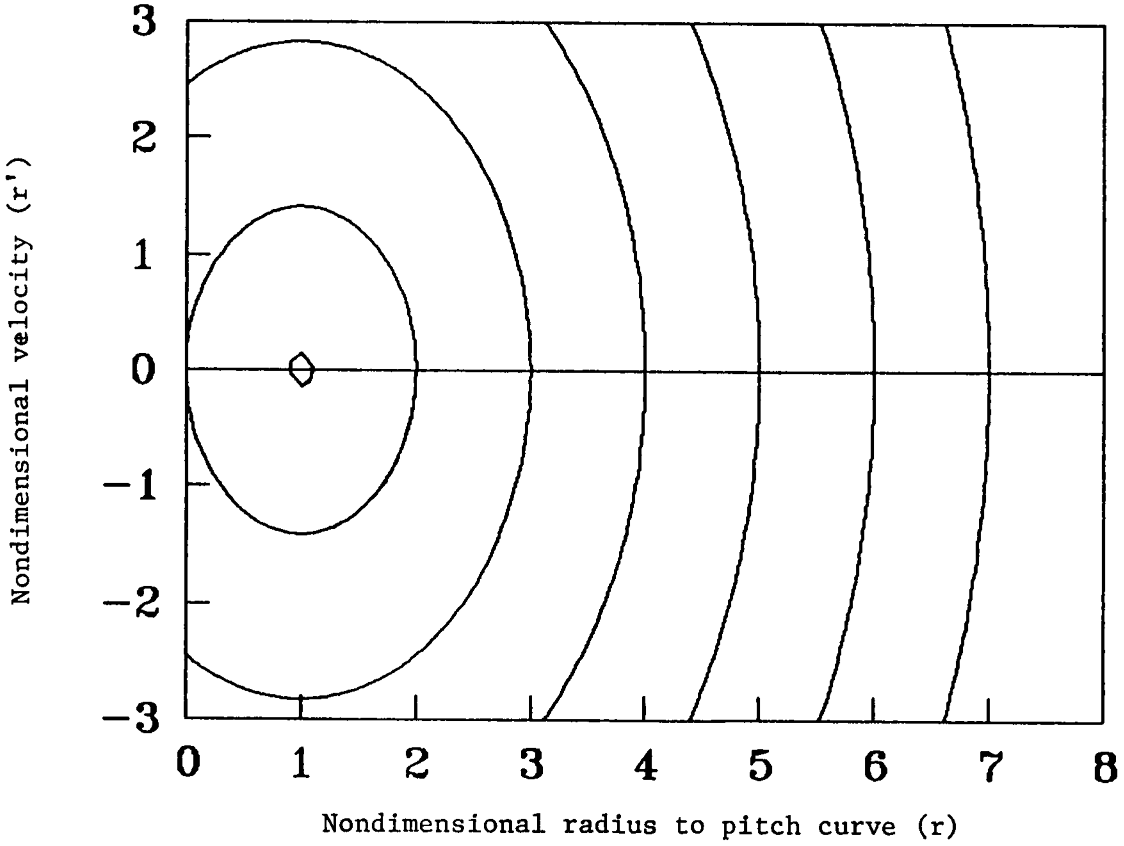

Figure 2.25. Low stress motion in the phase plane. $\alpha = 0$, $\beta = -1$, $\gamma = 0.5$.

$$\max\left(-\frac{R_f}{K_t}, -1\right)$$

will satisfy with the geometric inequality constraint (2.29). Now one must check the nondimensional stress given in inequality constraint (2.28). If the defined curve satisfies inequality (2.28) the problem has a feasible solution. Otherwise the solution for controlled curvature has to be reformulated.

We are interested first in the problem of low angular velocity. Putting $\gamma = 0$, inequality (2.28) reduces to

$$\alpha = \frac{1}{r} \frac{(\beta + r)[r^2 + (r')^2]^2}{[r^2 + (r')^2]^{3/2} - r^2 - 2(r')^2 + rr''} \leqq s \qquad (2.110)$$

Equation (2.110) tells us that the nondimensional stress is a decreasing function of the acceleration. According to reference [26] no positive acceleration of the follower will undercut the cam. That means that for the case of low angular velocity when we neglect the inertial forces we can use any definition of r as a function of θ ($r = r(\theta)$). Therefore a very high value of the positive acceleration can be reached. For practical reasons however we may define a minimum cam curvature (i.e., maximal concavity) as a number greater than -1 let us say $-\frac{1}{2}$, or the equivalent bounding the maximal acceleration by a value equal to M (i.e., $r'' < M : M >> 0$).

Now we must mention the validity of the formula for contact stresses which was developed by Hertz [8], which is used in this model.

Hertz mentioned that his model considers only a small area of contact compared with the size of the bodies in contact and he refers to the case of a sphere just fitting in a cylindrical cavity of the same radius as the sphere's, which will invalidate his model, as well as invalidate the case in the present study when a roller follower, which is a cylinder, fits in a cylindrical cavity of the same radius. But in this problem, by limiting the acceleration, we avoid the limit case and can thus be assured that the contact stress given by the Hertz's formula gives an acceptable value of the actual stress. Hertz did not give a recommendation for the range of validity of his contact stress formula which is used by many researchers in the combination of convex and concave bodies.

There is another viewpoint worthy of discussion, the cases of intermediate and high angular velocity. In those cases the inertial forces are important, the stress constraint is reached first. Therefore a big concavity will not occur.

CHAPTER 3

APPLICATIONS

In this chapter we apply the theory set forth in Chapter 2, for several cam lift problems. We then will display the phase plane using α and β to set the equilibrium points or extremal dwelling conditions. Then using β and γ we establish the area where the solution for stress constraint is feasible and draw the circle of singularity. Then we decide what type of movement is required. We will begin by studying cases in nondimensional form under the condition that we hope to have a short angle of rotation to complete the rise stroke. Then we will change the values of the parameters α, β, and γ to understand how they affect the solution. Later we use a practical example using numerical dimensional data to show how the solution is applied.

Solution of a Nondimensional Cam Lift Problem in Low Angular Velocity

Problem: Determine the rise profile in a nondimensional cam working with low angular velocity (i.e., use $\gamma = 0$). The material has a maximum nondimensional stress $\alpha = 6$. Set initially the prestress $\beta = 0$. The positive acceleration is limited by the maximum value of 4 and the initial value of the actual lower dwelling position is $r_{min} = 2$. Determine the best solution for the cam profile which gives the minimum angle of rotation subject to the stress constraint and to the maximal positive acceleration already mentioned. Use first $r_{max} = 3$ (i.e., nondimensional lift $h^* = 1$).

Solution. First we need to establish the function of the radius to the pitch curve r and its derivative r' as a function of the angle of rotation for the phase of positive acceleration. From the statement of the problem if follows that $r'' = 4$. On integrating, considering the following initial conditions $\theta = 0$, $r_0' = 0$, $r_0 = r_{min} = 2$, we get

$$r' = 4\theta \ . \tag{3.1}$$

With a second integration,

$$r = 2 + 2\theta^2 \ . \tag{3.2}$$

It is important to determine the equilibrium point for extreme dwelling conditions. Let us recall Eq. (2.34)

$$r_{1,2} = \frac{\alpha - \beta \pm \sqrt{\Delta}}{2}$$

where $\Delta = (\alpha - \beta)^2 - 4\alpha$.

Using the data $\alpha = 6$, $\beta = 0$, we obtain

$$r_1 = 4.73, \text{ and } r_2 = 1.27 \ .$$

We are using a $r_{min} = 2$ and $r_{max} = 3$ whose values are between the extreme dwelling conditions.

Now because we have low angular velocity using $\gamma = 0$, the negative acceleration is obtained by the maximal stress constraint which is defined using the data: $\alpha = 6$, $\beta = 0$, $\gamma = 0$. We run the numerical solution backward from the final conditions obtaining a table of values for θ, r, and r' using the initial condition $r_{max} = 3$; $r' = 0$.

The data of the first phase of the movement (i.e., positive acceleration) and the second phase of the movement (i.e., negative acceleration) are shown in Table 3.1. Also the data used in Table 3.1 can be represented in the phase plane (see Fig. 3.1). The intersection of the curve of positive acceleration and negative acceleration determine the transition point where the movement switchs from maximal acceleration to maximal deceleration.

The addition of the angles of rotation for first and second phase determine the total lift rotation going from the dwelling condition at $r_{min} = 2$ to the dwelling condition at $r_{max} = 3$. From Table 3.1 we find that for the rise of the roller follower;

positive acceleration $\theta = 19°$ of rotation,

negative acceleration $\theta = 61°$ of rotation,

total raise stroke $\theta = 80°$ of rotation.

See Table 3.2 and Fig. 3.2.

From the analysis it is seen that the positive acceleration acts quickly while the negative acceleration has a poor speed of response. Also in this case the nondimensional lift is one so that the dimensional lift is equal to the roller radius. This will result in a quite large roller. This can be seen in Fig. 3.3 where the cam profile is produced from the data of Table 3.2.

To determine the effect of changing the nondimensional stroke we change only $r_{max} = 4$ with the rest of the parameters remaining the same.

Table 3.1. Determination of Transition Point for Case 1.

Acceleration			Deceleration		
θ°	r	r'	θ°	r	r'
0	2.000	0.000	0	3.000	0.000
10	2.061	0.698	-50	2.467	1.143
11	2.074	0.768	-51	2.445	1.159
12	2.088	0.838	-52	2.425	1.174
13	2.103	0.908	-53	2.404	1.189
14	2.119	0.977	-54	2.383	1.204
15	2.137	1.047	-55	2.362	1.218
16	2.156	1.117	-56	2.341	1.232
17	2.176	1.187	-57	2.319	1.246
18	2.197	1.257	-58	2.297	1.259
19[a]	2.220	1.327	-59	2.275	1.271
20	2.244	1.396	-60	2.253	1.283
			-61[a]	2.230	1.295
			-62	2.208	1.306

[a]Transition point $r_{min} = 2$, $r_{max} = 3$, $\alpha = 6$, $\beta = \gamma = 0$.

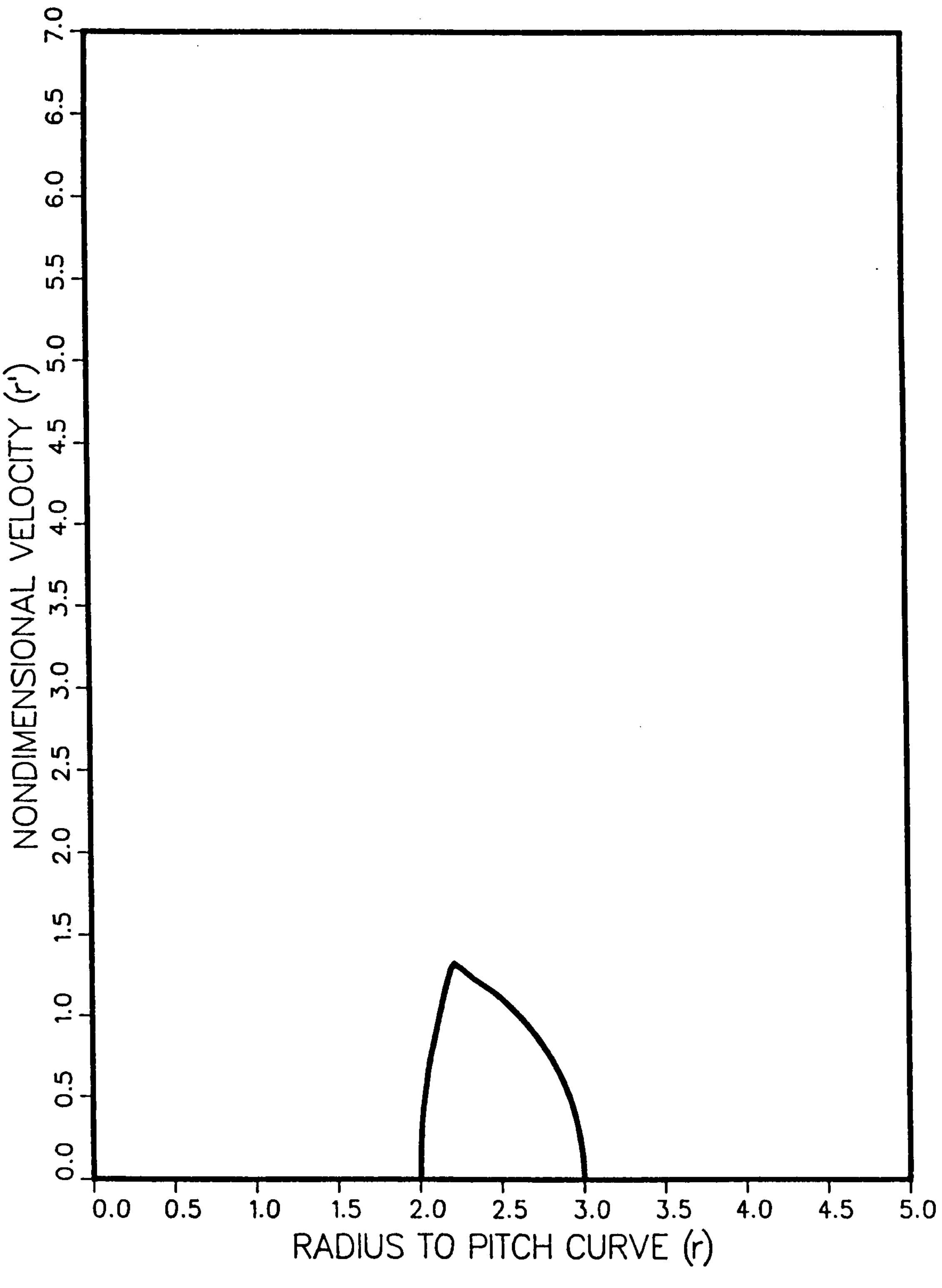

Figure 3.1. Rise movement in the phase plane for case 1.

Table 3.2. Trajectory of the Pitch Curve and Angle of Pressure Versus Cam's Rotation for Case 1.

$\theta°$	r	r'	$\psi°$
0	2.000	0.000	0.0
5	2.015	0.349	9.8
10	2.061	0.698	18.7
15	2.137	1.047	26.1
19[a]	2.220	1.327	30.9
20	2.253	1.283	29.7
25	2.362	1.218	27.3
30	2.465	1.143	24.9
35	2.561	1.057	22.4
40	2.649	0.962	20.0
45	2.729	0.859	17.5
50	2.799	0.749	15.0
55	2.860	0.634	12.5
60	2.910	0.513	10.0
65	2.949	0.388	7.5
70	2.977	0.261	5.0
75	2.994	0.131	2.5
80	3.000	0.000	0.0

[a]Transition point, $r_{min} = 2$, $r_{max} = 3$, $\alpha = 6$, $\beta = \gamma = 0$.

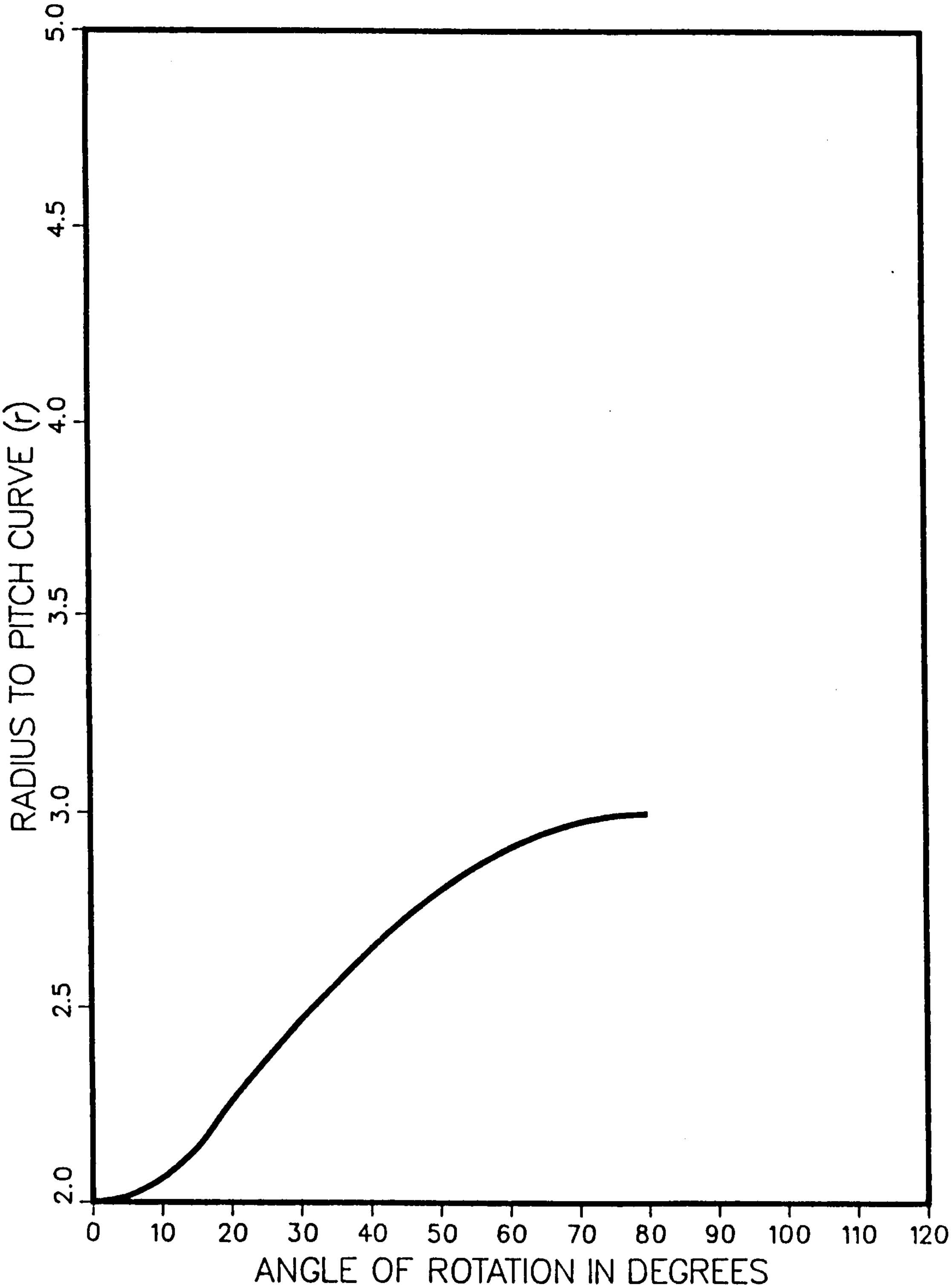

Figure 3.2. Displacement diagram for case 1.

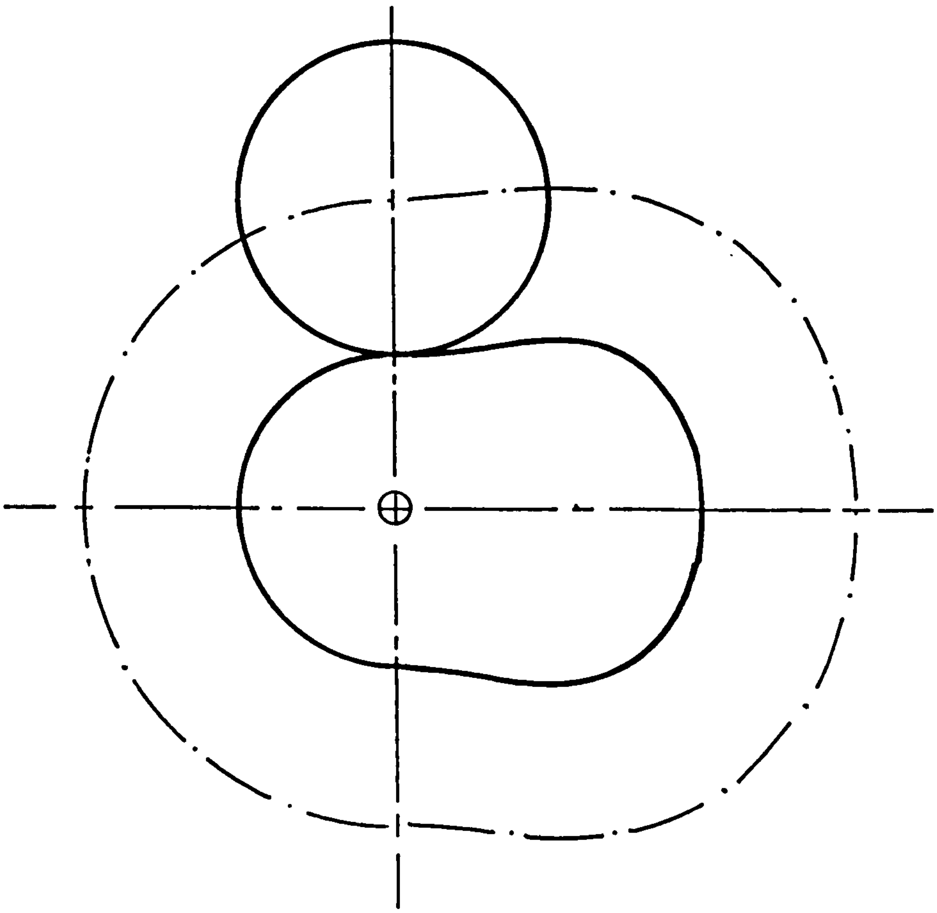

Figure 3.3. Cam contour for case 1.

For the solution of the lift problem using $r_{max} = 4$ we operate in the same way as the previous case. In this case the nondimensional lift is two, that is the radius of the roller follower is one-half of the lift. Thus, we have a solution using a smaller roller. Let us see what is the effect of this change in the total angle of rotation for completing the lift.

Table 3.3 and Fig. 3.4 shows that the transition point occurs after 26° of the cam's rotation and that there is 90° of cam rotation for the negative acceleration in the rise stroke. This makes a total rotation of 116° to complete the total lift.

In summary, enlarging the nondimensional lift will reduce the roller size but increases the total angle of rotation. Table 3.4 and Figs. 3.5 and 3.6 complete the information relating the movement.

Also as secondary information we may compare the maximal angle of pressure. Table 3.2 shows 30.9° for the first problem of lift equal to one and Table 3.4 shows a maximal angle of pressure of 37° for lift equal to two. This value has a secondary importance of increasing the side force and increases the friction of the stem. This effect is not considered in this dissertation.

As a second variation of the original problem we may reduce the prestress from the value $\beta = 0$ to $\beta = -1$.

In this case we reduce the spring force for all positions in the interval $r \in [2, 4]$. This affects the steepness of the cam because we keep all the other factors constant. That is $\alpha = 6$, $\gamma = 0$.

For this case the minimal dwelling condition occurs at $r_2 = 1$ and the maximal dwelling condition at $r_1 = 6$. We are working between

Table 3.3. Determination of Transition Point for Case 2.

Acceleration			Deceleration		
θ°	r	r'	θ°	r	r'
0	2.000	0.000	-0	4.000	0.000
10	2.061	0.698	-10	3.980	0.233
20	2.244	1.396	-20	3.919	0.466
22	2.295	1.536	-30	3.817	0.700
23	2.322	1.606	-40	3.675	0.931
24	2.351	1.676	-50	3.492	1.156
25	2.381	1.745	-60	3.272	1.367
26	2.412	1.815	-70	3.016	1.557
27[a]	2.444	1.855	-80	2.730	1.715
			-85	2.578	1.779
			-88	2.483	1.812
			-89[a]	2.452	1.821
			-90	2.420	1.830

[a]Transition point, $r_{min} = 2$, $r_{max} = 4$, $\alpha = 6$, $\beta = \gamma = 0$.

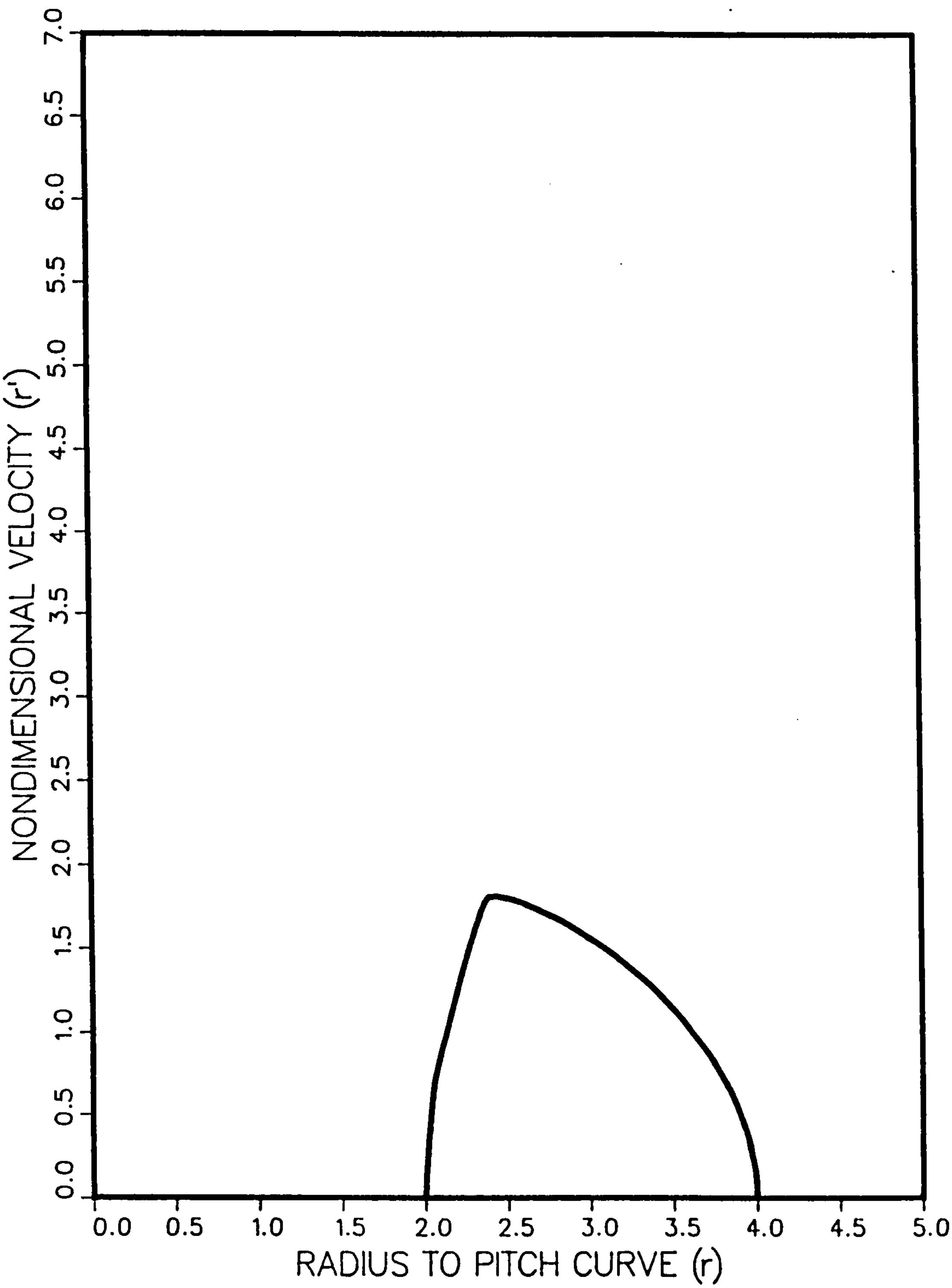

Figure 3.4. Rise movement in the phase plane for case 2.

Table 3.4. Trajectory of the Pitch Curve and Angle of Pressure Versus Cam's Rotation for Case 2.

$\theta°$	r	r'	$\psi°$
0	2.000	0.000	0.0
10	2.061	0.698	18.7
20	2.244	1.396	31.9
26[a]	2.412	1.815	37.0
30	2.547	1.790	35.1
40	2.848	1.657	30.2
50	3.123	1.484	25.4
60	3.365	1.285	20.9
70	3.570	1.067	16.6
80	3.736	0.839	12.7
90	3.863	0.606	8.9
100	3.948	0.373	5.4
110	3.993	0.140	2.0
116	4.000	0.000	0.0

[a]Transition point, $r_{min} = 2$, $r_{max} = 4$, $\alpha = 6$, $\beta = \gamma = 0$.

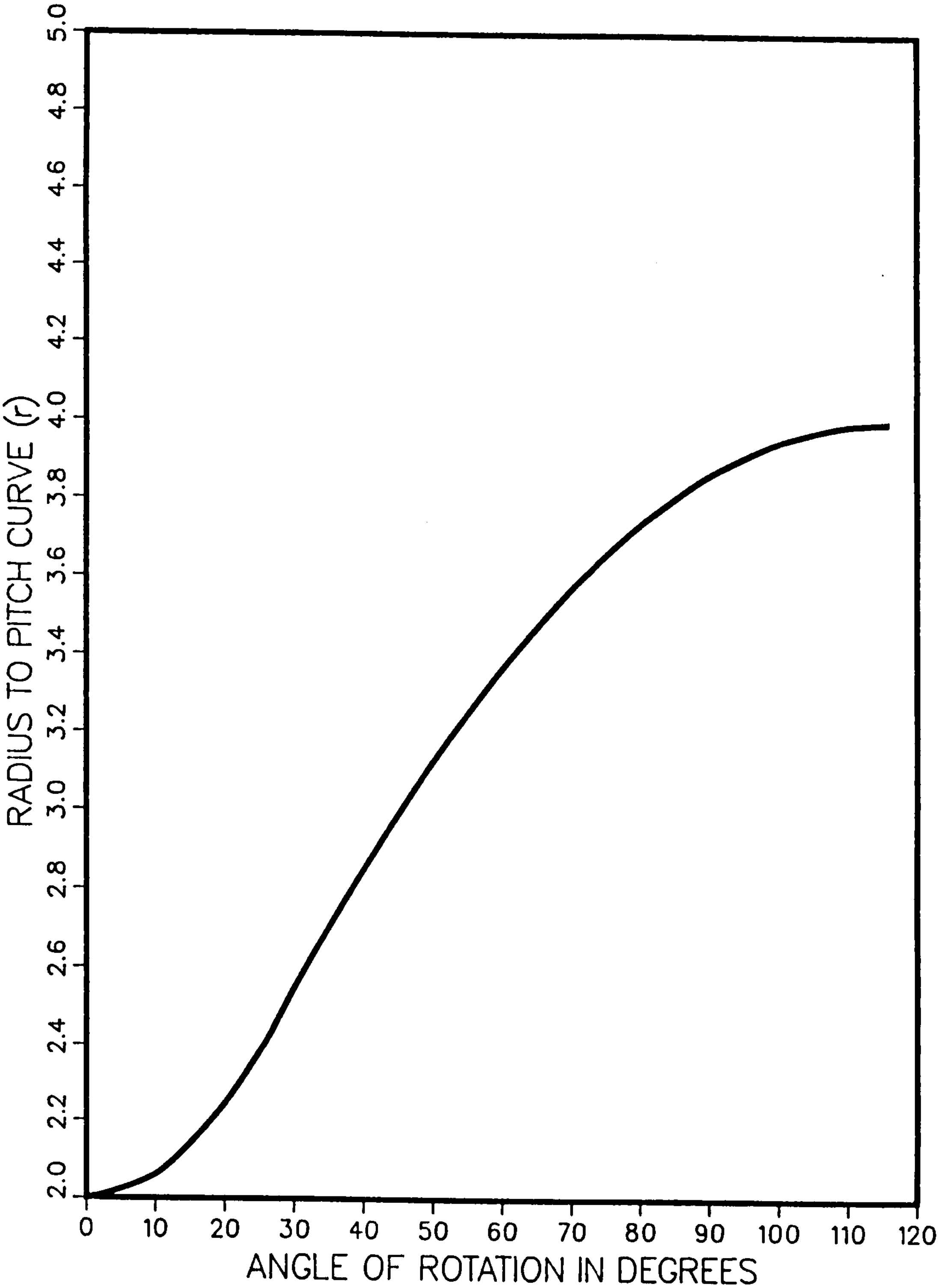

Figure 3.5. Displacement diagram for case 2.

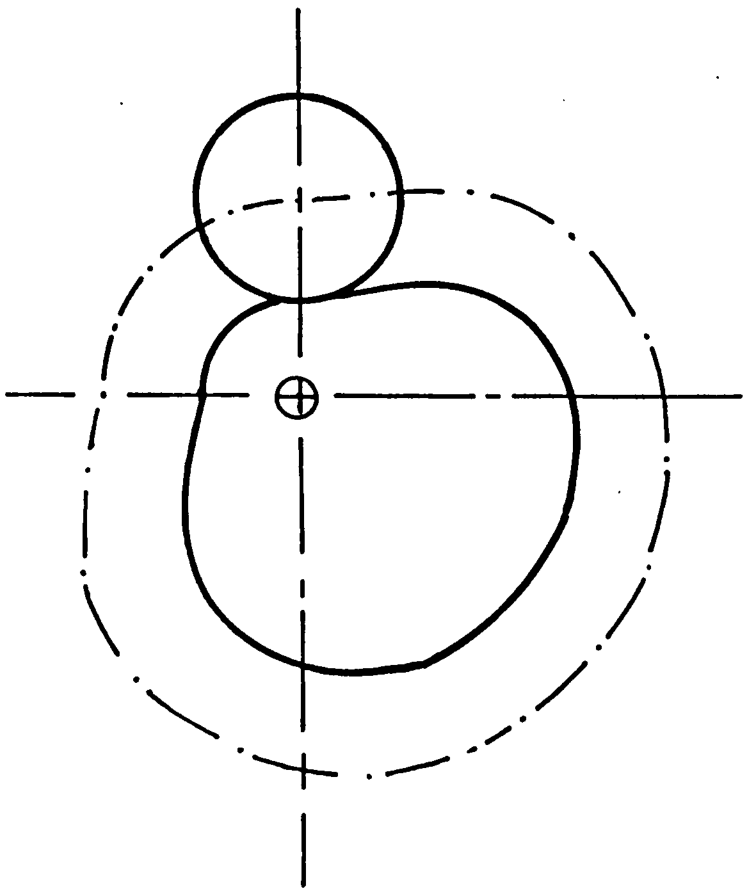

Figure 3.6. Cam contour for case 2.

$r_{min} = 2$ and $r_{max} = 4$, which is in the allowed interval and we know that for $r = 1$ we reach separation between cam and roller follower. From Chapter 2 it follows that all of the seminfinite plane defined for $r > 1$ are physical solutions for maximal stress constraint.

Solution. Table 3.5 and Fig. 3.7 shows the transition point at 40° of cam rotation at which follows 40° of cam rotation for the negative acceleration phase. That makes a total angle of rotation of 80° to complete the lift. We recover the performance in the speed of response of the first case but we retain the roller follower of the second case but as a negative secondary effect we increase the maximal pressure angle to 43.2° which is quite large (see Table 3.6). After observing Figs. 3.8 and 3.9 it is obvious that the average and maximal pressure angles increase when we try to reduce the angle of rotation for a given lift, however the contact force has been reduced from which the secondary effect of friction in the stem is reduced.

After analyzing this problem we find that a negative value of the prestress is a good choice and a large value of nondimensional lift is preferred for having a smaller roller follower.

The information available in the current literature states that increasing the base circle reduces the pressure angle but in opposition also results in an increase of the tangential velocity of the cam. In part that is the reason that we select $r_{min} = 2$, instead of a smaller value, which could be as smaller as $r_1 = 1.27$ for the first case in this problem.

Table 3.5. Determination of Transition Point for Case 3.

Acceleration			Deceleration		
θ°	r	r'	θ°	r	r'
0	2.000	0.000	-0	4.000	0.000
10	2.061	0.698	-10	3.939	0.697
20	2.244	1.396	-20	3.757	1.388
30	2.548	2.094	-30	3.455	2.076
35	2.746	2.443	-35	3.259	2.424
39	2.927	2.723	-39	3.079	2.712
40[a]	2.975	2.793	-40[a]	3.031	2.786

[a]Transition point, $r_{min} = 2$, $r_{max} = 4$, $\alpha = 6$, $\beta = -1$, $\gamma = 0$.

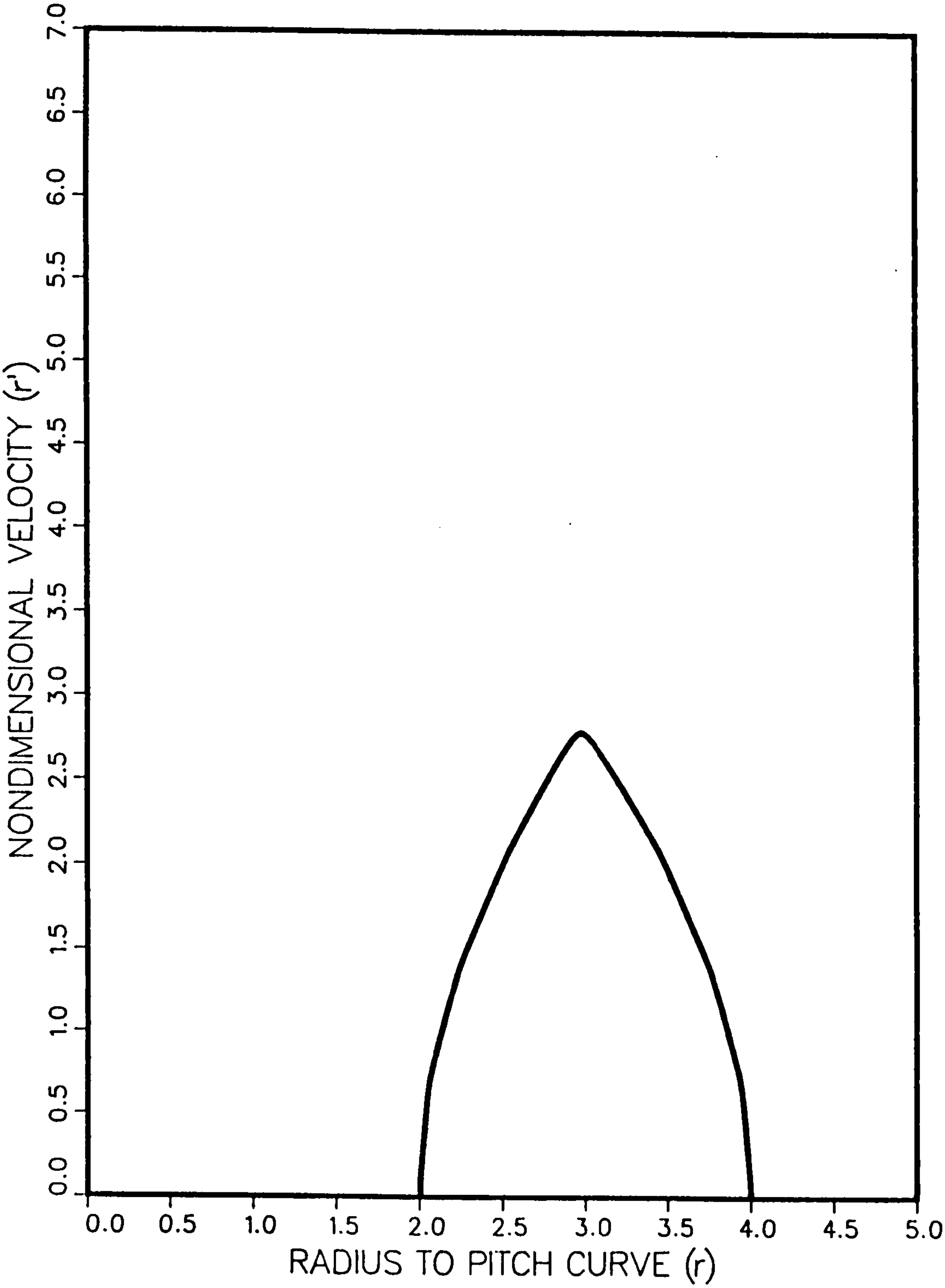

Figure 3.7. Rise movement in the phase plane for case 3.

Table 3.6. Trajectory of the Pitch Curve and Angle of Pressure Versus Cam's Rotation for Case 3.

θ°	r	r'	ψ°
0	2.000	0.000	0.0
10	2.061	0.698	18.7
20	2.244	1.396	31.9
30	2.548	2.094	39.4
40[a]	2.975	2.793	43.2
50	3.455	2.076	31.0
60	3.757	1.388	20.3
70	3.939	0.697	10.0
80	4.000	0.000	0.0

[a]Transition point, $r_{min} = 2$, $r_{max} = 4$, $\alpha = 6$, $\beta = -1$, $\gamma = 0$.

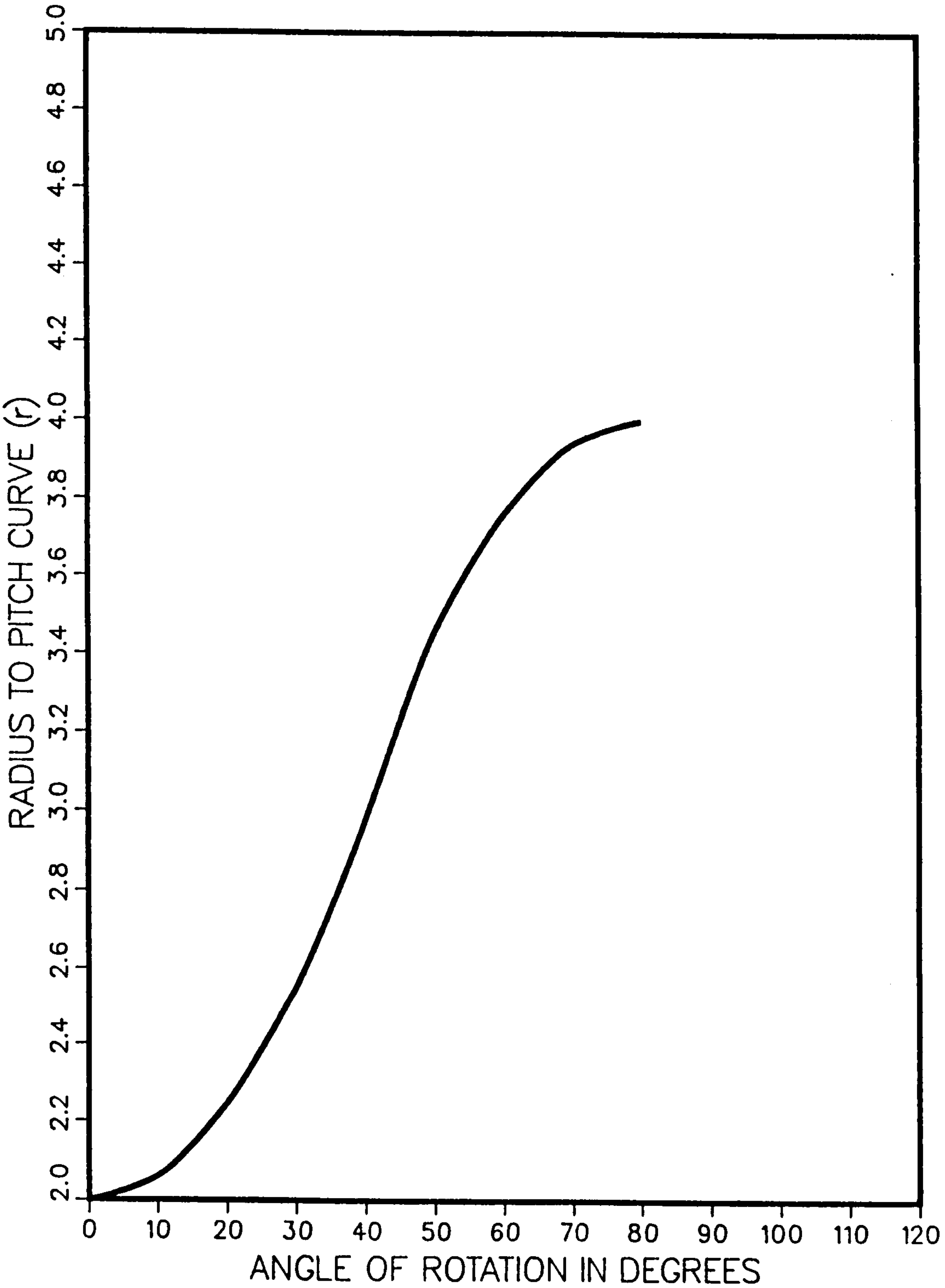

Figure 3.8. Displacement diagram for case 3.

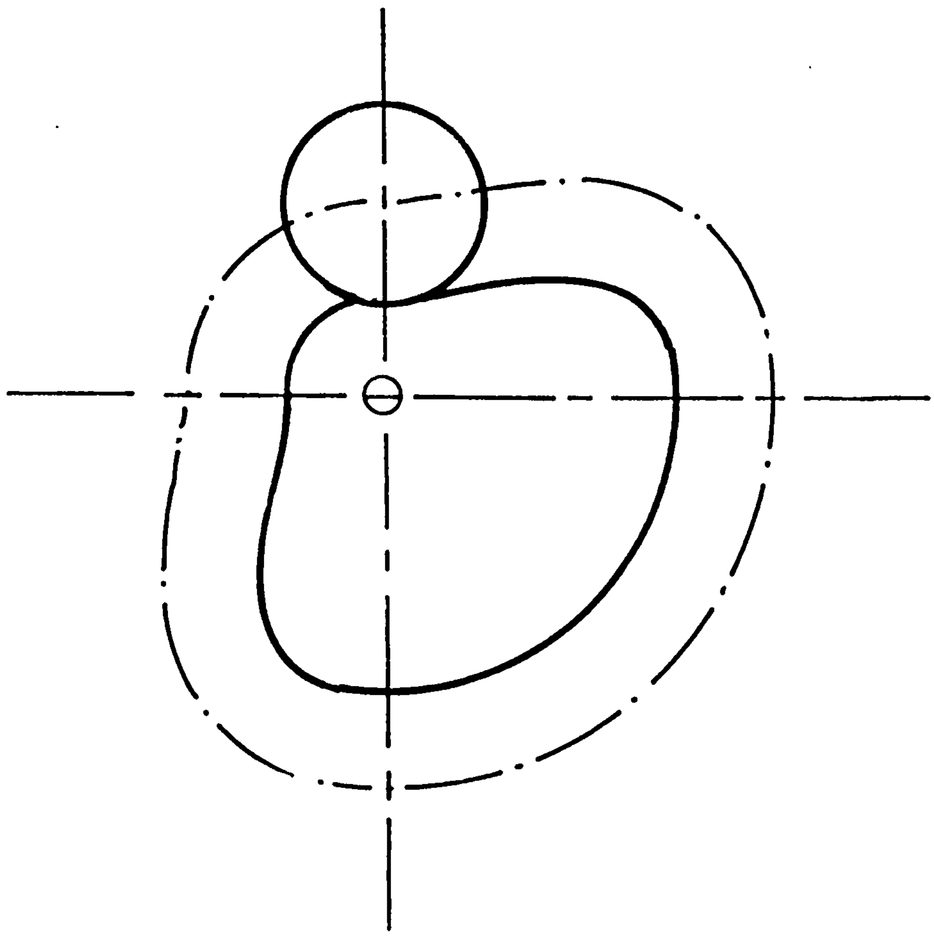

Figure 3.9. Cam contour for case 3.

Influence of the Nondimensional Stress

As a third variation of the original problem we increase the nondimensional stress from $\alpha = 6$ to $\alpha = 12$. We expect, without solving the problem, that the speed of response will increase in the second phase of deceleration. Because a higher value in the nondimensional stress α permits a higher convexity of the cam during the deceleration phase.

We solve the problem with the following data: $\alpha = 12$, $\beta = -1$, $\gamma = 0$, $r_{min} = 2$, $r_{max} = 4$. We are still bounded in the acceleration phase by $r'' = 4$. On solving the problem we will present the final results. We find that after 48° of rotation the transition point is reached. After that the maximal nondimensional stress $\alpha = 12$ is used, which gives maximal deceleration rate and the maximal position is reached in 21° of rotation. That makes a total of 69° for the lift ot the cam from $r_{min} = 2$ to $r_{max} = 4$ (see Fig. 3.10). We find a better speed of response in this case but on observing the phase plane this indicates that now the acceleration phase has the poor speed of response.

Influence of the Angular Velocity Ratio

The angular velocity ratio γ also has an influence on the speed of response of the cam because it affects the influence of the inertia force on the system. There are two known effects. First in the positive acceleration phase the inertia force is added, therefore, the stress increases, second in the deceleration phase the inertia force is subtracted, therefore, the stress decreases. This is general but depending on the value of γ and also on the initial conditions the

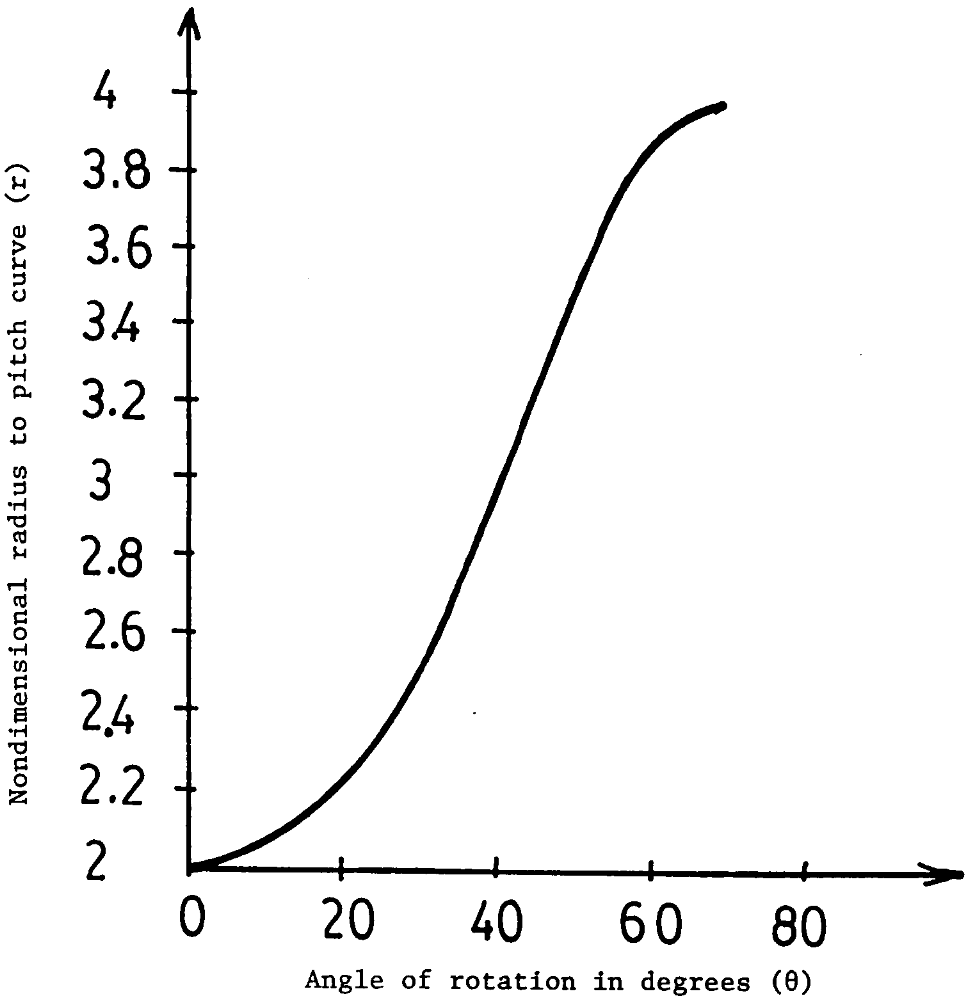

Figure 3.10. Displacement diagram for case 4.

behavior of the cam is different. To see this consider the profile obtained for γ equal to zero. Now use this for γ not zero but small, let us say $\gamma \simeq .1$, the circle of singularity defined by its diameter $\delta = \sqrt{\alpha/\gamma}$ contains inside both equilibrium points or extremum dwelling conditions. In this case the inertia force will not be important and the behavior of the cam will be similar to the solution given by $\gamma = 0$. That is, in the first phase of the acceleration during the rise stroke the stress will increase but will not approach α_{max} and the maximal acceleration rate M controls the movement, for the deceleration phase during the rise stroke the stress is lowered by the inertia force. Thus the stress will be lower than the maximum stress and the profile can be changed to reestablish the value of maximal stress which results in a higher deceleration. With these conditions we have a better speed of response.

Now for a high value of the angular velocity ratio one or both extreme dwelling conditions are outside of the circle of singularity of diameter δ. Also we have to consider Eq. (2.104) to determine the feasible region of solution in the phase plane. Given those conditions we have during the phase of acceleration that the maximum stress constraint, that is the value M of maximal acceleration does not control the movement, and in the phase of deceleration of the rise stroke we have again that the inertia force is dominant and we find that the stress α equal zero gives the best response.

Knowing that the value of the angular velocity ratio γ can be varied, the following question arises as to what is the maximal value that can be achieved. In reference [38] was explained that the value

$\gamma = 1$ represented a higher limit. The reason was explained that as γ approaches one then the natural angular frequency of the mass spring system is approached. But really the necessary demanding speed of response play the most important role. As an example the roller follower plate cam is used in the timing of valves of piston aircraft engines. The intake valve is open about 240° of rotation [12] of the crankshaft, but because in the four stroke cycle the camshaft rotates half the rate of the crankshaft that demands that the camshaft has to open and close the intake valve in 120° of rotation, which we will see in the examples is a very demanding situation. Actually in applications of aircraft engines the opening is reached in 45°, and is about the same for closing.

One conclusion can be mentioned. If a cam is working with $\gamma = 1$ a further increase in its speed will lower the positive acceleration phase, and also will lower the negative acceleration phase obtained for a low stress ($\alpha = 0$). This will result in a worse speed of response. This indicates that values less than $\gamma = 1$ provide a better speed of response.

<u>Solution for Angular Velocity Ratio</u>
<u>$\gamma = 0.1$</u>

With reference to the data given by

$$\alpha = 6\ , \quad \beta = -1\ , \quad \gamma = 0\ ,$$

$$r_{min} = 2\ , \quad r_{max} = 4\ ,$$

the total angle of rotation of the cam is $\theta = 80°$. We will try a variation in the angular velocity ratio from $\gamma = 0$ to $\gamma = 0.1$. We first have to establish the area of solution in the phase plane. For this we draw in the phase plane the circle of singularity whose diameter is given by $\delta = \sqrt{\alpha/\gamma}$, $\delta = 7.75$. We then find the roots of Eq. (2.104). Let us recall Eq. (2.104)

$$z = \frac{2\gamma + (1 - \gamma)\cos^2\psi \pm \sqrt{[2\gamma + (1 - \gamma)\cos^2\psi]^2 + 4\beta\gamma\cos\psi}}{2\gamma} .$$

Between the roots found by Eq. (2.104) the function z is positive. We draw the roots of z as a function of ψ and because all the smaller roots are in the area where $r < 1$ (unfeasible region) we do not draw them. The large roots form a shape similar to an ellipse, from $z = 10$ in the case $\psi = 0°$ to smaller values near the line $r = 1$ (see Fig. 3.11 and Table 3.7).

After seeing Fig. 3.11, we recognize it as a typical case of low angular velocity with both extremal dwelling points in the interior of the circle of singularity. Also the region between the dwelling points is inside the region where the second degree polynominal given by the numerator of inequality (2.100) is positive. Thus the intersection of these two areas is the feasible region in the phase plane (see Fig. 3.11).

After plotting in the phase plane the curve of constant acceleration $r'' = 4$ with initial dwelling position at $r = 2$ and plotting the curve of constant stress backward with initial condition of dwelling at $r = 4$ and using the parameters $\alpha = 6$, $\beta = -1$, $\gamma = 0.1$ we see in Fig. 3.11 that the trajectory is in the feasible region.

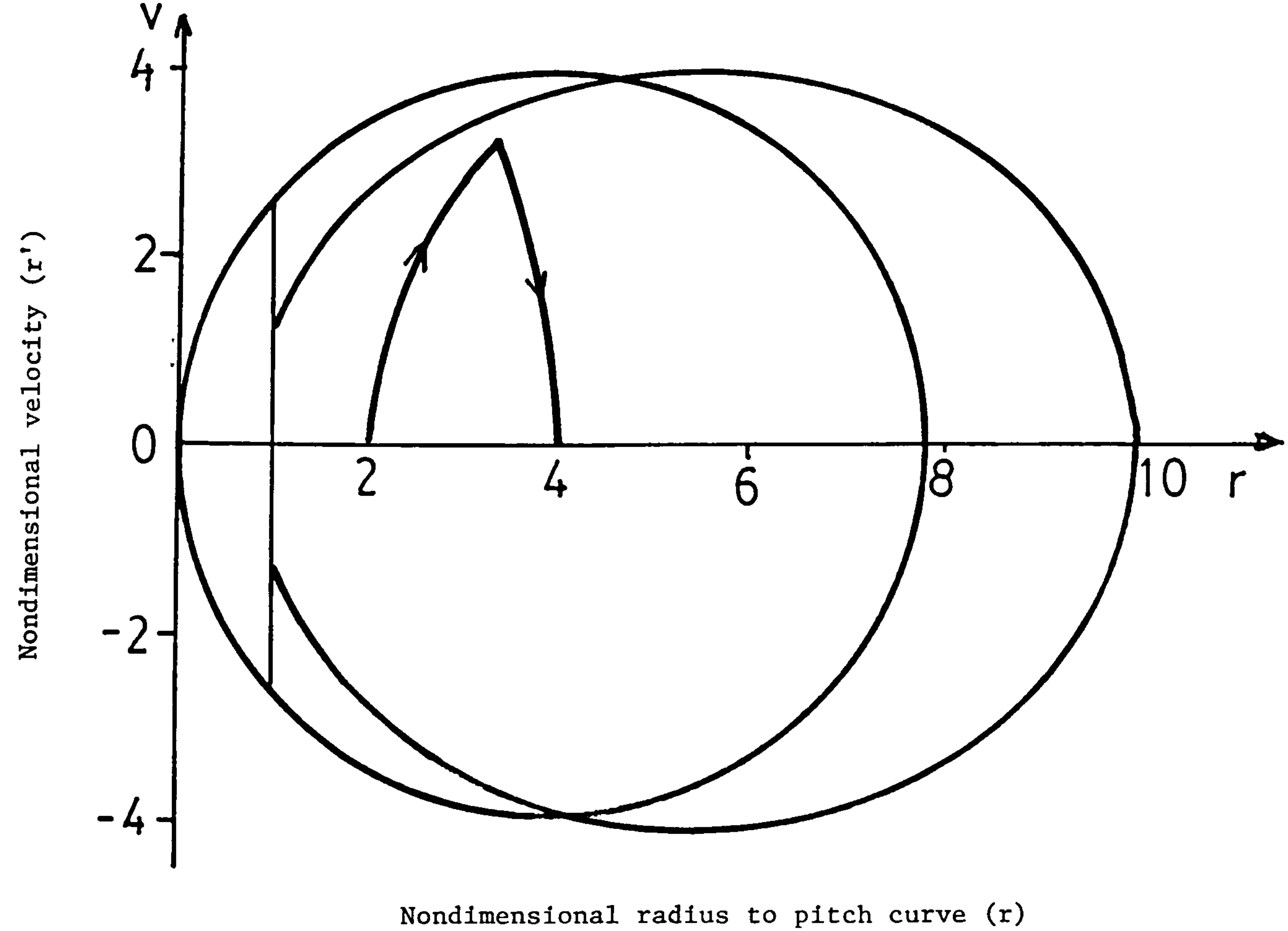

Figure 3.11. Rise movement in the phase plane for case 5.

Table 3.7. Values of the Roots Given by Equation (2.104).

$\psi°$	r_1	v_1	r_2	v_2
0	10.000	0.000	1.000	0.000
10	9.567	1.687	0.998	0.176
20	8.354	3.040	0.993	0.362
30	6.592	3.806	0.985	0.569
40	4.601	3.860	0.977	0.820
50	2.688	3.203	0.988	1.178
52	2.330	2.982	1.002	1.282
57	1.311	2.018	1.233	1.898

The movement is defined in Table 3.8. The acceleration at constant rate is maintained during 46° to the transition point. Then there is a switch to the maximal stress constraint using the nondimensional stress $\alpha = 6$. After 29° the maximal position is reached for $r_{max} = 4$.

Thus, the total angle of rotation to obtain a nondimensional lift $h^* = 2$ is 75°. We have improved the solution by lowering the rotation by 5° with respect to the value obtained for $\gamma = 0$. Figure 3.12 shows the lift versus rotation of the cam for the values of Table 3.8.

Solution for Angular Velocity Ratio $\gamma = 0.2$

With the better results obtained using $\gamma = 0.1$ in a low angular velocity case, we consider an increase in the speed in the low angular velocity to $\gamma = 0.2$. We first draw in the phase plane, the circle of singularity. Its diameter is $\delta = 5.48$.

The roots given by Eq. (2.104) are now smaller with $z = 5$ for $\psi = 0$ and approximately $z = 1.75$ for $\psi = 52°$. Now the upper dwelling position is outside the circle of singularity but our stroke from $r_{min} = 2$ to $r_{max} = 4$ is in the feasible region. However the velocity is restricted to a maximum value of $v = 2$ to stay in the feasible region. In the last case we used values of v as high as $v = 3.211$. Seeing Fig. 3.13 we conclude that is impossible to use an acceleration $r'' = 4$. We have to lower it to maintain movement inside the feasible region. On doing this we will lose immediately our speed of response in the positive acceleration and also in the total motion from $r_{min} = 2$ to $r_{max} = 4$. We will not go further for the case $\gamma = 0.2$ and it is better to study the case where the motion is in the region of high angular velocity.

Table 3.8. Trajectory of the Pitch Curve and Angle of Pressure Versus Cam Rotation for Case 5.

$\theta°$	r	r'	$\psi°$
0	2.000	0.000	0.0
10	2.061	0.698	18.7
20	2.244	1.396	31.9
30	2.548	2.094	39.4
40	2.975	2.793	43.2
46[a]	3.289	3.211	44.3
50	3.464	2.584	36.7
60	3.812	1.454	20.9
70	3.979	0.477	6.8
75	4.000	0.000	0.0

[a]Transition point.

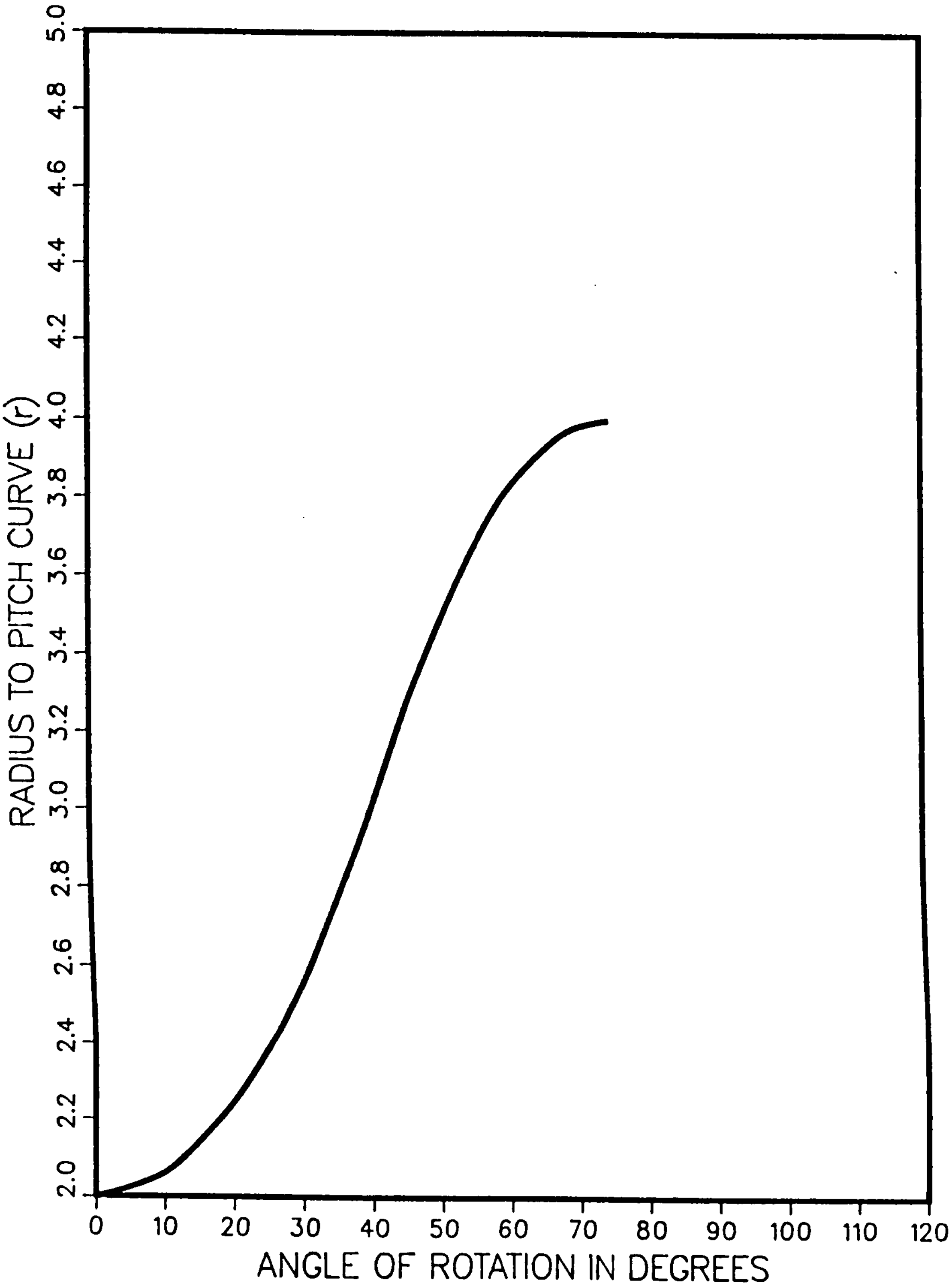

Figure 3.12. Displacement diagram for case 5.

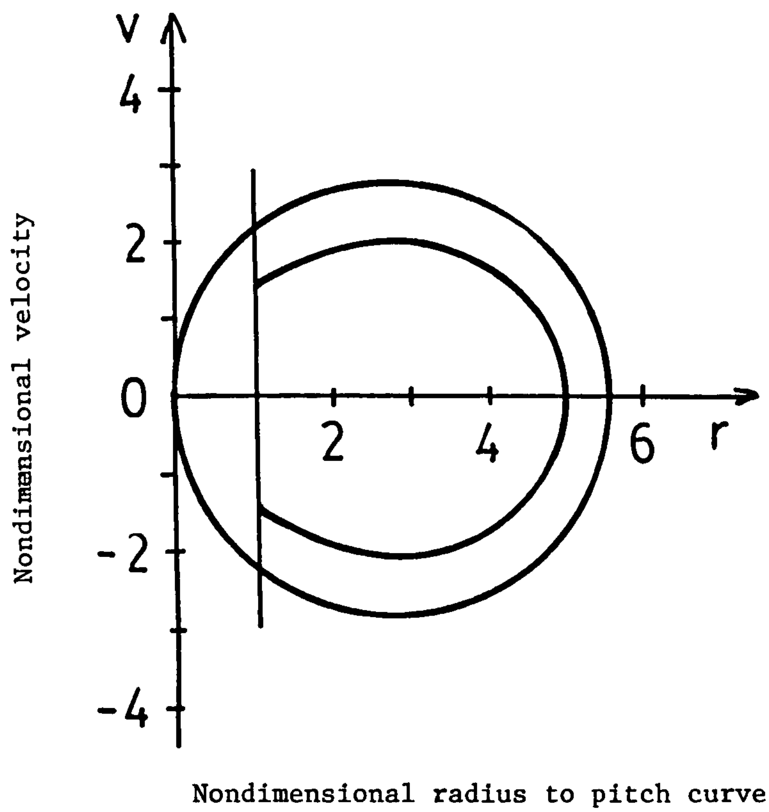

Figure 3.13. Phase plane diagram for case 6. $\alpha = 6$, $\beta = -1$, $\gamma = 0.2$.

Solution for Angular Velocity Ratio
$\gamma = 0.5$

We proceed as before. The data for this case is $\alpha = 6$, $\beta = -1$, $\gamma = 0.5$. We first draw in the phase plane the circle of singularity. Its diameter is $\delta = \sqrt{\alpha/\gamma} = 3.46$. Second, we plot the curve given by the roots of Eq. (2.104) as a function of ψ, we obtain a smaller curve with maximum value $z = 2$ that occurs at $\psi = 0$ (i.e., $r = 2$, $v = 0$), and a minimum value $z = 1.60$ that occurs at $\psi = 51°$. The plot stop in this angle because the region defined by $r < 1$ is unfeasible. All this information can be seen in Fig. 3.14. The situation is follows. The lower extremal dwelling position is at $r_2 = 1$ and is inside the circle of singularity. The upper extremal dwelling position $r_1 = 6$ is outside of the circle of singularity and is a center. Now the lower dwelling position set for this problem is $r_{min} = 2$ situated in the unfeasible region. The upper dwelling position is $r_{max} = 4$ and is situated in a feasible region of high angular velocity outside the circle of singularity. If we use the maximal stress constraint $\alpha = 6$ at $r = 4$, $v = 0$ we will obtain positive acceleration rather than deceleration. That indicates that we have to reformulate our lower and upper dwelling position. On doing that we set $r_{min} = 4$, $r_{max} = 6$, and $h^* = 2$.

Now our problem is a typical case of high angular velocity. We first obtain positive acceleration using maximal stress constraint with $\alpha = 6$. At the transition point we shift to low stress constraint with $\alpha = 0$. On following the ellipse in the phase plane we arrive at the upper dwelling position $r_{max} = 6$, which is also the maximal possible dwelling position (i.e., $r_1 = 6$).

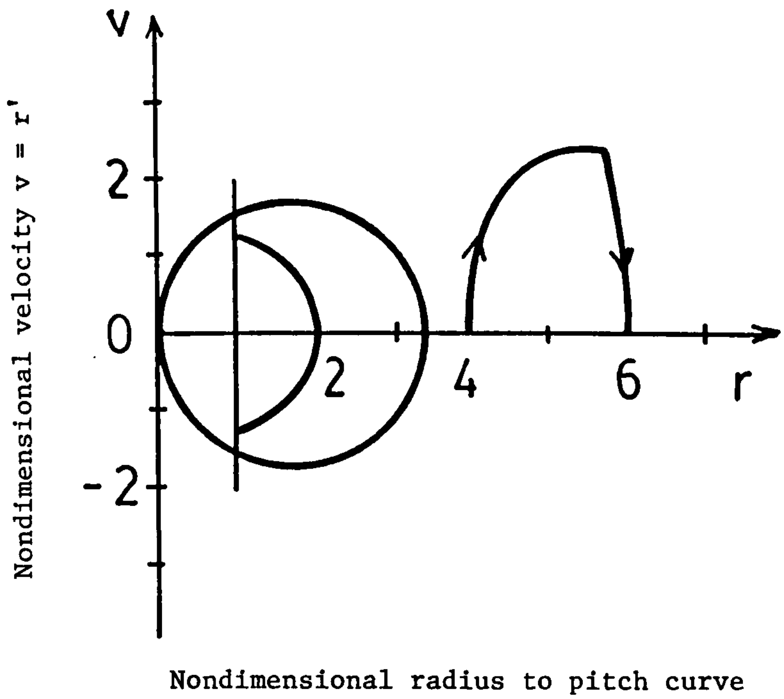

Figure 3.14. Rise movement in the phase plane at high angular velocity ratio. $\alpha = 6$, $\beta = -1$, $\gamma = 0.5$, $\theta_f = 64°$.

The solution can be described as follows. Using maximal stress constraint $\alpha = 6$ we go from $r = 4$, $v = 0$ to the transition point $r = 5.689$, $v = 2.418$ using 50° of rotation of the cam, then shifting to low stress $\alpha = 0$ we move from the transition point decelerating using all the spring force and arriving at the upper dwelling position after additional 14° of rotation of the cam, see Table 3.9 and Figs. 3.15 and 3.16.

The total angle of rotation for the lift $h^* = 2$ is 64°, which is 11° lower than the case studied using angular velocity ratio $\gamma = 0.1$.

We will stop here with the nondimensional application. We have already achieved a good understanding of the model, especially how the parameters α, β, and γ and the initial conditions influence the speed of response of the system.

Numerical Example

For completing the presentation of the applications, we will present an example with a case of a timing valve of an internal combustion engine. The valve train corresponds to a car engine of 302 cubic inches built by Ford Company. This engine uses a four stroke spark ignition cycle, the valves are situated in the cylinder head.

The system has a camshaft connected to the crankshaft with a speed reduction ratio of two. A flat follower is used and is connected with a push rod, rocker arm, and valve. A spring retainer and spring valve is mounted in the cylinder head to close the valve and to maintain contact between the follower and cam during the deceleration of the valve system (see Fig. 3.17).

Table 3.9. Trajectory of the Pitch Curve and Angle of Pressure Versus Cam Rotation for a High Angular Velocity Ratio.

$\theta°$	r	r'	$\psi°$
0	4.000	0.000	0.0
10	4.146	1.446	19.2
20	4.457	2.043	24.6
30	4.842	2.337	25.8
40	5.262	2.448	24.9
50	5.689	2.418	23.0
55	5.877	1.558	14.8
60	5.976	0.697	6.7
64	6.000	0.000	0.0

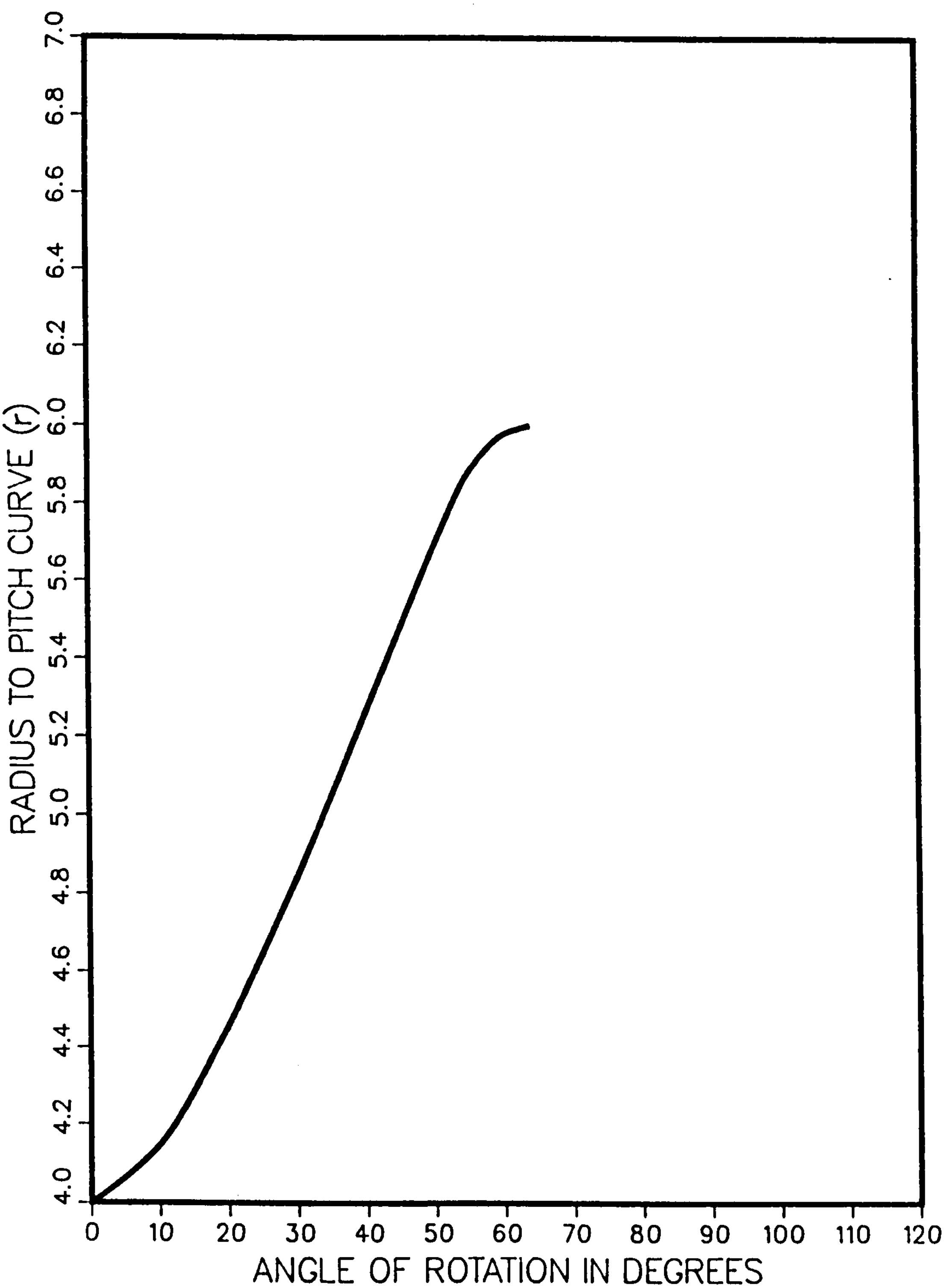

Figure 3.15. Displacement diagram at high angular velocity ratio.

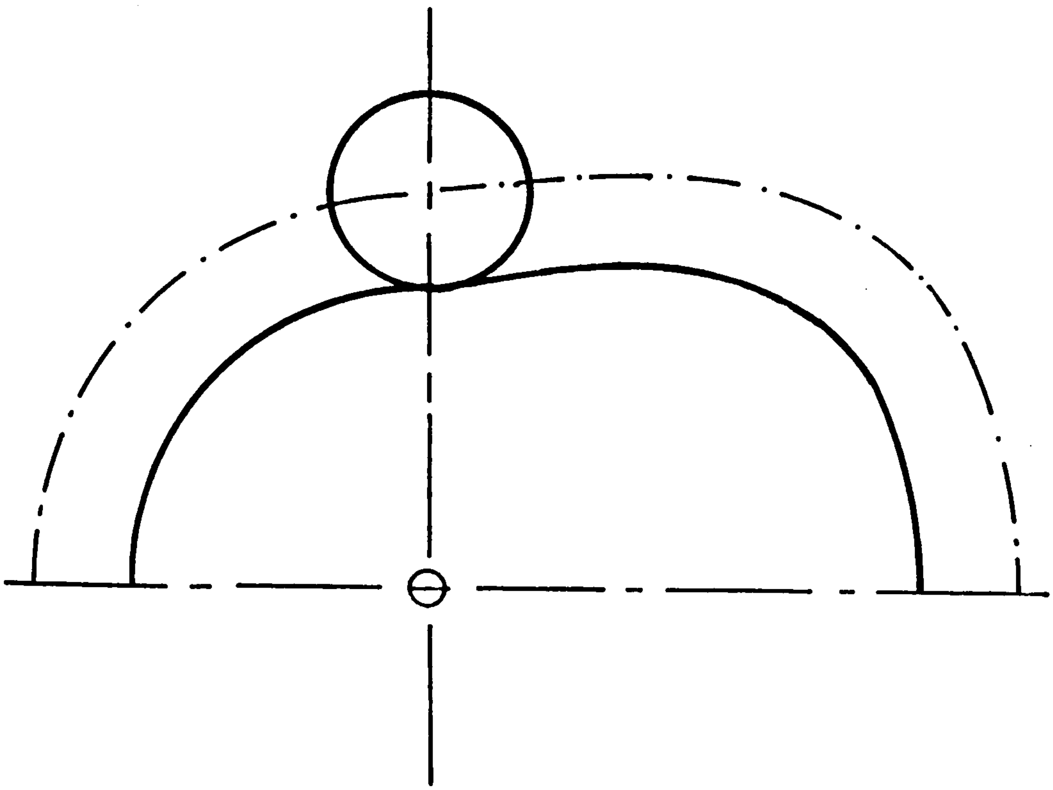

Symmetric with respect to the abscissa.

Figure 3.16. Cam contour at high angular velocity ratio.

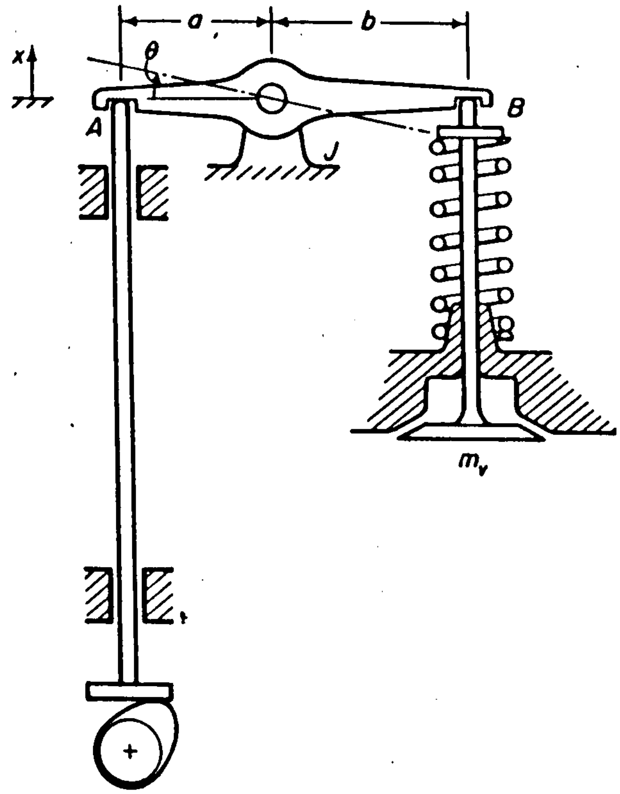

Figure 3.17. Engine valve system.

The system described uses a flat follower. We will modify the follower to a roller follower type, but will retain the rest of the components. The weight of the components is as follows:

valve:	0.1133 kg
spring retainer:	0.0321 kg
spring valve:	0.1204 kg
rocker arm:	0.1022 kg
push rod:	0.0439 kg
follower:	0.1055 kg

We determine the equivalent mass at A of the valve, spring retainer, spring valve, and rocker arm. To do this we need the geometrical dimensions of the rocker arm (see Fig. 3.17).

The equivalent mass at the point A is evaluated using the following expression

$$m_A = \frac{J + (m_v + \frac{1}{3}m_s)b^2}{a^2} \tag{3.1}$$

m_A: equivalent mass at A (valve, spring retainer, spring valve and rocker arm).

J: moment of inertia of the rocker arm with respect to the axis of rotation.

m_v: mass of the valve plus mass of the spring retainer.

m_s: mass of the spring.

a: arm distance of the rocker arm to the point of action of the push rod.

b: arm distance of the rocker arm to the point of action of the valve.

A measure of the rocker arm yielded a = 35 mm, and b = 22 mm. The moment of inertia of the rocker is estimated as

$$J = \frac{m_r l^2}{20} \tag{3.2}$$

where m_r: mass of the rocker arm.

l: length of the rocker arm.

With the data m_r = 0.1022 kg, and l = 76 mm and using Eq. (3.2) we find that J = 29.52 kg-mm^2.

Let us evaluate m_A using Eq. (3.1),

$$m_A = \frac{29.59 \text{ kg-mm}^2 + (0.1133 + 0.032 + \frac{0.1204}{3}) \text{ kg } (35 \text{ mm})^2}{(22 \text{ mm})^2} = 0.5305 \text{ kg}$$

Now to determine the total equivalent mass m we have to add to m_A the mass of the push rod and the mass of the follower (we estimate the mass of the roller follower to be about the same as the mass of the flat follower). On doing that,

$$m = 0.5305 + 0.0439 + 0.1055 \text{ [kg]}$$

$$m = 0.6799 \text{ kg.}$$

Next, the spring rate k is calculated using the well known formula,

$$k = \frac{G\, d^4}{64\, n\, r_m^3} \tag{3.3}$$

where k: spring rate,

G: shear modulus,

d: diameter of the wire,

n: number of turns of the coil, and

r_m: mean radius of the coil.

The data of the spring valve is:

$D_e = 38.1$ mm

$d = 5.6$ mm

$n = 4$

$G = 8 \times 10^5$ kp/cm^2

where D_e: exterior diameter of the coil,

kp: kilopond defined as the attraction force exerted by the earth over a mass of 1 kilogram (1 kp = 9.807N), and

N: Newton unit of force of S.I. system.

r_m can be evaluated using the geometrical relationship,

$$r_m = \frac{D_e - d}{2} = 16.25 \text{ mm}$$

Substituting the numerical values above into Eq. (3.3), yields

$$k = \frac{8 \times 10^3 \frac{\text{kp}}{\text{mm}^2} (5.6 \text{ mm})^4}{(64)(4)(16.25 \text{ mm})^3} = 7.162 \frac{\text{kp}}{\text{mm}}$$

or

$$k = 70{,}239 \frac{\text{N}}{\text{m}} .$$

Now that we have a physical model that corresponds to the model presented in this study, we can use it to study the speed of response of the roller follower cam driven system.

We assume that the car engine presented in this example is rotating at 2,600 rpm then the camshaft is rotating at 1,300 rpm or $\omega = 136.1$ rad/s.

At this time we can determine the angular velocity ratio γ. Let us recall Eq. (2.26)

$$\gamma = \frac{\omega^2}{k/m} .$$

Substituting values into Eq. (2.26), we obtain

$$\gamma = \frac{(136.1 \frac{rad}{s})^2 \ 0.6799 \text{ kg}}{70{,}239 \ \frac{N}{m}}$$

or,

$$\gamma = 0.179 \text{ (nondimensional)} .$$

The next step is to determine the maximum nondimensional stress s, which is

$$s = \frac{\sigma_{max}^2}{Ck}$$

where

$$\frac{1}{C} = \pi w\left(\frac{1 - \mu_1^2}{E_1} + \frac{1 - \mu_2^2}{E_2}\right) .$$

We select from reference [19, page 151], σ_{max} = 220,000 psi, $\mu_1 = \mu_2 = 0.3$, $E_1 = E_2 = 30 \times 10^6$ psi. Transforming to the S.I. system yields,

$$\sigma_{max} = 220{,}000 \text{ psi} \times 6.8948\ 10^3 \frac{\text{Pa}}{\text{psi}}$$

$$= 1516.9\ 10^6 \text{ Pa},$$

$$E = 30 \times 10^6 \text{ psi} \times 6.8948\ 10^3 \frac{\text{Pa}}{\text{psi}}$$

$$= 206.8\ 10^9 \text{ Pa}$$

On substituting into the expression for 1/C, we obtain

$$\frac{1}{C} = \frac{2\pi(0.91)w}{206.8\ 10^9 \text{ Pa}}, \quad (w \text{ in m})$$

and,

$$\frac{1}{C} = 0.02765\ 10^{-9}\ w \frac{\text{m}}{\text{Pa}}.$$

Now substituting σ_{max}, k, and 1/C into the above expression for s, yields

$$s = \frac{(1516.9\ 10^6 \text{ Pa})^2 \times 0.02765\ 10^{-9}\ w \frac{\text{m}}{\text{Pa}}}{70{,}239 \frac{\text{N}}{\text{m}}}$$

or

$$s = 905.8\ w;\ (w \text{ in m}), \tag{3.4}$$

s results nondimensional.

We have to select the roller follower for this problem. This will fix the value of s which is the maximal nondimensional stress. We select a roller with radius R_f = 10 mm and width w = 6.5 mm.

Substituting for w into Eq. (3.4), one obtains

$$s = 5.89 \text{ nondimensional}$$

Now we must select the prestress number β. For this we have to consider the base radius of the cam which is taken to be 16 mm, the free height of the spring and its maximum possible deflection. The geometrical data of the spring is

free height l = 53 mm.

maximum deflection Δ = 25 mm.

Also we need to know the lift of the cam h, which is related to the lift of the valve h_v by Eq. (3.5). Namely,

$$h = \frac{h_v a}{b} . \tag{3.5}$$

By knowing the diameter of the valve D_v, h_v can be obtained. Normally h_v is a quarter of D_v in this case D_v = 46 mm from which we find

$$hv = 11.5 \text{ mm.}$$

On substituting h_v into Eq. (3.5), one finds

$$h = 7.23 \text{ mm.}$$

For the prestress parameter we select $\beta = -1.4$. We must now check the spring's dimensional compatibility with its spring prestress β and deflection. Based on the definition of β, the equilibrium position of the center of the roller is -1.4 unit away from the center of the cam (the negative sign indicating that the roller center is above the cam center). Thus, the bottom surface of the roller at equilibrium is 0.4 units above the center of the cam. Since the roller follower has a radius $R_f = 10$ mm, then when the spring is at its free height the bottom surface of the roller is 4 mm away from the center of the cam. Since the base radius is 16 mm, the roller will be pushed 12 mm and the spring is compressed the same amount. As shown above, the lift of the follower is 7.23 mm so that the deflection of the spring will be

$$12 + 7.23 = 19.23 \text{ mm.}$$

The maximum deflection allowed for the spring is 25 mm. Therefore the selection of the value of $\beta = -1.4$ is adequate and we can begin to solve for the angle of rotation of the cam for the given lift h.

The nondimensional lift h^* is obtained with the formula

$$h^* = \frac{h}{R_f} ,$$

thus,

$$h^* = 0.723 \text{ (nondimensional)} .$$

With the values of $\alpha = 5.89$ and $\beta = -1.4$ we obtain the lowest dwelling condition at $r = 1.4$ and the upper extreme dwelling condition at

$$r_1 = \frac{\alpha - \beta + \sqrt{\Delta}}{2}$$

where $\Delta = (\alpha - \beta)^2 - 4\alpha$.

For $\alpha = 5.89$, and $\beta = -1.4$ we obtain

$$r_1 = 6.365.$$

In this problem we are working between $r_{min} = 2.6$ and $r_{max} = 3.323$, which are within the limits.

The diameter of the circle of singularity is given by

$$\delta = \sqrt{\frac{\alpha}{\gamma}}$$

and,

$$\delta = 5.74 \ .$$

r_{min}, r_{max} and the circle of singularity can now be drawn in the phase plane. The next step is to solve Eq. (2.104), which gives the geometrical constraint curve. That with the circle of singularity determines the feasible region in the phase plane.

With the data $\beta = -1.4$ and $\gamma = 0.179$ we run a computer program which solves numerically obtaining Table 3.10. The geometrical

Table 3.10. Values of the Geometrical Constraint Curve, for the Numerical Example.

$\psi°$	r_1	v_1	r_2	v_2
0	5.032	0.000	1.554	0.000
5	4.971	0.435	1.555	0.136
10	4.791	0.845	1.559	0.275
15	4.498	1.205	1.567	0.420
20	4.104	1.494	1.581	0.576
25	3.618	1.687	1.609	0.751
30	3.040	1.755	1.671	0.965
35	2.241	1.569	1.918	1.343

Parameters: $\beta = -1.4$; $\gamma = 0.179$.

constraint curve and the circle of singularity is then drawn in the phase plane (see Fig. 3.18).

The optimal solution for the lift problem in this numerical example, which stays within the feasible region, is obtained by accelerating at the constant rate $r'' = 2.7$ during 36° of cam rotation then switching to maximum stress constraint $\alpha = 5.89$ for the deceleration part of the rise stroke during 14°. The maximum lift of the valve is achieved in 50° of rotation and the performance can be considered acceptable for an adaptation (see Table 3.11). Furthermore because all data was real we can be sure that the example has geometrical compatibility.

The total figure for the timing of the valve will be:

rise 50°

dwell 20°

return 50°

dwell 240°

The lift diagram, and the contour of the cam can be seen in Figs. 3.19 and 3.20 respectively.

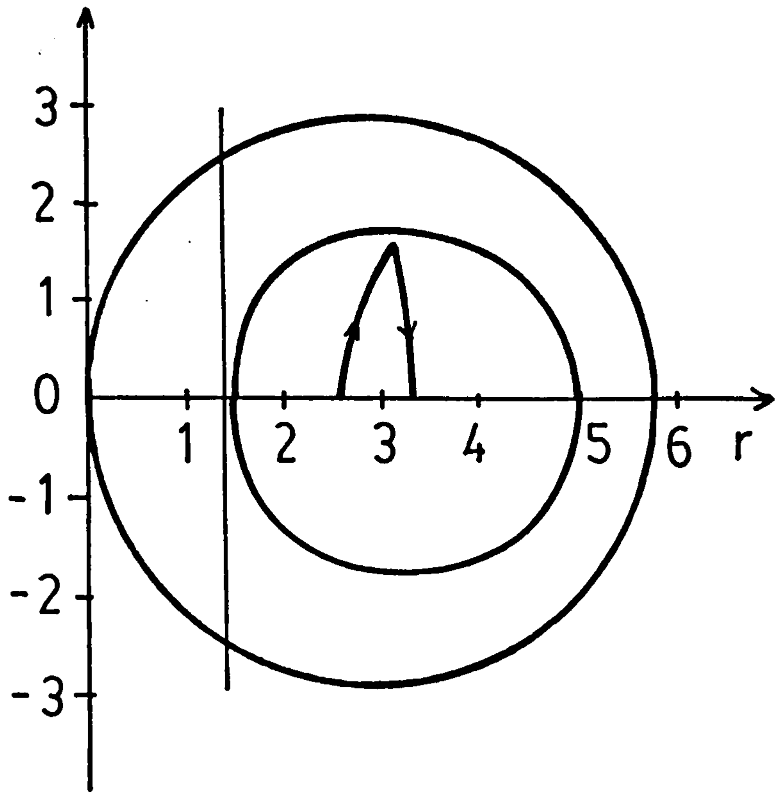

Figure 3.18. Phase plane trajectory for numerical example. $\alpha = 5.89$, $\beta = -1.4$, $\gamma = 0.179$.

Table 3.11. Trajectory of the Pitch Curve, Angle of Pressure and Stress Versus Cam Rotation for Numerical Example.

$\theta°$	r	r'	r''	$\psi°$	α
0	2.600	0.000	2.7	0.0	1.66
5	2.610	0.236	2.7	5.2	1.69
10	2.641	0.471	2.7	10.1	1.79
15	2.692	0.707	2.7	14.7	1.92
20	2.764	0.942	2.7	18.8	2.12
25	2.857	1.178	2.7	22.4	2.36
30	2.970	1.414	2.7	25.5	2.63
35	3.103	1.649	2.7	28.0	2.93
36[a]	3.129	1.683	-9.1	28.3	5.89
40	3.227	1.129	-7.1	19.3	5.89
45	3.299	0.546	-6.4	9.3	5.89
50	3.323	0.000	-6.2	0.0	5.89

[a]Transition point: $s = 5.89$, $\beta = -1.4$, $\gamma = 0.179$.

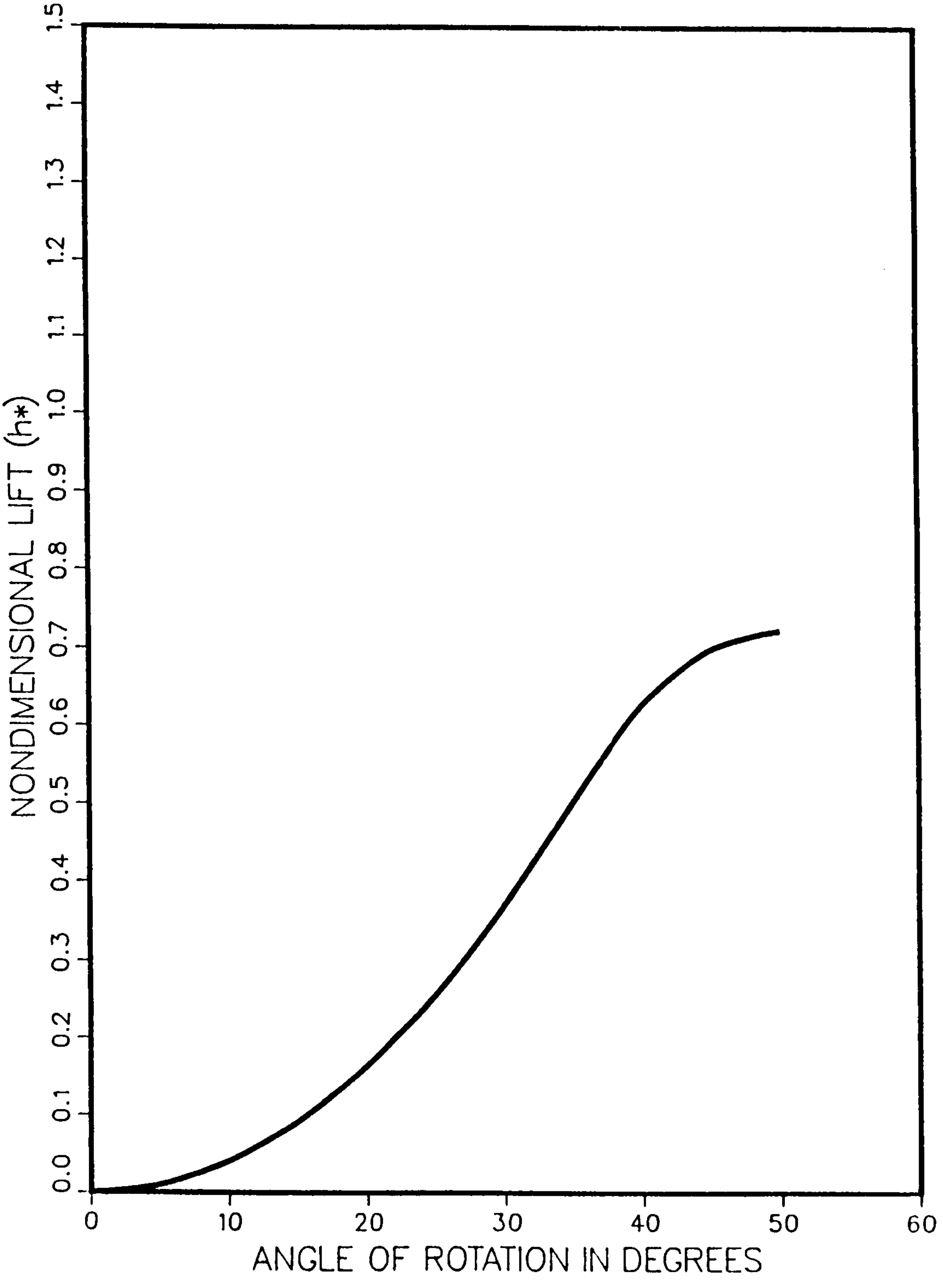

Figure 3.19. Displacement diagram for numerical example.

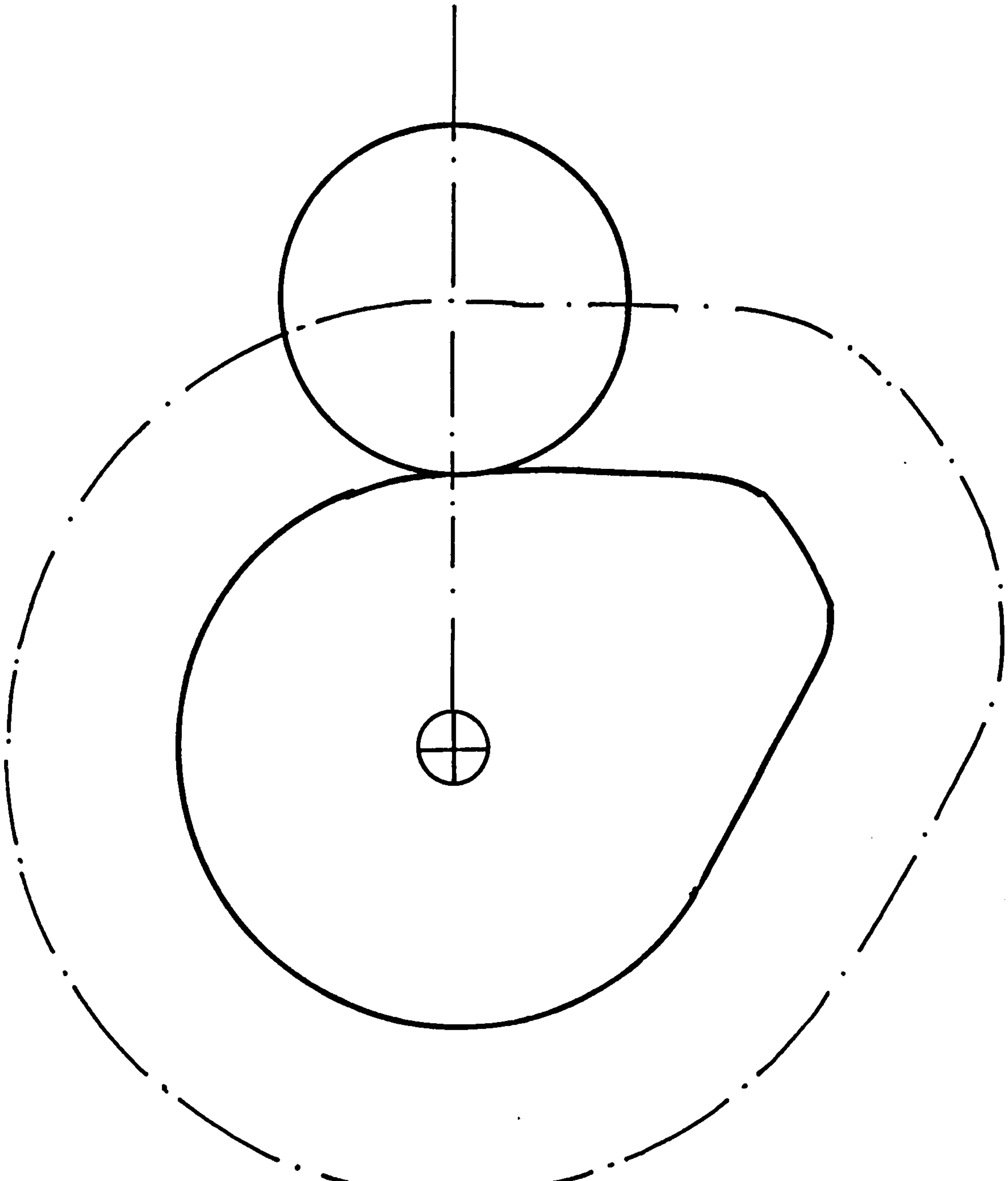

Figure 3.20. Cam contour for numerical example.

CHAPTER 4

CONCLUSIONS

The analogy of the simple Bang-Bang problem proved to be important in finding an approach on the solution of a maximal speed of response of a roller follower cam plate system.

The change of variable $z^2 = r^2 + (r')^2$ is efficient in showing the governing ordinary differential equation in a compact form in the original second order autonomous O.D.E. and in the first order O.D.E. in the phase plane.

The three nondimensional parameters α, β, γ, and the initial conditions define the type of solution, which for the general case has only numerical solution.

Giving the value zero to the nondimensional prestress (i.e., $\beta = 0$), the first order O.D.E. in the phase plane reduces to a linear one, which has always solution by quadratures. Also an additional restriction for the value of the angular velocity ratio equal to zero (i.e., $\beta = 0$, $\gamma = 0$) represent the homogenous solution of the linear O.D.E. in the phase plane.

The special case of only the parameter $\gamma = 0$ reduces the first order O.D.E. in the phase plane to the Abel equation but no close form solution was found. But a new change of variable reduces the Abel equation to only one governing parameter, which is interesting for the tabulation of the solution.

In low angular velocity the additional constraint of bounding the acceleration was necessary that means apply the old criteria, but the deceleration phase is governed by the stress constraint and the solution given in the work is optimal.

In high angular velocity the acceleration and deceleration are governed by the stress constraint and the solution of the initial value problem gives the optimal solution for the complete rise stroke.

The return stroke has symmetri with the rise stroke, that come from the even power of the velocity on the governing second order O.D.E.

The major finding is the region of true physical solution in the phase plane which result in the combination of the circle of singularity and the geometrical constraint curve.

The optimal result obtained in the numerical example angle of rotation for the lift or return of a valve was found to be 50° which is adequate. In the literature reference [12] states that for aircraft piston engines a rotation of 45° was achieved in lifting the valves, but in that case the design was optimized for a specific application where one could select the parameters in favor of an optimal result.

Future research in this area can be expanded to the possibility of adding viscous damping. This will introduce a fourth nondimensional parameter to the second order ODE and all of the solutions have to be reworked.

Another research area is to introduce the elasticity of the train valve mechanism, which implies a study of vibrations and dynamic response of the valve due to the forced displacement of the follower under the cam action.

LIST OF REFERENCES

LIST OF REFERENCES

1. Angel, Bellman, Dynamic Programming and Partial Differntial Equations (Mathematics in Science and Engineering), Vol. 88, Acedmic Press, New York, 1972.

2. Bateman, Harry, Differential Equations, Chelsea Publishing Company, New York, 1966.

3. Bazaraa, Mokhtar S., and Shetty, C. M., Nonlinear Programming, John Wiley and Sons, Inc., New York, 1979.

4. Bellman, Richard, Dynamic Programming, Princeton University Press, Princeton, New Jersey, 1957.

5. Beran, Thomas, The Theory of Machines, Longmans, Green and Co., London, New York, 1945.

6. Boutroux, Pierre, LeCons Sur Les Fonctions Definies Par Les Equations Differentielles Du Premier Ordre, Gauthier-Villars, Imprimeur-Libraire, Paris, 1908.

7. Chen, Fan Y., Mechanics and Design of Cam Mechanisms, Pergamon Press, 1982.

8. Cooper, Duane H., "Hertzian Contact-Stress Deformation Coefficients," Journal for Applied Mechanics, Transactions of the ASME, June 1969.

9. Davis, Harold T., Introduction to Nonlinear Differential and Integral Equations, Dover Publications, Inc., New York, 1962.

10. Elsgolc, L. E., Calculus of Variations, (International Series of Monographs in Pure and Applied Mathematics), Vol. 19, Pergamon, Press, New York, 1961, 1963.

11. Fel'Dbaum, A. A., Optimal Control System, (Mathematics in Science and Engineering), Vol. 22, Academic Press, New York, 1965.

12. Fraas, Arthur P., Aricraft Power Plants, McGraw-Hill Book Company, Inc., New York, 1943.

13. Gelfand, and Fommin, Calculus of Variations, Prentice-Hall, Inc., New Jersey, 1964.

14. Gottfied, and Weismann, Introduction to Optimatization Theory, (International Series in Industrial and Systems Engineering), Prentice-Hall, Inc., Englewood Cliffs, New Jersey, 1973.

15. Hagin, Frank G., A First Course in Differential Equations, Prentice-Hall, Inc., New Jersey, 1975.

16. Hochstadt, Harry, Differential Equations A Modern Approach, Dover Publications, Inc., New York, 1975.

17. Ince, E. L., Ordinary Differential Equations, Dover Publications, New York, 1944.

18. Jacobs, O. L. R., An Introduction to Dynamic Programming, The Theory of Multistage Decision Processes, Chapman and Hall LTD, London, 1967.

19. Jensen, Preben W., Cam Design and Manufacture, The Industrial Press, New York, 1965.

20. Jones, J. Rees, Cams and A Cam Mechanism, Mechanical Engineering Publications Ltd., Birmingham, Alabama, 1978.

21. Kamke, E., Differential Gleihungen Lösungsmethoden und Lösungen, Akademische Verlagsgesellschaft Becker & Erler Kom.-Ges., Leipzig, 1943.

22. Kaplan, Wilfred, Ordinary Differential Equations, Addison-Wesley Publishing Company, Inc., 1962.

23. Kreyszig, Erwin, Advanced Engineering Mathematics, 4th ed., John Wiley & Sons, Inc., 1979.

24. Martin and Reissmer, Elementary Differential Equations, 2nd ed., Addison-Wesley Publishing Company, Inc., Massachusetts, 1961.

25. Mayfeh and Mook, Nonlinear Oscilations, John Wiley & Sons, Inc., New York, 1979.

26. Neklutin, C. N., Mechanisms and Cams for Automatic Machines, American Elsevier Publishing Company, Inc., New York, 1969.

27. Petrov, Iu. P., Variational Methods in Optimum Control Theory, (Mathematics in Science and Engineering), Vol. 45, Academic Press, New York and London, 1968.

28. Pierre, Donald A., Optimization Theory With Applications, Dover Publications, Inc., New York, 1986.

29. Rainville, Earl D., Intermediate Differential Equations, 2nd ed., Chelsea Publishing Company, New York, 1972.

30. Rothbart, Harold A., Cams Design, Dynamics, and Accuracy, John Wiley & Sons, Inc., New York, 1956.

31. Roxin, Emilio O., Ecuaciones Diferenciales Ordinarias y Teoria de Control, Editorial Universitaria de Buenos Aires, 1968.

32. Selby, Samuel M., Standard Mathematical Tables, 18th ed., The Chemical Rubber Co., Cleveland, Ohio, 1970.

33. Speckhart, Frank H., and Euler, James A., "Design of Maximum Acceleration Plate Cam Profiles Subject to Stress and Curvature Constraints," American Society of Mechanical Engineering, 84-DET-131, 1984.

34. Stoker, J. J., Nonlinear Vibrations, (Mechanical and Eletrical Systems), Interscience Publishers, Inc., New York, 1950.

35. Struble, Raimond A., Nonlinear Differential Equations, McGraw-Hill Book Company, Inc., New York, 1962.

36. Szekely, Julian, and Foreman, Fred, "Megaflops and CAD/CAM in Metals Processing," The Journal of Metals, The Metallurgical Society, October 1986.

37. Tesar, Delbert, and Matthew, Gary K., The Dynamic Synthesis Analysis, and Design of Modeled Cam Systems, Lexington Books D. C. Heath and Company, Lexington, Massachusetts, 1976.

38. Westermann, Baldomero, Fast Movement of a Roller Follower Plate Cam Driven System, Master Thesis, University of Tennessee, Knoxville, August 1985.

APPENDIX

```
C         THIS PROGRAM DETERMINE PART OF THE PHASE
C       PLANE WHERE THE SOLUTION IS PHYSICALLY. VALUES
C       OF BETA AN GAMMA ARE REQUIRED THE SOLUTION WILL
C       BE IN POLAR FORM WITH THE PAIR PSI,Z. THEN WIL
C       BE CONVERT INTO CARTESIAN COORDINATES.
C
        REAL BETA,GAMMA,PSI,Z1,Z2,C,A1,DELTA,SQRTDEL
        INTEGER J
C
C       USE DO LOOP FOR GENERATING A SET OF VALUES
C
        BETA=-1.4
            GAMMA=0.179
        WRITE(41,*) 'BETA=',BETA,'GAMMA=',GAMMA
        WRITE(41,*) 'ANGLE,  R2,    V2,    R1,    V1'
        DO 10 J=1,91
            PSI=91-J
            THETA=PSI*3.14159/180
            C=COS(THETA)
            S=SIN(THETA)
            A1=2*GAMMA+(1-GAMMA)*C**2
            DELTA=A1**2+4*BETA*GAMMA*C
            IF (DELTA) 20,30,40
   20       WRITE(41,*) PSI,'COMPLEX ROOTS'
            GO TO 10
   30         Z1=A1/2/GAMMA
            Z2=Z1
            GO TO 50
   40       SQRTDEL=SQRT(DELTA)
            Z1=(A1+SQRTDEL)/2/GAMMA
            Z2=(A1-SQRTDEL)/2/GAMMA
   50       R1=Z1*C
            R2=Z2*C
            V1=Z1*S
            V2=Z2*S
            WRITE(41,*) PSI,R2,V2,R1,V1
   10     CONTINUE
        STOP
        END
```

```
C       PROGRAM STRESS
C       CALCULATE THE TRAJECTORY OF THE PITCH
C       CURVE WITH STRESS CONSTRAINT.
C
C       THIS PROGRAM USE THE SUBROUTINE DVERK
C       FROM THE IMSL LIBRARY (A SET OF FOR-
C       TRAN SUBROUTINES FOR MATHEMATICS AND
C       STATISTICS). DVERK IS A DIFFERENTIAL
C       EQUATION SOLVER RUNGE KUTTA-VERNER
C       FIFTH AND SIX ORDER METHOD.
C
        INTEGER N,IND,NW,IER,K,NTIME
        REAL*8 Y(2),C(24),W(2,9),X,TOL,XEND
        EXTERNAL FCN
        NW=2
        N =2
        A=5.89
        B=-1.4
        GAMMA=0.179
        WRITE(40,*) '   A=',A,'   B=',B,'   GAMMA=',GAMMA
        NTIME=50
        WRITE(40,*) '  THETA=',NTIME
        WRITE(40,*) '  THETA,   RADIUS,   VELOCITY,'
       *  '    PRESSURE   ANGLE,   AND   ACCELERATION'
        X =0.0D0
        Y(1) =3.323D0
        Y(2) =0.0D0
        Y1=Y(1)
        Y2=Y(2)
C
C       PREANG: PRESSURE ANGLE
C
        PREANG=(180/3.141593)*DATAN(Y(2)/Y(1))
C
C       DETERMINE THE ACCELERATION R2 AS A FUNCTION
C       OF A, B, GAMMA AND THE STATE VARIABLES Y(1)
C       AND Y(2).
C
        Z=SQRT(Y1**2+Y2**2)
        R2=(B+Y1)*Z**4
        R2=R2-A*Y1*(Z**3-2*Z**2+Y1**2)
        R2=R2/(A*Y1**2-GAMMA*Z**4)
        K=0
        WRITE(40,*) K,Y1,Y2,PREANG,R2
        TOL=0.001D0
        IND =1
        DO 10 K=1,NTIME
           XEND=0.017453D0*DFLOAT(K)
           CALL DVERK(N,FCN,X,Y,XEND,TOL,IND,
       *                   C,NW,W,IER)
           IF(IND.LT.0.OR.IER.GT.0)GO TO 20
```

```
C
C       Y(1) AND Y(2) ARE THE CURRENT
C       SOLUTIONS VALUES AT X.
C
      Y1=Y(1)
      Y2=Y(2)
      PREANG=(180/3.141593)*DATAN(Y(2)/Y(1))
      Z=SQRT(Y1**2+Y2**2)
C
C
C
C
      R2=(B+Y1)*Z**4
      R2=R2-A*Y1*(Z**3-2*Z**2+Y1**2)
      R2=R2/(A*Y1**2-GAMMA*Z**4)
          WRITE(40,*) K,Y1,Y2,PREANG,R2
   10 CONTINUE
      STOP
   20 CONTINUE
C
C         HANDLE IND.LT.0 OR IER.GT.0
C         ITEMS THAT MAY HELP DIAGNOSE THE
C         PROBLEM SHOULD BE OUTPUT HERE.
C         IND,TOL,N,W,Y(1),...,Y(N),XEND,AND
C         C(1),...,C(24).
C
      STOP
      END
      SUBROUTINE FCN(N,X,Y,YPRIME)
      INTEGER N
      REAL*8    A,B,C,Y(N),YPRIME(N),X
      A=5.89D0
      B=-1.4D0
      C=0.179D0
      YPRIME(1)=Y(2)
      YPRIME(2)=((B+Y(1))*(Y(1)**2
     *               +Y(2)**2)**2
     *               -A*Y(1)
     *               *((Y(1)**2+Y(2)**2)**(1.5D0)
     *               -Y(1)**2-2.0D0*Y(2)**2))
     *               /(A*Y(1)**2
     *               -C*(Y(1)**2+Y(2)**2)**2)
      RETURN
      END
```

```
C          THIS PROGRAM GENERATES A PARABOLA
C      IN THE PHASE PLANE USING CONSTANT
C      ACCELERATION.
C
       INTEGER THETA,I
       A=2.7
       RI=2.6
       B=-1.4
       C=0.179
       WRITE(39,*) '     BETA=',B,'     GAMMA=',C
       WRITE(39,*) 'ACCELERATION=',A,
      * '     BASE RADIUS=',RI
       WRITE(39,*) 'THETA,  RADUIS,  VELOCITY,'
      * ,'  PRESSURE  ANGLE,  AND  STRESS'
       DO 10 I=1,91
            THETA=I-1
            ANGLE=THETA*3.14159/180
            RPRIME=A*ANGLE
            R=RI+(A/2)*ANGLE**2
            Z=SQRT(R**2+RPRIME**2)
            ALPHA=(B+R+C*A)*Z**4
            ALPHA=ALPHA/(Z**3-2*Z**2+R**2+R*A)/R
            PRESSU=(180/3.14159)*ATAN(RPRIME/R)
            WRITE(39,*) THETA,R,RPRIME,PRESSU,ALPHA
   10       CONTINUE
       STOP
       END
```

VITA

Baldomero Westermann was born in Concepcion, Chile, on September 25, 1943. He graduated from Escuela Industrial Concepcion in December 1961. The following March he entered Universidad Tecnica del Estado in Concepcion, and in December 1966 he received the Licencia Industrial. The following March he entered The University of Santiago of Chile, and in January 1973 he received the Bachelor of Science degree in mechanical engineering. Since 1970 he has a teaching position in the University of Santiago in the Mechanical Engineering Department.

In the fall of 1982 he entered the graduate school of the University of Tennessee, Knoxville. He received the Master of Science degree in August 1985 and the Doctor of Philosophy degree in December 1987, both in mechanical engineering.

Mr. Westermann will be employed by the University of Santiago of Chile Department of Mechanical Engineering.